To the Graduate Council:

I am submitting herewith a dissertation written by Haoming Rong entitled “Structure and Properties of Cotton-based Biodegradable/Compostable Nonwovens.” I have examined the final electronic copy of this dissertation for form and content and recommend that it be accepted in partial fulfillment of the requirements for the degree of Doctor of Philosophy, with a major in Materials Science and Engineering.

Gajanan S. Bhat

_____

Major Professor

We have read this dissertation
and recommend its acceptance:

Kermit E. Duckett

_____

David C. Joy

_____

Larry C. Wadsworth

_____

Accepted for the Council:

Anne Mayhew

_____

Vice Chancellor and Dean of
Graduate Studies

(Original signatures are on file with official student records)

STRUCTURE AND PROPERTIES OF COTTON-BASED BIODEGRADABLE/COMPOSTABLE NONWOVENS

A Dissertation

Presented for the

Doctor of Philosophy

Degree

The University of Tennessee, Knoxville

Haoming Rong

May 2004

DEDICATION

This dissertation is dedicated to my parents, Mr. Xiaofeng Rong and Ms. Yamin Gu, and my parents-in-law, Mr. Guanzheng Wang and Ms. Mie Zhou, and my husband, Dr. Yizhong Wang, and the rest of my family.

ACKNOWLEDGEMENTS

First and foremost, I would like to express my deepest appreciation to my advisor, Dr. Gajanan S. Bhat, for his guidance and encouragement during my study, and for his help in bringing this thesis to fruition. I feel indebted to Dr. Kermit E. Duckett, Dr. Larry C. Wadsworth, and Dr. David C. Joy for taking the time to serve on my committee and the helpful suggestions they made during this work.

My gratitude can never be expressed enough to the people I met here in the University of Tennessee, Knoxville, especially those in the Textile Science program and Textile and Nonwovens Development Center (TANDEC).

I would like to give special thanks to Mr. Richard Meade and Mr. Van Brantley in TANDEC for their great assistances on running the pilot line and testing. I am very thankful to the following previous textile science graduate students for their precious assistances for running the thermal calendering machine: Mr. Shridhar Kurse, Ms. Xiao Gao, Mr. Praveen Jangala, and Mr. Ramaiah Kotra. The financial supports from Cotton Incorporated Inc., Raleigh, NC and Tennessee Agricultural Experimental Station and TANDEC at the University of Tennessee are most greatly appreciated.

Finally, I would like to thank my husband and the rest of my family for their unselfish support, sacrifices and understanding.

ABSTRACT

Cotton-based biodegradable nonwoven products have been receiving increasing attention in recent years with the growing environmental awareness throughout the world. A majority of the cotton-based nonwoven products are processed by carding with the binder fibers, and then point-bonding using a thermal calender.

In this work, different biodegradable binder fibers were used to produce cotton-based nonwovens. The structure and the properties of the resulting fabrics were studied. The effect of bonding temperature and binder fiber content on the bond morphology was investigated. The fracture and failure mechanisms of the fabrics produced with different binder fiber content and at different bonding temperature were analyzed.

Binder fiber distribution was determined by both qualitative and quantitative methods. The results show that DSC is a useful method to quantitatively characterize the binder fiber distribution in the carded cotton-based nonwovens. By determining the specific enthalpy from crystallization of one of the binder fiber components in the fabrics, it is possible to calculate the fiber composition.

Tensile properties of the resultant nonwovens under different processing conditions were studied. The optimal processing conditions for the nonwovens processed using different binder fibers were determined based on their tensile properties. Consequently, effects of binder fiber type, binder fiber content, and bonding temperature on the tensile property of the nonwoven fabrics are discussed. The best binder fiber under the experimental conditions was selected based on the tensile property of the resulting fabrics. Based on the interactions of binder fiber composition and bonding temperature, empirical models have been developed to predict the breaking load of the

webs bonded by the best binder fiber using the General Linear Models Procedure in JMP 5.0 statistical analysis software.

The absorbent behavior and flexural rigidity of the nonwoven fabrics bonded by one of the binder fibers were investigated. The results indicate that the resultant fabrics have low flexural rigidity and good absorbency which show that the fabrics have potential applications as absorbent materials.

TABLE OF CONTENTS

LIST OF TABLES

LIST OF FIGURES

NOMENCLATURE AND ABBREVIATIONS

Nomenclature

σ	standard deviation
C.V.	coefficient of variation
T	temperature
T_c	crystallizing temperature
T_o	onset temperature
T_p	peak temperature
ΔH_c	specific enthalpy for the crystallization exothermic peak
ΔH_f	heat of fusion
T_g	glass transition temperature
T_m	melt temperature
T_s	softening temperature
G	flexural rigidity
M	fabric mass per unit area
c	bending length
θ	contact angle
γ_{SV}	surface free energy of the solid-vapor interfaces
γ_{SL}	surface free energy of the solid-liquid interfaces
γ_{LV}	surface free energy of the liquid-vapor interfaces
C	absorbent compacity
Q	absorbency rate
A	area of the web
T	thickness of the web

W_f	mass of the dry web
ρ_f	density of the dry fiber
V_d	amount of fluid diffused into the structure of the fibers
α	ratio of the increase in volume of a fiber upon wetting to the volume of fluid diffused into the fiber
t	fluid penetration time
S	distance through which the fluid penetrated in time t
r	mean pore radius of the capillary
γ_l	surface tension of the fluid
η	viscosity of the fluid
ξ	a constant with a value of 9×10^5
d	fiber denier
ρ	fiber density (g/cc)
f	mass fraction of a fiber in blend
α	significant level

Abbreviations

CA	Cellulose Acetate
PLA	Polylactic Acids
CD	Cross Direction
PCL	Poly(ω-Caprolactone)
DSC	Differential Scanning Calorimeter
PTAT	Poly(Tetramethylene Adipate-co-terephthalate)
MD	Machine Direction
PVA	Poly(Vinyl Alcohol)
PHB	Poly(3-Hydroxybutyrate)
PHBV	Poly(3-Hydroxybutyrate-*co*-3-hydroxyvalerate)
PCA	Plasticized Cellulose Acetate
OCA	Ordinary Cellulose Acetate
CAP	Cellulose Acetate Propionates
CAB	Cellulose Acetate Butyrates
PE	Polyethylene
PET	Poly(Ethylene Terephthalate)
PP	Polypropylene
DS	Degree of Substitution
SEM	Scanning Electron Microscopy
TANDEC	Textile and Nonwoven Development Center
Eastar	Eastar *Bio*® GP Copolyester Unicomponent Fiber
ATS	Absorbency Testing System
GLM	General Linear Model Procedures
PI	Prediction Interval
gsm	Grams per Square Meter

Chapter 1

INTRODUCTION

§1.1 BIODEGRADABLE NONWOVEN MATERIALS

Nonwoven fabrics have been widely used in home furnishings, automotive products, geotextiles, industrial filters and medical sanitary materials. The wide variety of the applications can be generally classified into two groups; one is single-use disposable materials and the other is long-lasting durable applications. Over the past 30 years, fiber usage by the nonwoven industry has grown by a factor of ten. Demand for nonwoven materials in the United States is expected to increase 3.9 percent per year to nearly $5 billion in 2007. The main demand for nonwovens in 2002 was disposable markets, which accounted for a 64-percent share [1]. The majority of these products are made of synthetic fibers, such as polypropylene, polyethylene, polyester and polyamide, which are not biodegradable and end up as solid waste. With the growing environmental awareness throughout the world, environmentally compatible nonwoven products have been receiving increasing attention in recent years [2, 3].

Population and environmental concerns, litter abatement, public policies, and seasonal agricultural needs are providing an incentive to develop and use biodegradable or environmentally friendly textiles, especially disposable nonwoven products [4]. Biodegradation is defined as “an event which takes place through the action of enzymes

and/or chemical decomposition associated with living organisms (bacteria, fungi, etc.) or their secretion products" [5]. It is worth noticing that some other abiotic reactions, such as photodegradation, oxidation, and hydrolysis, may also associate with the biodegradation due to environmental factors such as soils, rivers, lakes, and seas. Generally, the biodegradable material loses its weight over time and the whole material disappears and leaves no trace of remnants [6]. Thus the target for biodegradable nonwovens is to replace non-biodegradable synthetic fibers with biodegradable fibers in the disposable nownovens.

Natural fibers, such as cotton, kenaf, coir, flax, jute, hemp, sisal, and wood, become the first choice due to their biodegradability. The biodegradable materials from biodegradable natural fibers and polymers will render a contribution in the 21st century due to serious environmental problem. Currently, both natural fibers and synthetic biodegradable fibers are available in the market for nonwoven applications. Some synthetic biodegradable fibers, such as cellulose ester (CA), Rayon, Lyocell, polyesters (PLA, PCL, PHB, PHBV, Biomax, PTAT), and water soluble PVA, have been used for nonwoven applications.

§1.2 MOTIVATION FOR THE PRESENTED WORK

Because biodegradable/compostable cotton-based nonwovens are sustainable materials, there is increasing interest in them and the expansion of nonwovens into novel applications. One of the major applications of disposable nonwovens is in absorbent materials, which constitute a broad range of products, including baby diapers, personal

hygiene and adult incontinent pads, tampons, paper towels, tissues, and medical wipes and pads. Most cotton-based nonwoven products are processed by carding with the binder fibers and then point-bonded using a thermal calendering machine. At the beginning of cotton-based nonwoven research, synthetic fibers such as polypropylene, polyethylene, and polyester were used as binder fibers [7-10]. However, these binder fibers are not biodegradable, thereby contributing to environmental pollution. Therefore, it has become important to find a suitable biodegradable binder fiber.

Cellulose Acetate (CA) fiber has been shown to be a good binder fiber for cotton-based biodegradable/compostable thermal calendered nonwoven products by the research conducted at the University of Tennessee, Knoxville. CA is a thermoplastic, hydrophilic and biodegradable fiber. However, the softening temperature of cellulose acetate fiber is relatively high (T_s: 180-205˚C). Acetone solvent pre-treatment has been applied to decrease the softening temperature and to lower the calendering temperature [11]. Because acetone is flammable and toxic, and it is undesirable from the point of environmental concern. In this research, two alternative methods were used for cotton/cellulose acetate nonwovens:

1) Water as external plasticizer instead of acetone solvent
2) Plasticized cellulose acetate (PCA) instead of ordinary cellulose acetate (OCA) binder fiber.

Also, Eastar *Bio*® GP Copolyester [12], in the form of unicomponent and bicomponent fibers, was selected as the binder fiber instead of cellulose acetate to make thermally calendered nonwoven products. Eastar *Bio*® GP copolyester can be totally

degraded into CO_2, H_2O and biomass. Another advantage of this binder fiber is its relatively low melting temperature (110˚C), which means that the thermal calendering process temperature can be relatively low.

The objectives of this research was to:

1) Design and prepare biodegradable nonwovens with improved processability, without compromising tensile properties
2) Select the best available binder fiber for biodegradable cotton-based nonwovens
3) Determine the optimal processing conditions for the best compositions
4) Investigate the relationship among process, structure, and properties of the resulting nonwovens.

Chapter 2

LITERATURE REVIEW

§2.1 NONWOVENS

Nonwovens are flat, porous sheets that are made directly from separate fibers or from molten plastic or plastic film, and not from weaving or knitting of yarns. Nonwoven fabrics are broadly defined as sheet or web structures bonded together by entangling fiber or filaments (and by perforating films) mechanically, thermally or chemically [13]. The nonwoven process begins by making a "web" of loosely entangled fibers or filaments by carding, air-laying, wet-laying, or polymer-laying. The fibers in the web can be directionally or randomly orientated. The webs are then bonded together either by chemical, mechanical or thermal means. Chemical bonding involves the use of various adhesives or binders to bond the fibers together, in which the most commonly used adhesive is latex. Mechanical bonding includes needlepunching, stitchbonding, and hydraulic entanglement using water jets, while thermal bonding supplies heat in combination with pressure to fuse the components or binder fibers so that upon solidification, the web is bonded together. Thermal bonding can be further classified as thermal calendering, through-air bonding, ultrasonic bonding, or radiant bonding based on the heating method. A thermoplastic component in the form of fiber, powder, or film is necessary for the thermal bonding process. The melting point of the thermal plastic

component must be lower than that of the carrier fiber. Alternatively, carrier (base) fibers with low softening temperatures can themselves function as binding components. For example, spunbond PP is normally thermally point-bonded.

Nonwoven fabrics are engineered fabrics that may be classified as durable for life long applications or disposable for limited life and single-uses. Nonwoven fabrics can be produced with different properties such as softness, absorbency, resilience, liquid repellency, flame retardancy, stretch, strength, cushioning, washability, filtering, bacterial barrier and sterility. These functions are often combined to create fabrics for specific applications. They can be as bulky as the thickest paddings and can mimic the appearance, texture and strength of woven fabrics. Nonwoven fabrics may be used alone or as components of apparel, home furnishing, health care, or engineering, industrial and consumer goods [13].

§2.2 BIODEGRADABLE FIBERS

Fibers are the basic units of nonwoven fabrics: they can be continuous filaments or short staple fibers. A variety of fiber types, both natural and synthetic, have been employed in the production of nonwoven products. Almost every fiber known to mankind has been used in a nonwoven structure at one time or another. However, commercially important nonwoven fabrics have been limited to relatively few fiber types. The dominant fibers include polypropylene, polyester, nylon, cotton and rayon. In Western Europe, the three fibers, polypropylene, polyester, and rayon accounted for nearly 70% of staple fiber consumption by the nonwoven industry in 1997 [14].

The popularity of synthetic fibers in the nonwoven industry is attributed to low cost, uniformity, ease of processing etc. However, with the growing demand and consciousness for environmentally friendly products, manufactures are now paying more attention to biodegradable fibers.

Biodegradable fibers are fibers which can degrade to lower molecular weight components, owing to the action of enzymes and/or chemical decomposition associated with living organisms (bacteria, fungi, etc.) and their secretion production [15]. Biodegradable fibers often have chain backbones with oxygen or nitrogen links and/or pendant groups containing oxygen or nitrogen atoms. Most natural fibers and fibers made of natural polymers fit this description.

As it is well known, cotton is a natural cellulosic fiber. The importance of natural biodegradability of the cotton fiber makes it the best choice for the carrier fiber of biodegradable nonwovens. Besides, cotton fiber has good absorbency, softness, and breathability. These properties have made the cotton fiber to be widely used in baby diapers, adult incontinence coverstocks, wipes, medical/surgical products, feminine hygiene coverstocks, sanitary towels, and some other health care products. Some of the biodegradable synthetic fibers which are currently available for use in the production of nonwoven fabrics are discussed below [16-21].

§2.2.1 Cellulose Esters

Cellulose acetate (CA) is considered as a potentially useful polymer in biodegradable applications. Cellulose esters are produced by the chemical modification

of cellulose and include the family of cellulose acetates (CA), cellulose acetate propionates (CAP) and cellulose acetate butyrates (CAB) [22]. CA, CAB and CAP can be obtained from Eastman Chemical Co. Inc. Kingsport, TN under the trade name Tenite [17]. Cellulose acetate (CA) is produced by the partial hydrolysis of cellulose triacetate. The structure of cellulose diacetate is represented in Figure 2.1. Since the hydroxyl groups in cellulose acetate are blocked and substituted by acetyl groups in different degrees, the biodegradability of cellulose acetate is less certain. Cellulose acetate only biodegrades under certain circumstances as the three hydroxyl groups on the glucopyranosyl rings are replaced by more hydrophobic ester groups. The extent of biodegradability is highly related to the degree of substitution (DS) [5].

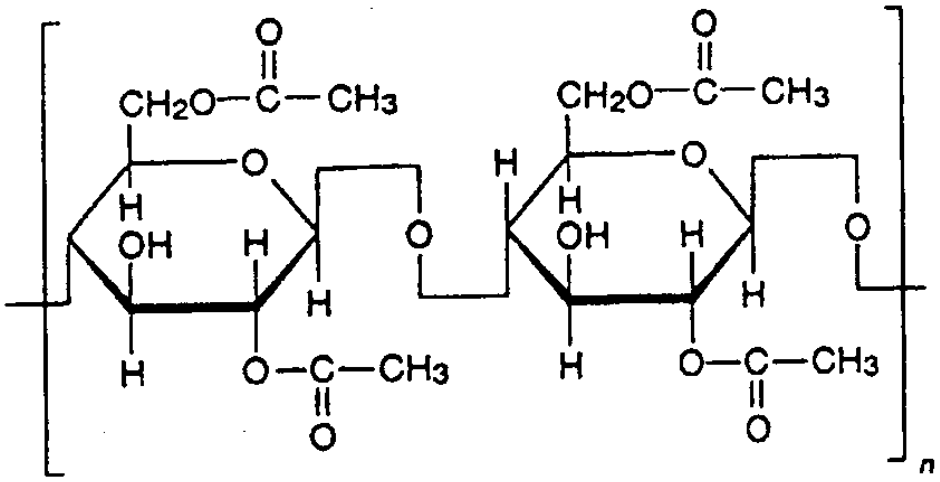

Figure 2.1 Chemical structure of cellulose diacetate.

§2.2.2 Polylactic Acids

Polylactic acids (PLA) received considerable attention because of the biodegradability and biocompatibility. It can be used in biomedical applications, such as surgical suture and drug delivery systems. The chemical structure of PLA is illustrated in Figure 2.2. Recently PLA has been highlighted by Cargill Dow Polymers because of its availability from renewable resources like corn [23]. PLA resins are composed of chains of lactic acid, a natural food ingredient, which can be produced by converting starch into sugar and then fermenting it to yield lactic acid. PLA can be degraded into lactic acid and finally into CO_2 and H_2O by hydrolysis of ester bonds. PLA has the advantage of being not only biodegradable but also renewable since the raw material, lactic acid, may be produced by microbial fermentation of biomass. One interesting feature of PLA is that its processing temperatures are more typical of polyolefins (approximately 220°C) but its properties are more like those of polyesters. PLA's biggest potential use may be as a lower cost competitor for PET in films, fibers and fabrics, and bottles for water and other noncarbonated liquids.

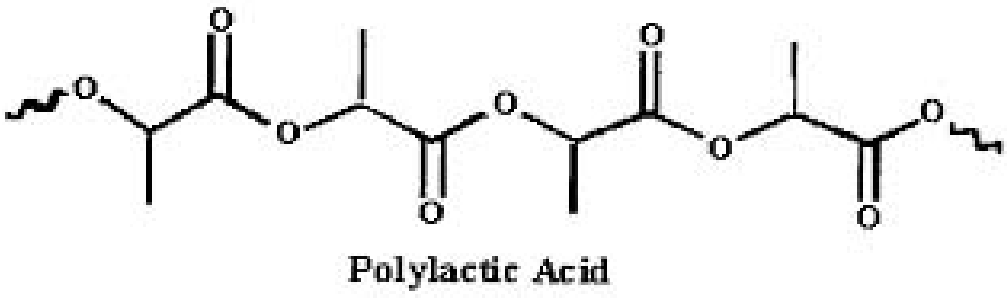

Figure 2.2 Chemical structure of PLA.

§2.2.3 Poly(ω-Caprolactone)

Poly(ω-caprolactone), PCL**,** is an example of poly(ω-hydroxyalkanoate), a preferred biodegradable aliphatic polyester. PCL is prepared from cyclic ester monomer, lactone, by a ring-opening reaction with a catalyst like stannous octanoate in the presence of an initiator that contains an active hydrogen atom. The chemical structure of PCL [24] is illustrated in Figure 2.3. It has been shown that PCL is degraded by enzymes, lipases, secreted from microorganisms [25, 26].

PCL polymers are available from Union Carbide Corporation under the trade name Tone. Glass transition and melting temperatures of PCL are – 60°C and 61°C, respectively.

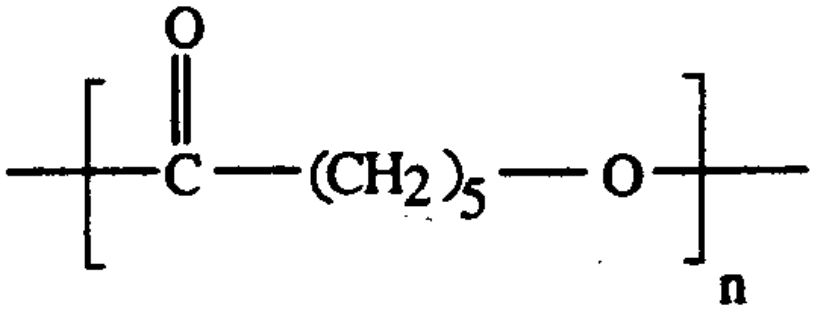

Polycaprolactone (PCL)

Figure 2.3 Chemical structure of PCL.

§2.2.4 Poly(Tetramethylene Adipate-co-terephthalte)

Poly(tetramethylene adipate-co-terephthalte) (PTAT) is a patented product developed by Eastman Chemical Company in August 1995 and commercialized in November 1997 with a trade name Eastar *Bio*® GP Copolyester. It is a random copolymer derived from conventional diacids and glycols. The building blocks are shown in Figure 2.4 [16].

Eastar *Bio*® GP Copolyester can be fully degraded into CO_2, H_2O and biomass in a commercial composting environment in 180 days and becomes invisible to the naked eye in twelve weeks [16]. The extent and rate of biodegradation depend on several factors including environmental conditions, such as moisture and temperature, geometry, and manufacturing method of the finished product.

The biodegradable copolyester is a semicrystalline polymer with a tensile strength comparable to LDPE, but with very high elongation and low modulus. The melting temperature of the polymer is around 110°C. Eastar *Bio*® copolyester can be spunbonded and meltblown. It can also be mixed with materials from renewable resources, such as starch and wood floor, or can be applied in extrusion coating applications.

Fiber and fabrics made from Eastar *Bio*® copolyester have very soft hand. The main applications for the biodegradable copolyester are in food packaging, ground covers, gardening bags, seed mats, and nonwovens [27].

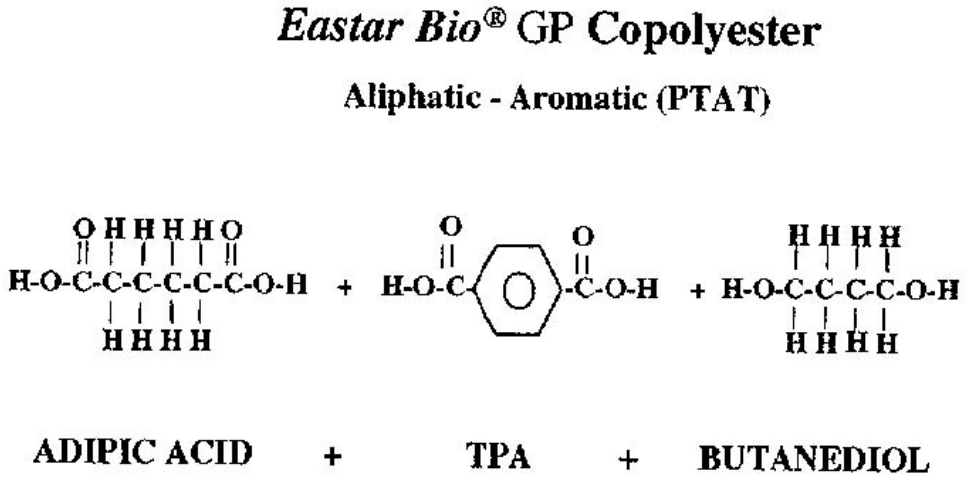

Figure 2.4 Building blocks of Eastar *Bio*® GP copolymer.

§2.3 NONWOVEN PROCESSING

The web formation in nonwoven production is a critical part of end-use product performance. Strength, absorbency, and stiffness in a nonwoven fabric are primarily determined by the fiber orientation distribution during web formation, fiber type and strengths of the constituent fibers, and the degree of bonding. Four basic methods are used to form a web: dry-laying (carding and airlaying), wet-laying, spunbonding and meltblowing. Webs, other than spunlaid, have little strength in their unbonded forms. The web must therefore be consolidated in some way. There are three basic types of bonding: chemical (latex bonding, saturation bonding, spray bonding, foam bonding), thermal (calendering, through-air bonding, ultrasonic bonding, radiant bonding), and mechanical (needlepunching, stitchbonding, hydraulic entanglement).

§2.3.1 Carding

Carding is the most common process for producing nonwoven fabrics from staple fibers. The objective of carding is to separate the fiber stock into individual fibers with minimum fiber breakage. The carding process consists of opening and thoroughly blending different species of fibers. It is performed by the mechanical action in which the fibers are held by one surface while the other surface combs the fibers, causing the separation of individual fibers. For cotton-based thermally point-bonded nonwovens, it is important that the low-melting adhesive components (the binder fibers) be distributed evenly throughout to ensure uniformity of fabric properties. However, the carded webs always have area irregularities of mass distribution caused by machine variables, such as

the nature and conditions of card clothing, the relative speeds and settings of the carding elements, fiber properties, such as fiber staple length, cross sectional shape, crimps, stiffness, fiber surface roughness, tensile properties, spin finishes applied to the fibers, fiber morphologies, and area irregularities of the fed fiber matt [28]. For any application, the most important characteristic of a carded web is the uniformity of fiber areal density.

§2.3.2 Thermal Bonding

Thermal bonded nonwovens have "come of age" in the 1990s [29]. Thermal bonding is the process of using heat to bond or stabilize a web structure that contains a thermoplastic binder. It is the most popular method of bonding used in nonwovens because of favorable process economics, the absence of chemical binders, the availability of new fibers and machinery, and process and product enhancement.

There are three key components in thermal bonding: structure of carrier or base fiber, heat activated binder fiber, and the bonding process [30]. The carrier fiber is the skeleton structure of the nonwoven fabric. It gives the fabric strength, integrity and certain properties depending on the fiber composition. The adhesive component, distributed in a nonwoven web is in the form of a unicomponent binder fiber, bicomponent binder fiber, powder particle, film, hot melt, netting or the outer surface of a homogeneous carrier fiber that is subjected to heat [30]. As the adhesive approaches its melting point, its surface softens and contacts areas with more stable fibers to form potential bonding sites. The adhesive attaches to a network fiber upon melting and flows along the network fiber into a crossing of two or more fibers, or an adhesive bead is

formed. When cooled, the adhesive solidifies and forms a bond or thermal fusion at each fiber/binder contact. Individual bond strength is a function of the amount of fiber surface area joined or shared at fiber intersections and the inherent strength of the bonding adhesive. Binder distribution and binder concentration also affect the bond. Fabric properties such as strength, resilience, softness, and drape are influenced by individual bond strength, bond placement, and the total bonded area. A properly produced thermal bonded nonwoven can approach the idealized nonwoven structure, that is, one in which individual fibers are attached flexibly at every fiber crossing [29].

Thus, all thermal bonding processes have two common features. First, the melting point of the binder fiber must be lower than that of the carrier fiber. Second, heat must be applied either alone, combined with pressure, followed by pressure as in the case of calenders, ovens and radiant heat sources or simply generated as part of the process (e.g. ultrasonic bonding). There are four methods of thermal bonding [31]. They are hot calendering, oven bonding, ultrasonic bonding, and radiant heat bonding. Hot calendering can be further classified as area bond hot calendering, point bond hot calendering, and embossing hot calendering. Among the various types of thermal bonding methods, point bonding using embossing rolls is the most desired method used by the cover-stock industry for baby diapers. It employs direct contact, with heat and pressure, to produce localized bonding in a nonwoven. Also it adds softness and flexibility to the fabric by the embossing rolls compared to smooth rolls used in area bond hot calendering.

§2.3.3 Point Bonding Process

Point-bonding is applicable to carded, spunbond, and meltblown webs. This method produces fabrics which range from thin, closed, strong, inelastic, and stiff to open, bulky, weak, flexible and elastic depending on the size, density, and the pattern of the bond points.

In the point bonding process, the web is fed to a calender nip consisting of one engraved roll and one smooth roll. As the web enters the hot calender nip, fiber temperature is raised to the point at which tackiness and melting cause fiber segments caught between the tips of engraved points and smooth roll to adhere together. The process is schematically shown in Figure 2.5 [32].

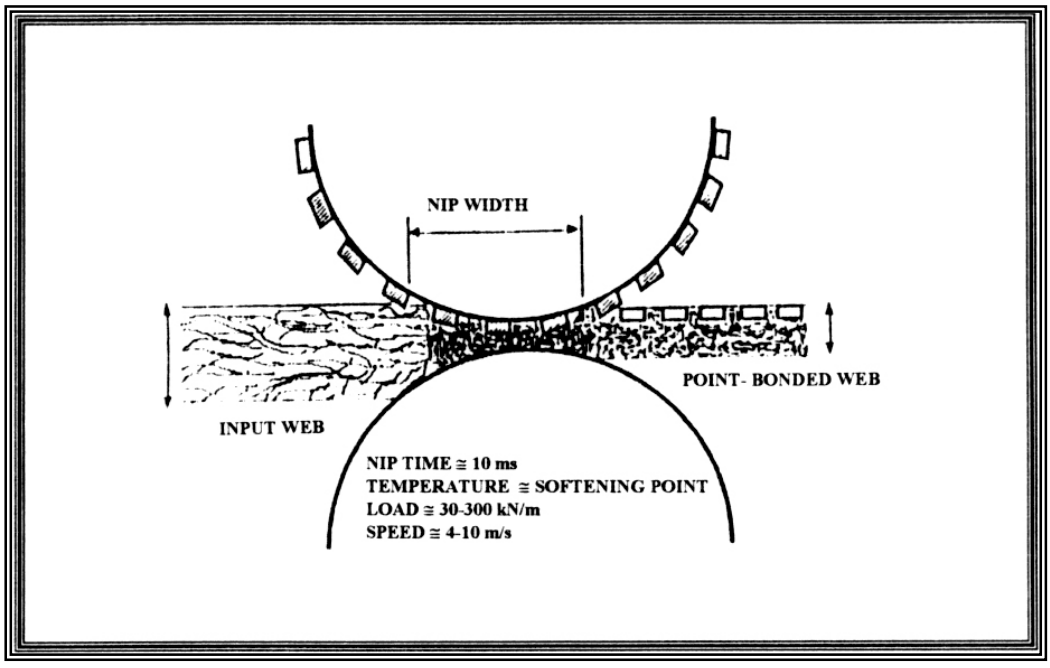

Figure 2.5 Schematic of thermal point bonding process [32].

The main process variables affecting fabric properties are bonding temperature, bonding pressure, and contact time (or calendering speed). In general, bonding temperature is considered the primary parameter influencing bonded fabric strength [33, 34]. At fixed bonding pressure and calendering speed, there is an optimal bonding temperature which gives maximum bond strength [34-37]. Bonding pressure was found to be less significant in determining fabric properties as compared to bonding temperature [36]. However, a certain pressure is essential to achieve contact between fibers and roll surfaces. Higher pressures may have the effect of increasing the melting point of the polymer fibers due to the Clapeyron effect [38]. The contact time of the web in the nip is primarily controlled by the production speed and roll diameters. Generally, increasing the calender speed while maintaining the roll temperature and pressure constant reduces the breaking strength [34]. The roll speeds used are a tradeoff between maximum productivity and sufficient contact time of fibers and rolls. An increase in production rate, when compensated by an appropriate increase in temperature and reduction of the bond point area, may actually increase the fabric strength.

§2.4 **BOND FORMATION**

Bonding has been ascribed to adsorption/wetting, van der waals attractive forces, electrostatic attraction, development of contact at the interface by viscoelastic deformation, diffusion of molecules, chemical bonds and mechanical interlocking, which are schematically shown in Figure 2.6. It is well known that the properties of an interface

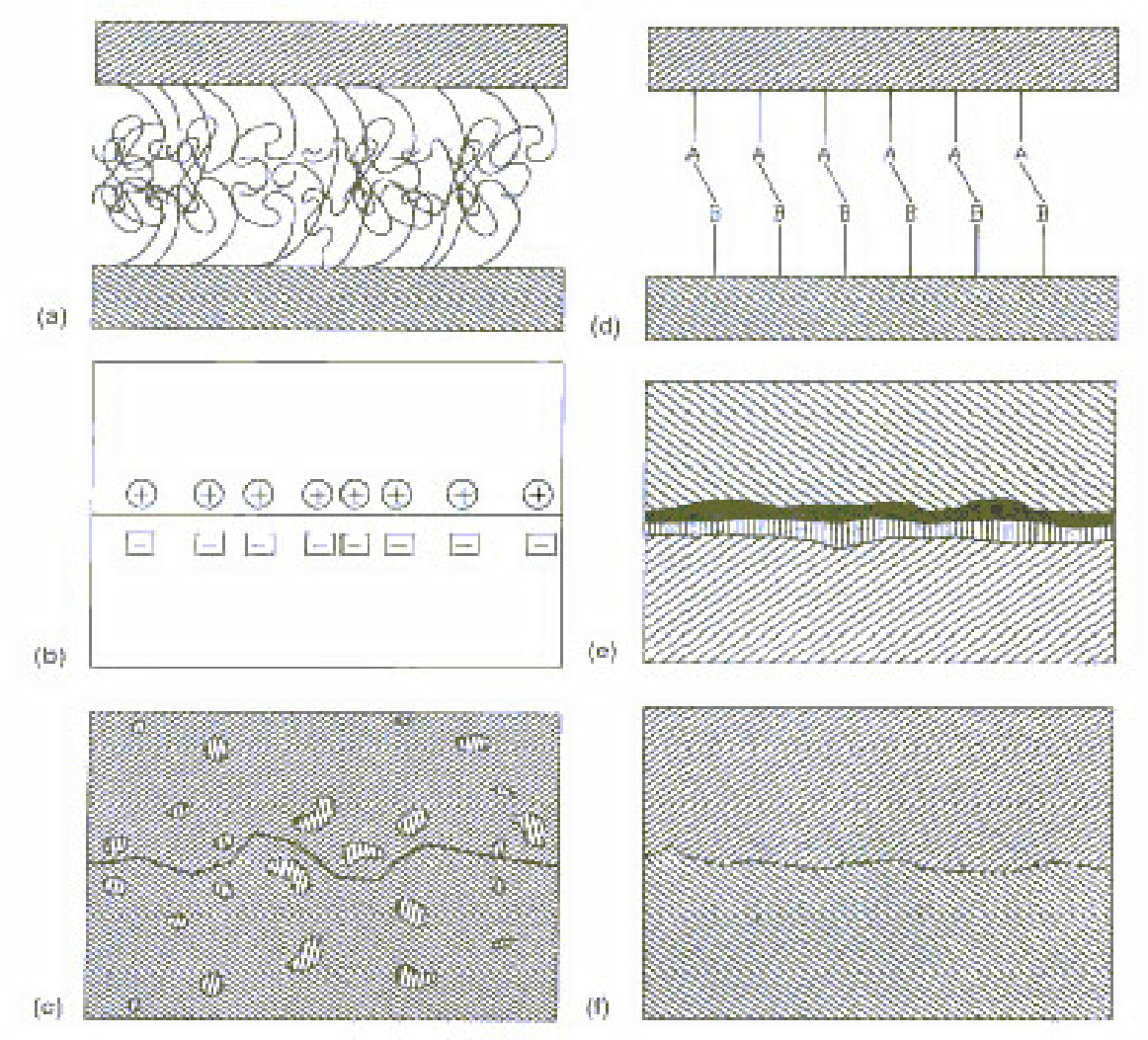

Figure 2.6 Interface bonds. Bonds are formed (a) by molecular entanglement; (b) by electrostatic attraction; (c) by interdiffusion of elements; (d) by chemical reaction between groups A on one surface and groups B on the other surface; (e) by chemical reaction following forming of a new compound(s); (f) by mechanical interlocking [40].

are controlled largely by the chemical/morphological nature and physical/thermodynamic compatibility between the two [39, 40].

Wetting can be quantitatively expressed in terms of contact angle and surface energy according to Young's equation:

$$\gamma_{SV} = \gamma_{SL} + \gamma_{LV} \cos\theta \tag{2.1}$$

where γ_{SV}, γ_{SL} and γ_{LV} are the surface free energies of the solid-vapor, solid-liquid and liquid-vapor interfaces, respectively, and θ is the contact angle as shown in Figure 2.7. Liquids that form contact angles greater than 90° are called "Non-wetting", while liquids that form contact angles less than 90° are called "wetting". If the liquid does not form a droplet, i.e. θ=0°, it is termed "spreading" and in this case, γ_{SV} - γ_{SL} > γ_{LV}. The surface energy of a solid, γ_{SV}, must be greater than that of a liquid, γ_{LV}, for proper wetting to take place. According to the diffusion theory, wetting at the interface is followed by diffusion of molecular segments across the interface and ensuing entanglements with

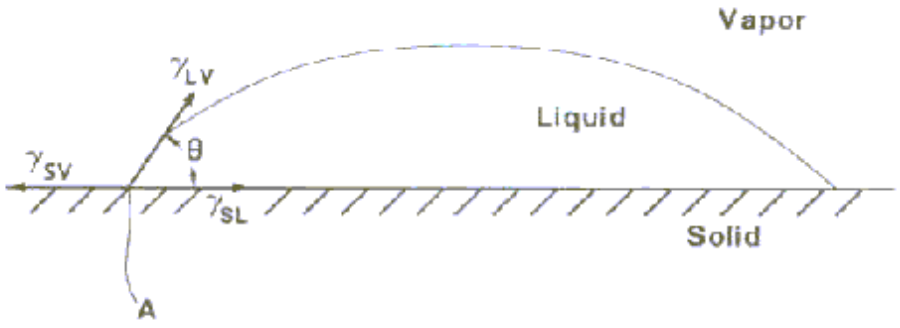

Figure 2.7 Contact angle. Contact angle θ, and surface energies, γ_{LV}, γ_{SL}, and γ_{SV}, for a liquid drop on a solid surface.

other molecules contributing to bond formation. A bond between two surfaces may be formed by the interdiffusion of atoms or molecules across the interface. A fundamental feature of the interdiffusion mechanism is that there must exist a thermodynamic equilibrium between the two constituents [40]. The phenomenon of bonding has been explained in terms of adhesive and cohesive forces in the bonded nonwovens. If fibers are to be bonded firmly with an adhesive, a strong mechanical and/or chemical bond must be formed between the adhesive and the fiber. Therefore, the coherence of the product will be determined by the harmony of the two types of bonding forces involved, that is, the adhesive forces acting on the contact interface and the cohesive forces acting within the bonding layer [39].

The bond strength in polymer matrix composites will depend on the amount of molecular entanglement, the number of molecules involved and the strength of the bonding between the molecules. The interfacial region has a substantial thickness, and its chemical, physical and mechanical properties are different from those of either of the two bulk components. An analysis of the bonding procedure reveals the following main steps in the process [39]:

- Getting both the phases into contact
- Wetting of the surface of carrier/base fibers with the softening of binder fiber
- Interfacial diffusion

Factors that affect bonding can be classified in two groups, physical and chemical. Physical factors are listed as surface tension, cleanness and size of the surface, thickness of the adhesive layer, pressure and the time for which it is applied, and temperature and

the time for which it is applied. Chemical factors include chemical composition and properties of the two constituents, degree of polymerization and polydispersity of the two constituents, polarity of the two constituents, adsorption property of the carrier fiber, viscosity of the binder in the course of the bonding process, and its rheological properties [39].

§2.5 FABRIC FAILURE

A thermally point-bonded fabric is a network of fibers bonded together at discrete points called bond points. The fibers connecting the bond points are called bridging fibers. Most of the fibers in thermally point-bonded fabrics are unbonded, and result in a fabric that is soft to touch. The strength of thermally point-bonded fabrics is rarely proportional to the aggregated single fiber strength. It depends on both the properties of the bond points and the bridging fibers, the bond shape, bond arrangement, mechanical damage of the fibers during thermal calendering.

Chidambaram [41] mentioned the following two factors, which affect the failure of the fabric:

1. Non-uniform lengths of bridging fibers caused by different crimps of carrier fiber and binder fiber and the diamond shape of the bond points result in strain inhomogenieties during the test. The higher the crimp level, the longer the bridging fiber interval. For the diamond shape bond pattern, fibers at the edges of bonds are longer than the fibers in the center of the bond. Thus, the fibers close to the center bear higher strains and support higher loads than the fibers at the edges.

2. Elongation variability of bridging fibers. Two idealized shapes of fiber stress-strain curves are shown in Figure 2.8. Fibers with concave-down stress-stain curves (A) are believed to be a better choice for thermally point-bonded nonwovens than those with concave-up stress-strain curves (B), when load sharing is considered [41]. For fabrics containing more than one type of constituent fibers, the elongation variability may cause strain inhomogenieties. For the same fiber, elongation properties may vary from fiber-to-fiber, which can further increase inhomogeneous straining.

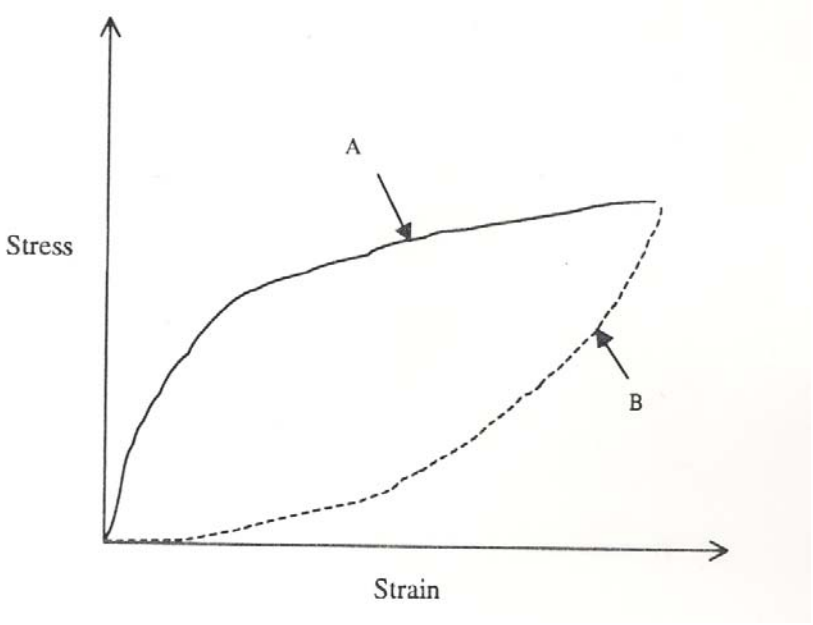

Figure 2.8 Two idealized stress-strain relationships [41].

Failure of nonwoven fabrics can occur by failure of the constituent fibers, failure within the adhesives or at the fiber-binder bonding interfaces, or by a combination of these modes. The nonwoven fabric failure mechanism is influenced by fiber physical properties, adhesive properties, and structural properties including the relative frequency and structure of the bonding elements, fiber orientation and the degree of freedom for movement of the fibers between the bond points. Physical properties of the nonwovens will be controlled by the first failure occurring in the fabric sample [42]. The following observations were made according to previous study on the fabric failure mechanism of thermally point-bonded nonwovens [33-34, 36-37, 43-46]:

a) At low bonding temperatures, the bond failure mechanism was found to be the loss of interfacial adhesion at the bond site, leading to bond disintegration due to poor bonding.

b) At higher bonding temperatures, the failure mechanism was cohesive failure of the fibers near the bond site attachment point, either at the bond perimeter or between two bond points.

c) At extremely high temperatures, bond points lose fiber integrity and formation of film-like spots resulting in brittle bonds, which cracked and caused fabric failure at lower strength, that is, the fracture of bond itself.

§2.6 MORPHOLOGY OF BOND POINTS AND BRIDGING FIBERS

Fabric failure was determined by the character of the bond points and by the stress-strain relationship of the bridging fibers. During point bonding, the bond points and

the bridging fibers develop distinct properties, different from those of the virgin fibers, depending on the process variables employed.

Warner [38] suggested that fibers break at the bond periphery because of the local thermo-mechanical history of the polymer. The material at the perimeter is weak and brittle, and he attributed this brittleness to crystallization in an unoriented state, especially at the perimeter where polymer is a result of extrusion from under the pin. Thus, he suggested that the strength of point-bonded fabrics would be governed by the bond-periphery strength. Mi et al. [47] suggested that bond strength is important in determining the strength of point-bonded fabrics. Theoretical results of their model indicated that 'high-strength' bonds defined by fabric failure, caused by failure of the bridging fibers, led to the strongest fabrics. Wei et al. [48] observed that "significant morphological changes occur in the bonding regions, and the physical properties of thermally bonded fabrics are a manifestation of the nature and quality of the bonding regions". Akai and Aspin [49] indicated that embossing increased crystallinity, improved crystal perfection, and caused some molecular orientation in the manufacture of embossed PP tapes.

Although considerable knowledge has been gained on how the structure of a nonwoven affects its properties as stated above, it is still not clear on how to translate fiber morphology and properties to the end-product properties due to the lack of reliable data and the complexity of the structure of nonwovens. Recently some breakthroughs have been made by several researchers via reliable methods that measure how the fiber morphology and properties are transformed during bonding.

Bhat et al. [50] found that fibers with relatively less developed morphology yielded stronger and tougher webs as compared to fibers with more developed morphology. The fibers with high molecular orientation and cystallinity tended to form a weak and brittle bond mainly due to lack of polymer flow and the presence of fibrillation of the fibers in the bonded regions. Also they observed fiber breaking extension is as important as fiber strength in governing web properties. Higher breaking extension of the fibers leads to a greater degree of load sharing between the fibers during deformation, thus improving the mechanical properties of the web. Fibers with less developed morphology showed lower optimum bonding temperature.

Wang and Michielsen [51] applied Raman microspectroscopy to isotactic polypropylene nonwovens to determine the morphology of these materials on a micro scale size of about 3μm. Several discoveries have been made. First, the morphology of the fibers between bond points and at locations greater than 30μm from the bond edges is unchanged from the original fibers. Second, the morphology of the bonded regions is considerably different from that of the original fibers, and the extent of the difference depends directly on bonding conditions. Birefringence is higher and the crystallinity is lower in the thermal point bonds compared to the original fibers. Third, there is a sharp gradient in the morphology at the bond edge over a distance of about 30μm.

§2.7 ABSORPTION

One of the major applications of disposable nonwovens is in absorbent materials, which constitute a broad range of products, ranging from baby diapers, personal hygiene

and adult incontinent pads to tampons, paper towels, tissues and sponges. The key requirement for absorbent materials is its ability to imbibe rapidly and hold large amount of fluid under pressure. Absorbency rate and absorbent capacity are the two most important performance parameters to be considered for absorbent applications of nonwovens. The absorbent capacity is mainly determined by the interstitial space between the fibers, the absorbing and swelling characteristics of the material and the resiliency of the web in the wet state. The absorbency rate is governed by the balance between the forces exerted by the capillaries and the frictional drag offered by the fiber surfaces. For non-swelling materials, these properties are largely controlled by the capillary sorption of fluid into the structure until saturation is reached [52]. Gupta et al [53-57] found that absorbency rate and absorbent capacity are affected by fiber mechanical and surface properties, structure of the fabric (i.e., the size and the orientation of flow channels), the nature of fluids imbibed, and the manner in which the web or the product is tested or used. Among those factors, the surface wetting characteristics (contact angle) of the fibers in the web and the structure of the web, such as the size, shape, orientation of capillaries, and the extent of bonding, are most important.

The polymer type of the fibers in the fabrics, hydrophilic or hydrophobic, influences the inherent absorbent properties of the fabrics. A hydrophilic swellable fiber provides the capacity to absorb liquid via fiber imbibition, giving rise to fiber swelling. It also attracts and holds liquid external to the fiber, in the capillaries, and structure voids. On the other hand, a hydrophobic fiber has only the latter mechanism available to it normally [58]. The effect of the small amount of fiber finish (generally 0.1 to 0.5% by

weight) is also important since it is on the fiber surface. The particular finish applied on the fiber can significantly change surface wetting property of the fiber.

Fiber linear density and its cross-section area affect void volume, capillary dimensions and the total number of capillaries per unit mass in the fabrics. Fiber surface morphology, surface rugosity, and core uniformity can influence the absorbency performance to some extent. Fiber crimps influence the packing density of the fabrics and further affect the thickness per unit mass, which affects the absorbency of the nonwoven fabrics. The nature of the crimps, whether it is two-dimensional or three-dimensional, also has some effect [58].

The size of capillaries is affected by the thickness per unit mass and the resiliency of the web, and the size, shape and the mechanical properties of the fibers. The resiliency of the web is influenced by the nature and level of bonding of the fabrics as well as the size, shape, and mechanical properties of the constituent fibers [57].

Models have been built to characterize the two parameters, absorbent capacity (C) and absorbency rate (Q). C (cc/g fluid/g) is given by the volume/mass of fluid absorbed at equilibrium divided by the dry mass of the specimen, while Q is given by the slope of the absorbency curve divided by the dry mass of the specimen. The model to calculate C is based on determining the total interstitial space available for holding fluid per unit dry mass of fiber. The equation is shown as follow [56, 57]:

$$C = A\frac{T}{W_f} - \frac{1}{\rho_f} + (1-\alpha)\frac{V_d}{W_f} \tag{2.2}$$

where, A is the area of the web

T is the thickness of the web

W_f is the mass of the dry web

ρ_f is the density of the dry fiber

V_d is the amount of fluid diffused into the structure of the fibers

α is the ratio of increase in volume of a fiber upon wetting to the volume of fluid diffused into the fiber.

In the above equation, "the second term is negligible compared to the first term, and the third term is nearly zero if a fiber is assumed to swell strictly by replacement of fiber volume with fluid volume" [57]. Thus, the dominant factor, which controls the fabric absorbent capacity, is the web thickness per unit of dry mass (T/W_f).

For absorbency rate, the Washburn-Lucas's equation [59, 60] is applied.

$$S^2 = \frac{r\gamma_l \cos\theta}{2\eta} t \tag{2.3}$$

where, S is the distance through which the fluid penetrated in time t

r is the mean pore radius of the capillary

γ_l is the surface tension of the fluid

θ is the contact angle of the fiber

η is the viscosity of the fluid

t is the fluid penetrated time

Modifications are given to Washburn-Lucas's equation when applied to the nonwoven webs in which the fluid radially spreads outward from a point in the center. The modified equation is shown as follow:

$$Q = \frac{\pi r \gamma_l \cos\theta}{2\eta}\left(\frac{T}{W_f} - \frac{1}{A\rho_f}\right) \tag{2.4}$$

where, r is the mean pore radius of the capillary

γ_l is the surface tension of the fluid

θ is the contact angle of the fiber

η is the viscosity of the fluid

T is the thickness of the web

W_f is the mass of the dry web

A is the area of the web

ρ_f is the density of the dry fiber

In a given web and fluid system, only mean pore radius r and thickness per unit mass (T/W_f) in above equation are not constant. Gupta [54] predicted the value of r by the following equation based on the assumption that a capillary was bound by three fibers, oriented parallel or randomly, and the specific volume of the capillary unit cell equaled that of the parent web.

$$r = \left[\frac{1}{6\pi\xi} \left(A \frac{T}{W_f} \times \frac{\rho_1 \rho_2}{f_1 \rho_2 + f_2 \rho_1} - 1 \right) \left(\frac{d_1 n_1}{\rho_1} + \frac{d_2 n_2}{\rho_2} \right) \right]^{\frac{1}{2}} \tag{2.5}$$

for $n_1 = 3 - n_2$, $n_2 = \dfrac{3 f_2 d_1}{f_1 d_2 + f_2 d_1}$

where the subscripts $_1$ and $_2$ represent different fiber types and

ξ is a constant with a value of 9×10^5

d is fiber denier

ρ is fiber density (g/cc)

f is mass fraction of a fiber in blend ($f_1 + f_2 = 1$)

Chapter 3

MATERIALS, PROCESSING, AND CHARACTERIZATION

§3.1 MATERIALS

Six different staple fibers were used in this study: cotton fiber, ordinary cellulose acetate (OCA) fiber, plasticized cellulose acetate (PCA) fiber, Eastar *Bio*® GP copolyester unicomponent (Eastar) fiber, Eastar bicomponent (Eastar/PP) fiber, and PE/PET bicomponent fiber. The cotton fiber, the carrier fiber, was supplied by Cotton Incorporated, Cary, NC. The scoured and bleached commodity cotton fiber had a moisture content of 5.2%, a micronaire value of 5.4 and an upper-half-mean fiber length of 0.96 inches. Both the OCA and PCA binder fibers were provided by Celanese Corporation, Charlotte, NC, while the Eastar and Eastar/PP bicomponent binder fibers were provided by Eastman Chemical Company, Kingsport, TN. The plasticizer used in PCA binder fiber is triethyl citrate ester ($C_{12}H_{20}O_7$) with a weight concentration around 2%. The PE/PET bicomponent fiber, provided by Kosa, Inc., Charlotte, NC, was selected as the control binder fiber. Both the bicomponent fibers have a sheath/core structure, with PE and Eastar as the sheaths, and PET and PP as the stiffer cores, respectively.

§3.2 PROCESSING

The nonwoven fabrics in this research were produced by first carding the cotton and binder fibers, followed by thermal bonding of the carded webs. The fiber components were prepared by separately opening and then hand mixing the two fiber types for homogeneity. The fiber blend was then carded to form a web using a modified Hollingsworth card with the conventional flats installed at the licker-end of the machine. The resulting carded webs had basis weights of about 40 or 80grams/m^2 (gsm). After carding, water dip-nip treatment was applied to some of the carded webs. Then the treated or untreated webs were thermally point-bonded using a Ramisch Kleinewefers 60cm (23.6inches) wide calender. The embossed roll has a diamond pattern, covering approximately 16.6% of the surface area.

§3.3 DESIGN OF EXPERIMENT

Two blend ratios (75/25, 50/50) and three calendering temperatures (150°C, 170°C, and 190°C) were used for the cotton/cellulose acetate series. Three blend ratios (85/15, 70/30 and 50/50), and two sets of calendering temperatures, (90°C, 100°C, 110°C, and 120°C) and (110°C, 120°C, 130°C, and 140°C) were used for cotton/Eastar(/PP) series and cotton/(PE/PET) series, respectively. All the webs were calendered under the same nip pressure of 0.33MPa at a constant speed of 10m/min. Table 3.1 lists the parameters and their various levels taken up for the study.

Table 3.1 Process parameters and their levels.

Process parameters and their various levels selected for testing			
Cotton/Binder	Process parameters	Number of levels	Levels
Cotton/OCA	Bonding temperature °C	3	150, 170, 190
	Blend ratio (%)	2	75/25, 50/50
Cotton/OCA + water dip-nip	Bonding temperature °C	3	150, 170, 190
	Blend ratio (%)	2	75/25, 50/50
Cotton/OCA + 20% acetone	Bonding temperature °C	3	150, 170, 190
	Blend ratio (%)	2	75/25, 50/50
Cotton/PCA	Bonding temperature °C	3	150, 170, 190
	Blend ratio (%)	2	75/25, 50/50
Cotton/Eastar	Bonding temperature °C	4	90, 100, 110, 120
	Blend ratio (%)	3	85/15, 70/30, 50/50
	Basis weight (g/m^2)	2	40, 80
Cotton/(Eastar/PP)	Bonding temperature °C	4	90, 100, 110, 120
	Blend ratio (%)	3	85/15, 70/30, 50/50
Cotton/(PE/PET)	Bonding temperature °C	4	110, 120, 130, 140
	Blend ratio (%)	3	85/15, 70/30, 50/50

§3.4 CHARACTERIZATION

§3.4.1 Tensile Strength

Tensile properties of single filaments, single bonds, and fabric strips were tested using the United Tensile Test. All the tensile property tests were carried out under the standard atmosphere for testing textiles, with the temperature of 21 ± 1°C and the relative humidity of 65 ± 2%. Strip tests were done according to *ASTM D 5035-95 Standard Test Method for Breaking Force and Elongation of Textile Fabrics (Strip Method)* with a gauge length of 5 inches. Single filament tests were run at 0.5 inches gauge length with an extension speed of 0.5 inches/min. Results from average of 15 tests are reported.

A schematic illustration of the sample preparation of single bond test is shown in Figure 3.1. A strip of size 80mm x 5mm was cut from the web. The strip was cut across the width direction from the two sides to leave only one bond uncut in the middle of the strip. The strip was then subjected to a conventional tensile test. The test was conducted on the United Tensile Tester with a gauge length of 1 inch (2.54cm) and extension rate of 0.5 inches/min (1.27cm/min). A total of twenty tests were done for each sample.

§3.4.2 Thermal Analysis

Thermal analysis was carried out using the Mettler Differential Scanning Calorimeter (DSC), Model DSC-821. Thermal behavior of the binder fibers was determined with a scanning rate of 20°C/min under nitrogen atmosphere. DSC was also used to determine the weight/weight concentration of the binder fiber in the thermally

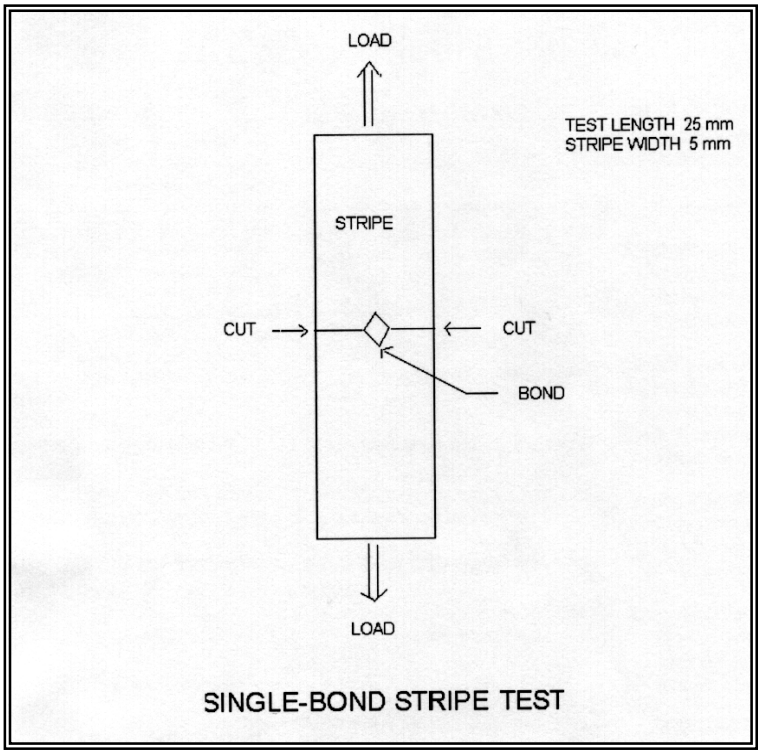

Figure 3.1 Schematic of single bond strip tensile test.

point-bonded cotton/(PE/PET) and cotton/(Eastar/PP) webs. The uniformity of the binder fiber distribution of the carded webs was evaluated by taking several measurements of the specific enthalpy of cooling across the width of the web. Additional details are summarized in the published paper (Appendix).

Temperature calibration was performed using indium with the melting temperature of 156.56°C and heat of fusion (ΔH_f) of 28.54J/g. In order to eliminate the effect of different heat histories of the two binder fibers during processing, the crystallization behavior of one of the binder fiber components was measured. For the cotton and PE/PET binder fiber series, the crystallization behavior of PE was measured. Approximately 5mg samples were first heated under nitrogen atmosphere (at a flow rate of 200ml/min) at 150°C for 10 minutes to make sure the PE component of the binder fiber was fully melted, and then cooled to 50°C at a cooling rate of 10°C/min. For the cotton and Eastar/PP binder fiber series, the crystallization behavior of PP was recorded. Approximately 5mg samples were first heated under a nitrogen atmosphere (at a flow rate of 200ml/min) at 180°C for 10 minutes to make sure the PP component of the binder fiber was fully melted, and then cooled to 50°C at a cooling rate of 10°C/min.

§3.4.3 Basis Weight

Basis weights of the nonwoven fabrics were determined according to *INDA Standard Test 130.1-92 Standard Test Method for the Mass Per Unit Area of Nonwoven Fabrics*.

§3.4.4 Stiffness

Stiffness of the fabrics was determined according to ASTM D 1388 – 64 Standard Test Method. Five 1"×10" specimens were cut along the machine direction for each sample and each test specimen was measured with four readings on each end of both sides. The test result is expressed as flexural rigidity (G), a measure of the interaction between weight and stiffness, G was calculated using the following equation:

$$\mathbf{G = 9.809 \times 10^{-6}\, M\, c^3}\ (\mu N.m) \qquad (3.1)$$

where M is the fabric mass per unit area (g/m^2), and c is the bending length which is calculated as half of the overhang length (mm).

§3.4.5 Scanning Electron Microscopy

Scanning Electron Microscopy (SEM) images were obtained for the bonded fabrics and ruptured specimens using a Hitachi S - 3500 N Scanning Electron Microscope. To avoid the charging problem of the nonconductive fabric samples, back-scattered electrons were used to capture the images. The sample chamber was controlled under low pressure to decrease the charging problem.

§3.4.6 Absorbency

Absorbency of the fabrics was tested using the Sherwood ATS-600 optical Absorbency Testing System (ATS). The instrument was designed for sophisticated

absorption and desorption rate and capacity measurements based on time and the amount of fluid displaced from the fluid reservoir. A directional flow plate and distilled water were used. A "slope" limited test was selected as the mode of operation. Tests were carried out at an absorption slope of 0.005 grams per 5 seconds or 0.005 grams per 20 seconds. When the flow rate drops below the specified setting, the instrument will stop the test and transfer the data to the computer. Absorption, absorption rate and directional flow rate were reported. Three 2" ×2" specimens were cut along the cross direction for each sample. The reported absorption curve is the average among the three specimens.

§3.4.7 Contact Angle

Contact Angle of the single fiber was measured by a Krüss Processor Tensiometer, K121 Dynamic Contact Angle and Adsorption Measuring System. Water was selected as the test liquid. Immersion length was set at 1mm for all the fibers in order to avoid the effect of crimps of the binder fiber. Sensitivity of all the tests was set at 0.0001 gram due to the small cross section area and lightweight of a single fiber. The reported contact angle value is an average of six fibers for each sample.

§3.4.8 Disperse Dyeing

Disperse dyeing was applied to cotton/Eastar webs to qualitatively study the Eastar binder fiber distribution in the webs using a TEXOMAT dyeing machine (AHIBA AG Lalorapparate, Chemie, Textile). The dye solution was prepared in 1-liter volumetric flasks using 50ml Terasil Blue and 50ml Direct Blue. Both of the solutions have a

concentration of 2grams/liter. CIBA-GEIGY Terasil Blue R and CIBA-GEIGY Direct Blue B were used as the solutes, respectively. The cut webs were first wetted with 0.1% solution of Triton X-100. Then 165ml distilled water, 30ml Triton X-100 solution (5%), and 30ml Irgacarrier OSD (5%) were added to the dyeing beaker. The bath temperature was first raised to 110°F. The wet-out webs were entered and run 10 to 20 minutes at 110°F. Add total of 100ml of the predissolved dye solution. The bath temperature was elevated to 212°F and dyed for 30 minutes. A 25ml sodium chloride solution (8%) was added. The bath temperature was then cooled to 170°F for 30 minutes.

Chapter 4

RESULTS AND DISCUSSIONS

§4.1 FIBER PROPERTIES

The physical properties of all the fibers used in this research are listed in Table 4.1. It is worth noticing that the peak extension of Eastar unicomponent (Eastar) fiber is much higher than that of cotton fiber, while the initial modulus of Eastar unicomponent fiber is much lower than that of cotton fiber. This is clearly observed in Figure 4.1, which is the illustration of the load-elongation curves of the selected fibers. It can be seen from Figure 4.1 that Eastar/PP and PE/PET binder fibers have a concave-down shaped curve. Based on Chidambaram's observations [41] these two binder fibers should be better choices when load sharing is considered.

The DSC traces of PCA, PE/PET, Eastar, and Eastar/PP binder fibers are shown in Figure 4.2. It is obvious that the softening temperature of PCA is around 150°C, which is lower compared to that of OCA (which has a softening temperature in the range of 180-205˚C) [3] by adding the plasticizer. A plasticizer is a chemical added to polymers/resins to reduce rigidity and to improve processability by penetrating to the noncrystalline area of the polymer, by breaking the interactive forces between polymer

Table 4.1 Properties of selected fibers (Single filaments).

	Cotton	OCA	PCA	Eastar	Eastar/PP	PE/PET
Filament density (g/cm^3)	1.50	1.3	1.30	1.20	1.10	0.95
Filament denier (denier)	2.20	1.1	2.90	4.00	4.00	3.00
Filament tenacity (g/denier)	1.83	1.2	1.32	1.58	2.18	3.42
Peak load (gram)	4.02	1.3	3.83	6.31	8.73	10.25
Peak extension (%)	7.81	25	50.63	296.06	148.66	62.0
Staple length (inches)	0.96*	1.7	1.80	1.0	1.50	1.50
Crimps (/inch)	***	more	13	Not Measur-able	11	18
Softening temperature (°C)	-	~190	~110	~80	~80**	~110**
Contact angle (°)	31.90	-	43.04	56.75	63.02	85.43

* upper-half-mean fiber length
** softening temperature of sheath
*** cotton has natural convolution

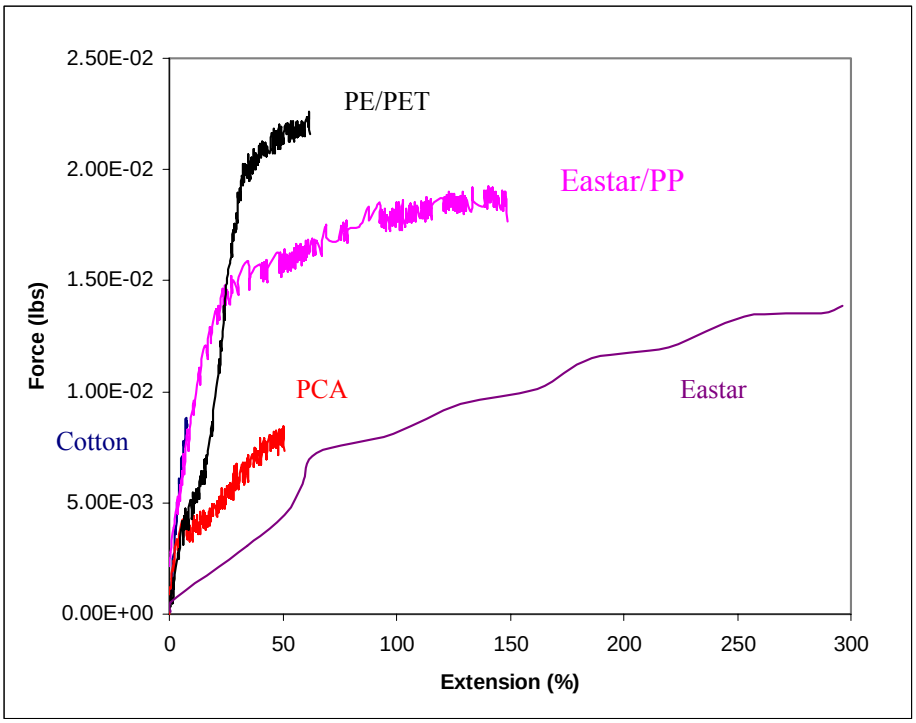

Figure 4.1 Load-elongation curves of selected fibers.

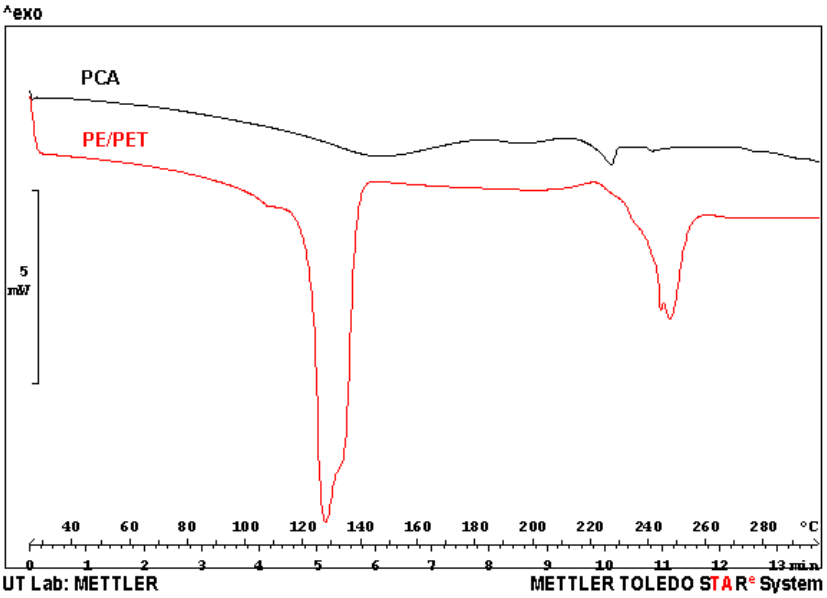

(a) PCA and PE/PET binder fibers

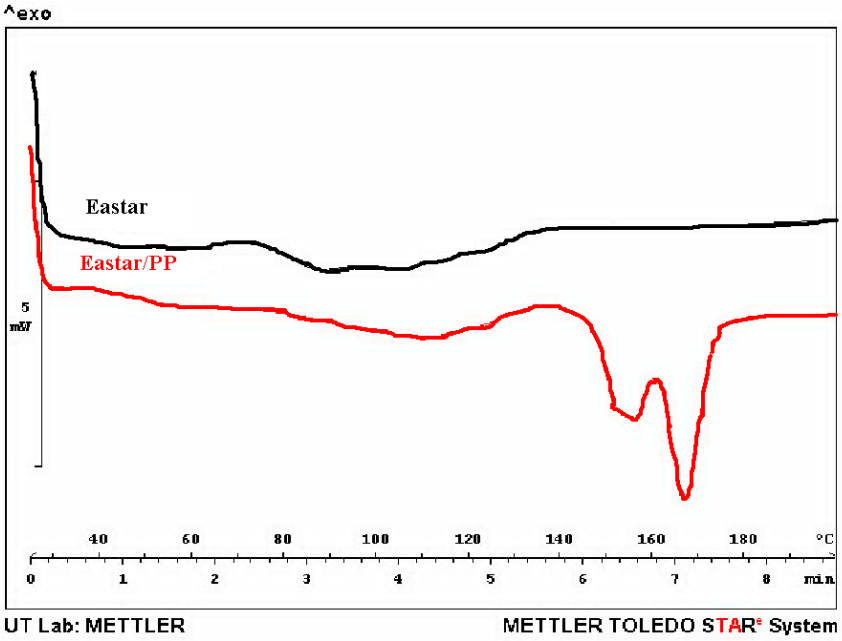

(b) Eastar and Eastar/PP binder fibers

Figure 4.2 Thermal behaviors of the binder fibers.

molecules and by replacing polymer molecule interactions with polymer-plasticizer interactions. The result increases the segmental mobility of the polymer that leads to molecular relaxation, and to lowering the glass transition temperature (T_g) and/or melt temperature (T_m). A strong sharp PE peak is found in the PE/PET binder fiber, indicating the high crystallinity and the relatively uniform crystal sizes of the PE component.

Eastar unicomponent fiber shows a broad melting endotherm around 110°C. The Eastar/PP shows a strong peak for PP, which is broad and double melting and different than typical PP. This is probably due to the crystal size distribution in the PP component. The Eastar component in the bicomponent fiber also shows a broad endotherm.

Surface properties of the binder fibers are important in both web preparation and in subsequent bonding. Binder fibers interact with the fiber network during bonding. The strength of the fabric is affected by the strength of the interface. According to the contact angle values listed in Table 4.1, it seems that Eastar and Eastar/PP binder fibers, which have lower contact angle values, may have better wettability than PE/PET binder fiber. When the contact angle is greater than 90°, it is called "Non-wetting"; while the contact angle is less than 90°, it is called "Wetting". Therefore, the smaller the contact angle the better the wettability.

§4.2 STRUCTURE OF THE BIODEGRADABLE NONWOVENS

§4.2.1 Bonding Structure

Since all the nonwoven fabrics were carded and then thermally point-bonded using the same thermal calendering machine, the bond pattern of all the fabrics are similar with diamond shaped bond points as shown in Figure 4.3. The bond structures at

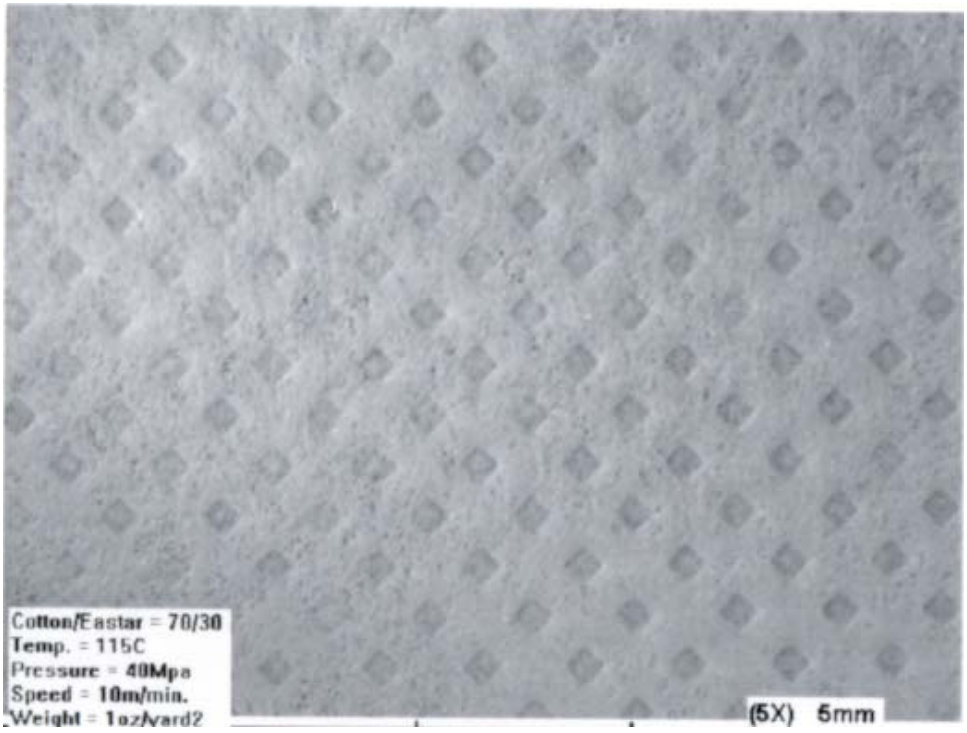

Figure 4.3 Optical micrograph showing the typical bonding pattern of cotton-based nonwovens.

different bonding temperatures and binder fiber contents are illustrated in the following sections.

§4.2.1.1 Effect of bonding temperature

The effect of bonding temperature on the bond structure was observed. Figure 4.4 shows the bond structure of cotton/Eastar nonwovens with the binder fiber content of 30% and basis weight around 80g/m^2. Figure 4.5 shows the bond structure of cotton/(Eastar/PP) nonwovens with the blend ratio of 70/30 and basis weight around 40g/m^2. It is found that with an increase in the bonding temperature, the shape of the bond becomes well-developed and the surface of the bond points becomes smoother. The regular shape of the bond points and smooth surface of the fabrics bonded at high bonding temperature show the well-developed bond structure, as shown in Figure 4.4(b) and Figure 4.5 (b, c). More binder fibers within an embossed region become soft and melt at the higher bonding temperatures. The molten part of the binder fiber acts as the bridge, which adheres the cores of the binder fibers and/or the carrier fibers together. Thus, better adhesion is expected at higher bonding temperatures.

For further analysis of the effect of bonding temperature, the bond points were observed at higher magnifications and the cross sections of the bond points were also studied. Figure 4.6 (a) illustrates part of the bond point at higher magnification (x 500) for cotton/(PE/PET) at a blend ration of 70/30. The fluffy transparent top layer is the PE sheath that melted and bonded the carrier fibers and/or the PET cores together, showing the good adhesion between the binder fibers and the carrier fibers, and between the

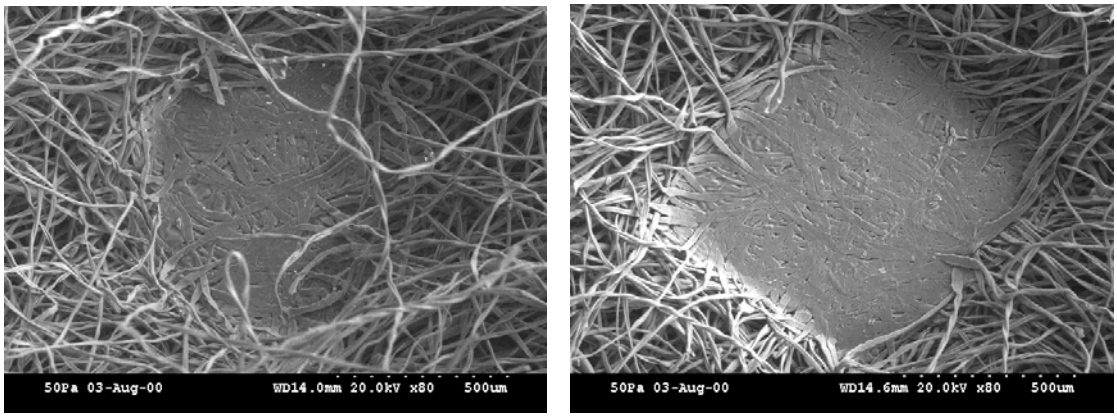

(a) Bonding temperature = 100°C (b) Bonding temperature = 120°C

Figure 4.4 Bond points for cotton/Eastar=70/30 with basis weight of 80gsm.

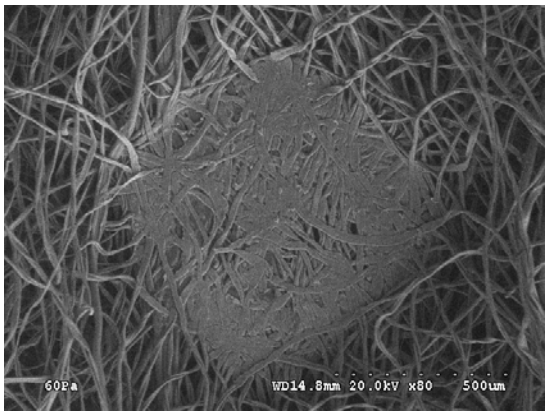

(a) Bonding temperature = 100°C

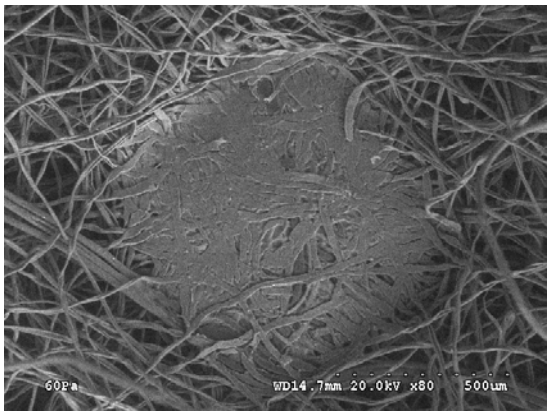

(b) Bonding temperature = 110°C

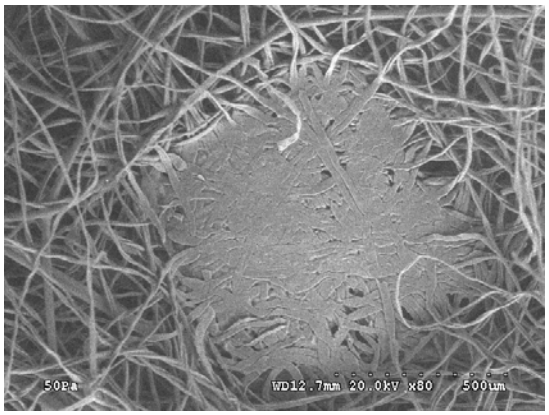

(c) Bonding temperature = 120°C

Figure 4.5 Bond points for cotton/(Eastar/PP)=70/30 with basis weight of 40gsm.

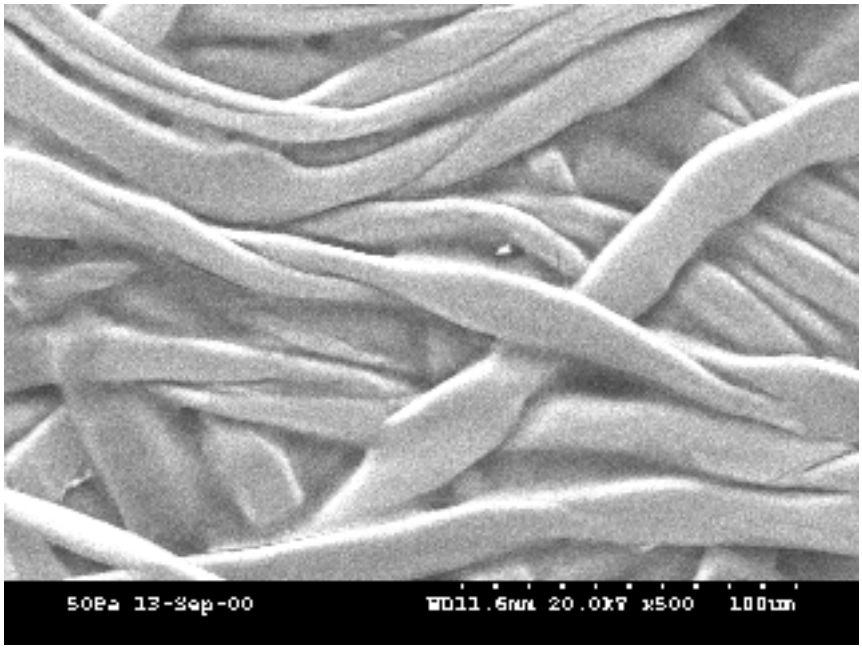

(a) Cotton/(PE/PET) = 70/30 web, bonded at 130°C

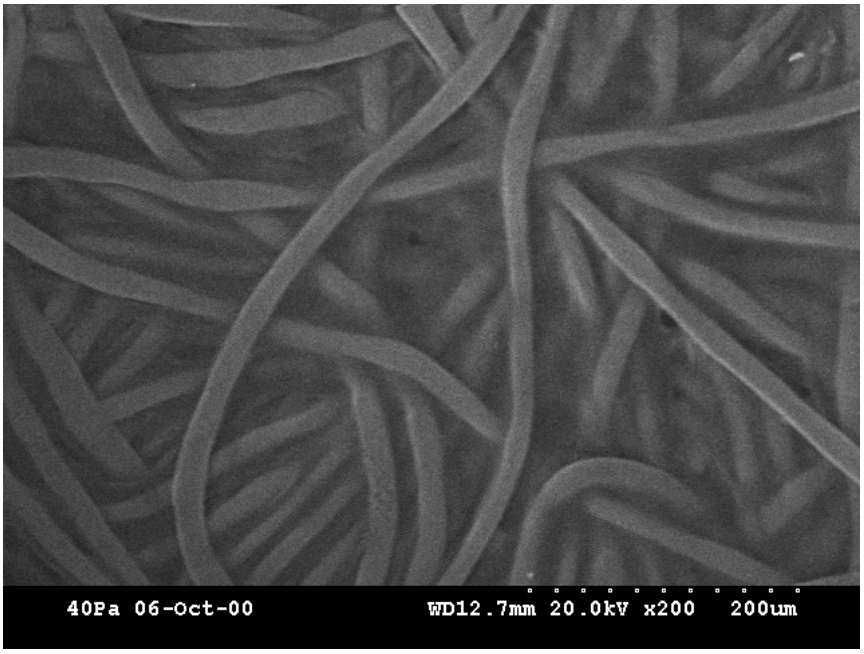

(b) 100% PE/PET web, bonded at 120°C

Figure 4.6 Adhesion at the bond point (40gsm).

binder fibers themselves at the bond points. The fibers at the bond points were deformed during the thermal calendering process; thus, it is hard to differentiate between the binder fiber cores and the carrier cotton fibers. The good adhesion among binder fibers themselves and the deformed binder fiber cores can be seen from Figure 4.6 (b) from the bond point of the web made of 100% binder fibers. The cross-sections of the bond points for cotton/(Eastar/PP) webs with a binder fiber content of 50%, but bonded at different temperatures of 100°C are 120°C, are shown in Figure 4.7. It is apparent that the melted Eastar binder fiber sheath penetrated into the carrier fiber networks and bonded the carrier fibers and the cores of the binder fibers together to form a well-developed bond structure. Also, it was observed that the cores of the binder fibers were deformed from round to oval shape by the thermal bonding process.

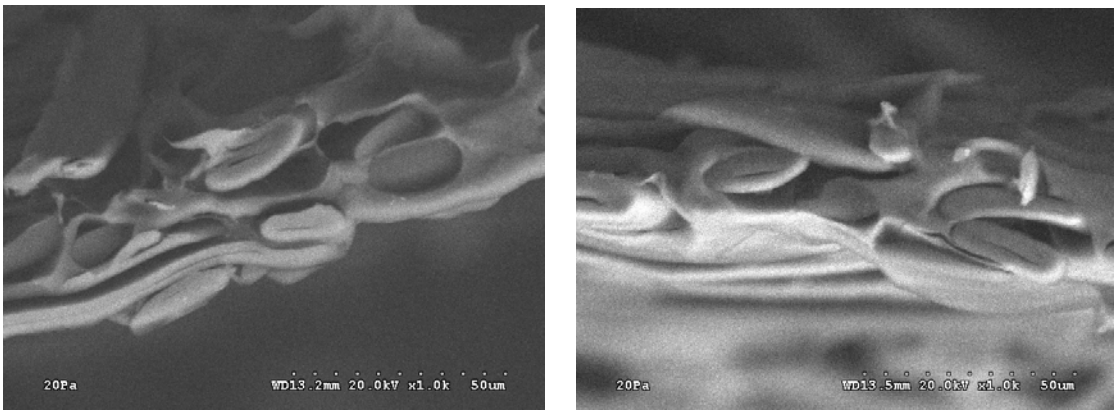

(a) Bonding temperature = 100°C (b) Bonding temperature = 110°C

Figure 4.7 Cross-sections of bond points for cotton/(Eastar/PP)=50/50 webs (40gsm).

§4.2.1.2 Effect of binder fiber content

The effect of the binder fiber content on the bond structure was also investigated. Figure 4.8 shows the bond structure of cotton/(Eastar/PP) nonwovens, which have a basis weight around 40g/m^2 and bonded at 100°C. It is clear that when the bonding temperature is sufficient, the shape of the bond becomes well-developed and the bond point becomes more film like with the increase in the binder fiber content. The reason is that more binder fibers are involved in the bonding with the increase of the binder fiber content, leading to the increases in the number of bond points and the effective bond areas. That is, there is more binder fiber melt in a single bond point.

§4.2.2 Failure Analysis

The fracture structures of cotton/Eastar, cotton/(Eastar/PP), and cotton/(PE/PET), with 50% binder fiber content and thermally bonded at different temperatures, are shown in Figure 4.9 – 4.11. It is found that the fractures for cotton/Eastar webs are generally brittle. This may result from the weak bonds caused by the non-uniform Eastar binder fiber distribution, which is discussed in section 4.3.3 and the different tensile properties of Eastar and cotton fibers. Eastar fiber has very high elongation (is 295%) compared to cotton (is 8%), which may lead to inhomogeneous load-sharing during the failure. The fractures of cotton/(Eastar/PP) webs is not as brittle as those of cotton/Eastar webs; however, the webs are not as ductile as that of cotton/(PE/PET) webs, indicating better load sharing in the later fabrics. According to Chidambaram's finding [41], fibers with a concave-down stress-strain curves are better for thermally bonded nonwovens when

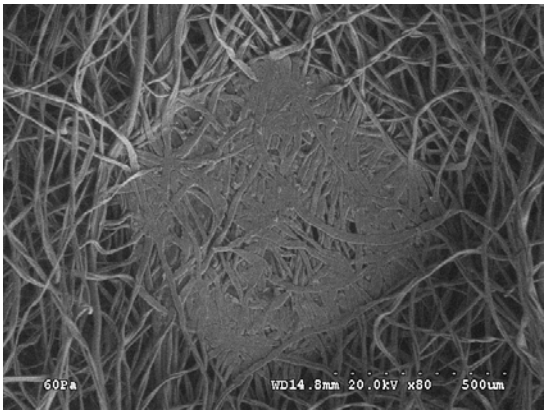

(a) Eastar/PP = 30%

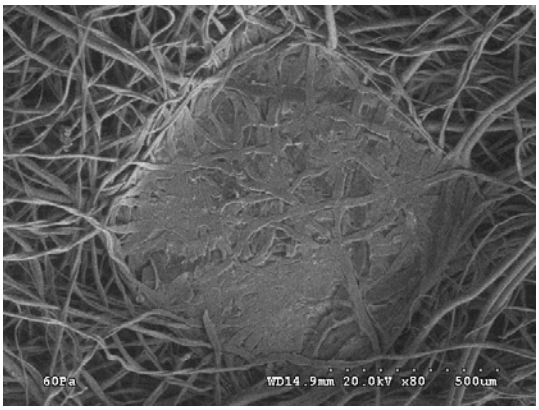

(b) Eastar/PP = 50%

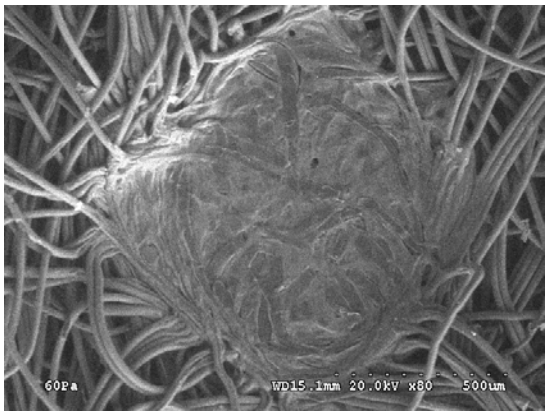

(c) Eastar/PP = 100%

Figure 4.8 Bond points for cotton/(Eastar/PP), bonded at 100°C (40gsm).

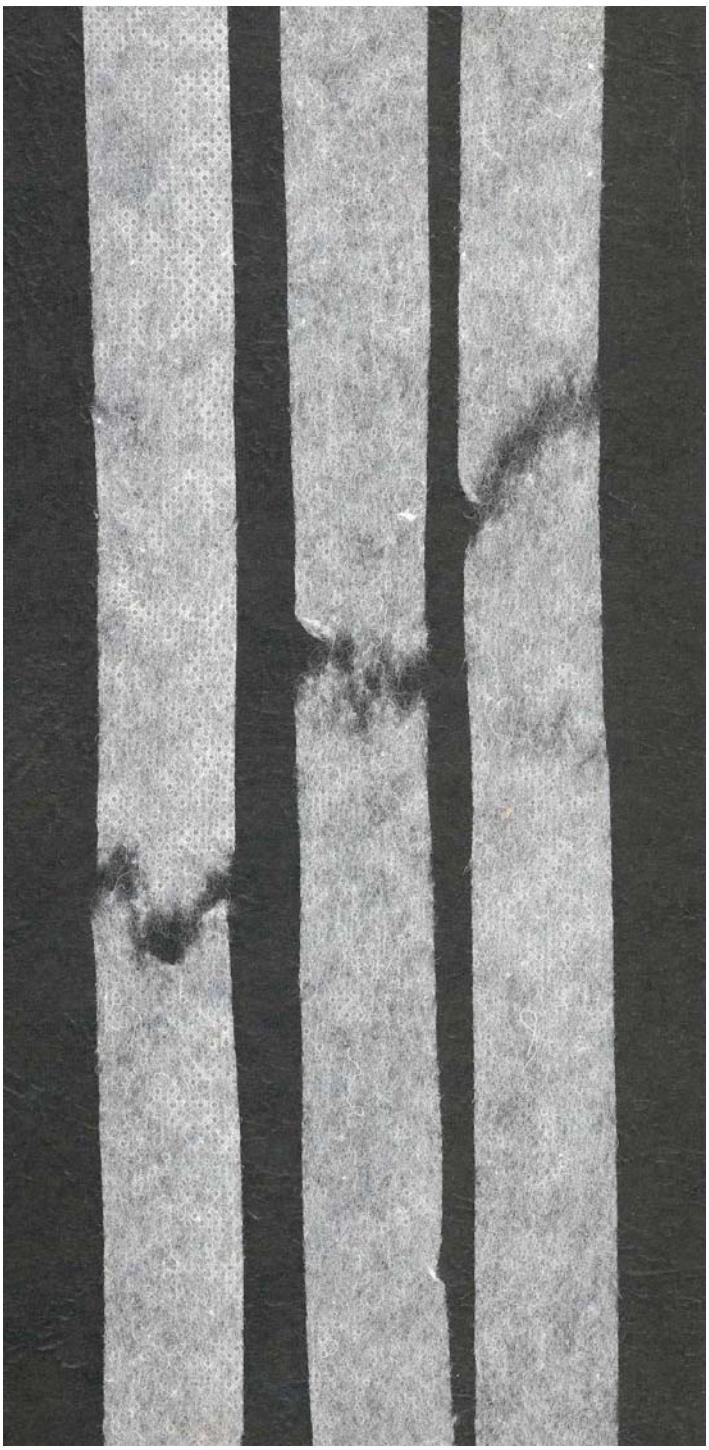

(a) bonded at 100°C (b) bonded at 110°C (c) bonded at 120°C

Figure 4.9 Fracture of cotton/Eastar fabrics after tensile test (40gsm).

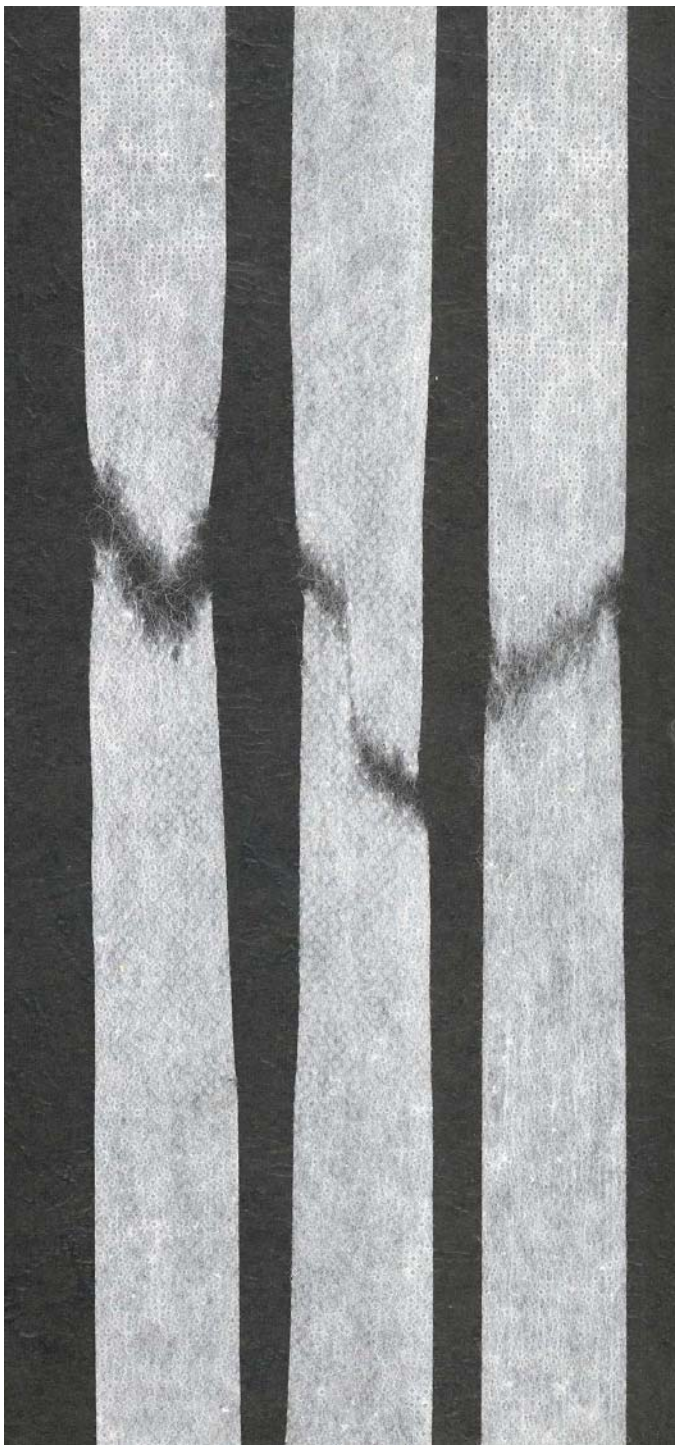

(a) bonded at 100°C (b) bonded at 110°C (c) bonded at 120°C

Figure 4.10 Fracture of cotton/(Eastar/PP) fabrics after tensile test (40gsm).

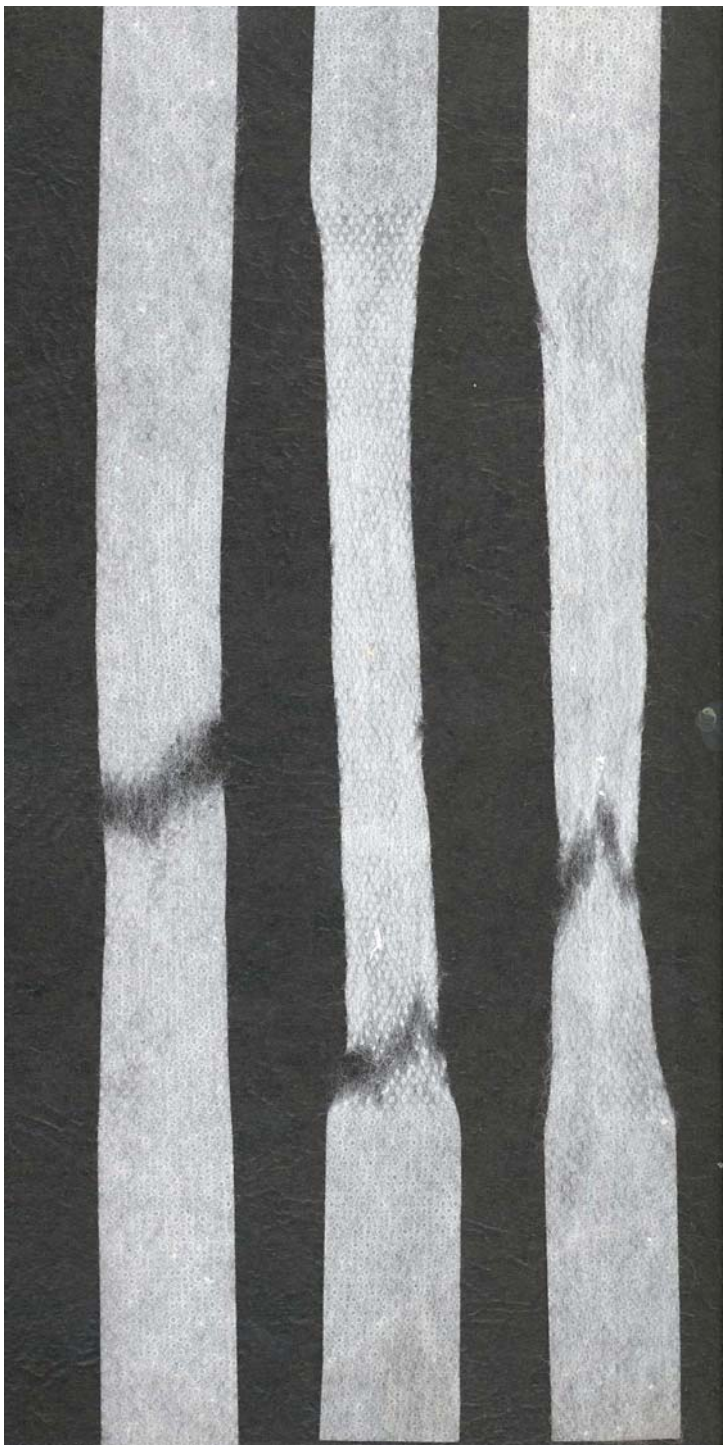

(a) bonded at 120°C (b) bonded at 130°C (c) bonded at 140°C

Figure 4.11 Fracture of cotton/(PE/PET) fabrics after tensile test (40gsm).

load sharing is considered important. Our observation is consistent with his finding. Both Eastar/PP and PE/PET binder fibers have prominent concave-down stress-strain curves as shown in Figure 4.1. As a result, these fabrics stretch a lot more before failure (details in section 4.4), with a ductile failure mechanism.

Failure of nonwoven fabrics can occur by fiber breakage, binder breakage or cohesive failure or at the fiber-binder bonding interface, or by a combination of these modes. The interaction of component properties, structures, and fabric deformation mechanisms can lead to a variety of unique failure mechanisms for nonwoven fabrics. The nonwoven fabric failure mechanism is influenced by the fiber physical properties, binder properties, and structural properties including the relative frequency and structure of the bonding elements, fiber orientation, and the degree of liberty of movement of the fibers between the bond points.

In order to analyze the failure mechanism, the failure structures of nonwoven fabrics were observed. Figure 4.12 shows the failure structures of cotton/Eastar high basis weight webs, around 80g/m^2. Both the fabrics were bonded at a high temperature of 120°C but with different binder fractions. The failure mechanism of the fabric of a lower binder fiber content of 30% (Figure 4.12(a)) is observed to be the loss of interfacial adhesion at the bond site leading to the bond disintegration. The failure mechanism of the fabric of a higher binder fiber content of 50% as shown in Figure 4.12(b) is the result of the cohesive failure of the fibers in the bond point and/or near the bond periphery due to the loss of fiber integrity and formation of film-like spots at high temperatures, as well as the reduction in load transfer from fibers to film [43, 44].

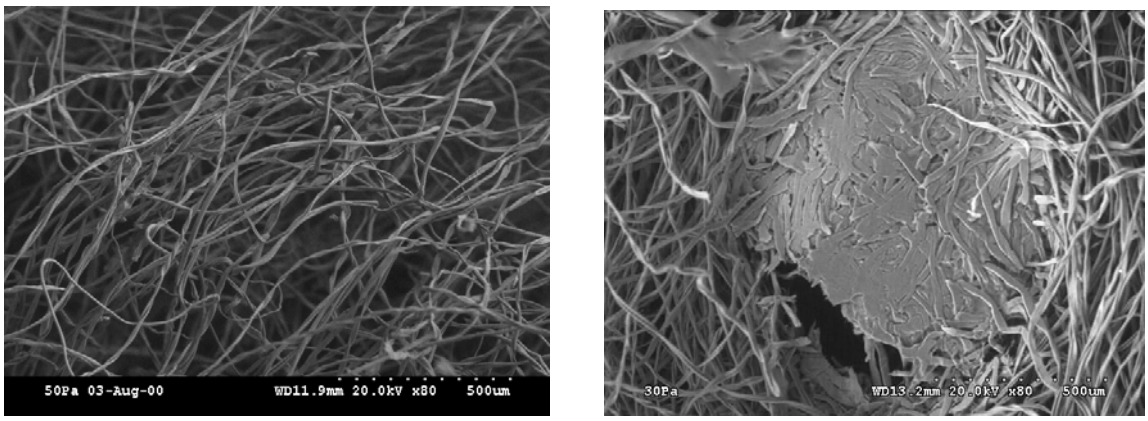

(a) Cotton/Eastar = 70/30 (b) Cotton/Eastar = 50/50

Figure 4.12 Failure structures of cotton/Eastar webs bonded at 120°C (80gsm).

Similar observations can be found for webs at the same binder fiber fraction but different bonding temperatures. Figure 4.13 shows the failure structures of cotton/(Eastar/PP) low basis weight webs, around 40g/m^2. Both the fabrics have the same binder content of 30% but bonded at different temperatures. The failure mechanism of the fabric bonded at a lower bonding temperature of 100°C as shown in Figure 4.13(a) was found to be the loss of interfacial adhesion at the bond site leading to bond disintegration. On the other hand, the failure mechanism of the fabric bonded at a higher bonding temperature of 120°C as shown in Figure 4.13(b) is the result of the cohesive failure of the fibers in the bond point and/or near the bond periphery. These observations are consistent with those of Gibson and McGill [45], who studied the failure mechanism of thermal point-bonded polyester nonwovens as a function of the bonding temperature.

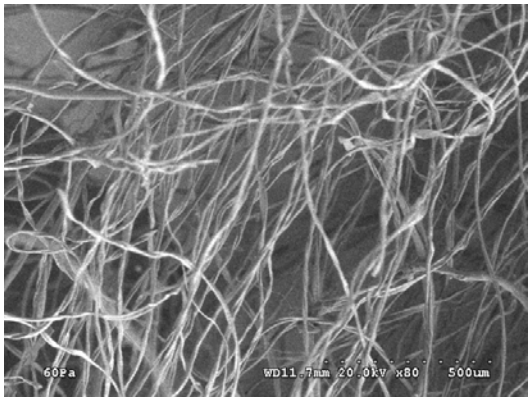

(a) Bonded at 100°C

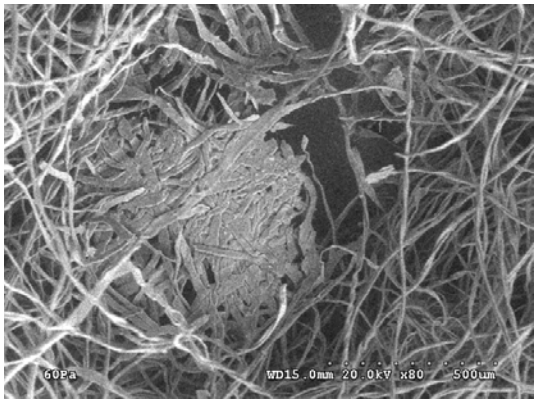

(b) Bonded at 120°C

Figure 4.13 Failure structures of cotton/(Eastar/PP)=70/30 webs after tensile test (40gsm).

§4.2.3 Binder Fiber Distribution

§4.2.3.1 Qualitative Description

4.2.3.1.1 Cotton/Eastar low basis weight webs

Carding is the basic process in the production of nonwoven fabrics. One shortcoming of the carding process is that the carded webs always have areal irregularities of mass distribution caused by machine variables, fiber properties and area irregularities of the fed fiber matt [22]. Besides, there is always some weight loss during the carding process. This fiber loss may be caused by flying fibers and by sticking of fibers on the cleaning rollers. Or as a result of the selected carrier and/or binder fiber distribution. Longer fibers are picked up with higher probability than the shorter ones, due to some fibers sticking on the metal wires and/or collected by the cleaning roller.

Large weight loss was observed in the carding process for cotton/Eastar webs with a basis weight around 40g/m^2, as shown in Table 4.2. It was found that the weight losses are relatively high for all the three binder contents. For the web with a binder fiber content of 50%, the weight loss was as high as 44%. The weight loss during carding increases with the increase of Eastar binder fiber content. This indicates that Eastar binder fiber is not suited for the carding process. Several factors may affect the resulting carded webs. From the point of the fiber properties, the influential factors may be staple length, crimps, fiber stiffness, spin finishes applied to the fibers, fiber surface roughness, fiber tensile properties, and fiber crystallinity and orientation. From the point of carding machines, both settings of the carding elements and conditions of the card clothing may have an effect.

Table 4.2 Weight loss during carding for cotton/Eastar webs.

Blend ratio	Basis weight	Weight loss
Cotton/Eastar = 85/15	40g/m^2	23.5%
Cotton/Eastar = 70/30	40g/m^2	33.4%
Cotton/Eastar = 50/50	40g/m^2	44.0%

According to Table 4.1, Eastar binder fiber has lower staple length, hardly any crimps, and high peak extension. All these factors may be responsible for the poor carding processability. Disperse dyeing was used to further observe Eastar binder fiber distribution in the carded webs. It was also observed that the Eastar binder fibers are not uniformly distributed in the webs, as shown in Figure 4.14. The white areas indicate that there is no binder fiber there, while the blue lines indicate the existence of Eastar fiber bundles.

4.2.3.1.2 Cotton/Eastar high basis weight webs

High basis weight cotton/Eastar webs were produced to reduce the weight loss during the carding process. However, high weight loss was also observed in the carding for the high basis weight cotton/Eastar webs, as shown in Table 4.3, although the weight loss was lower compared with the low basis weight cotton/Eastar webs (Table 4.2). The pictures of high basis weight webs after disperse dyeing (Figure 4.15) show that the cotton/Eastar webs are not uniform in binder fibers distribution. Bundles of binder fibers

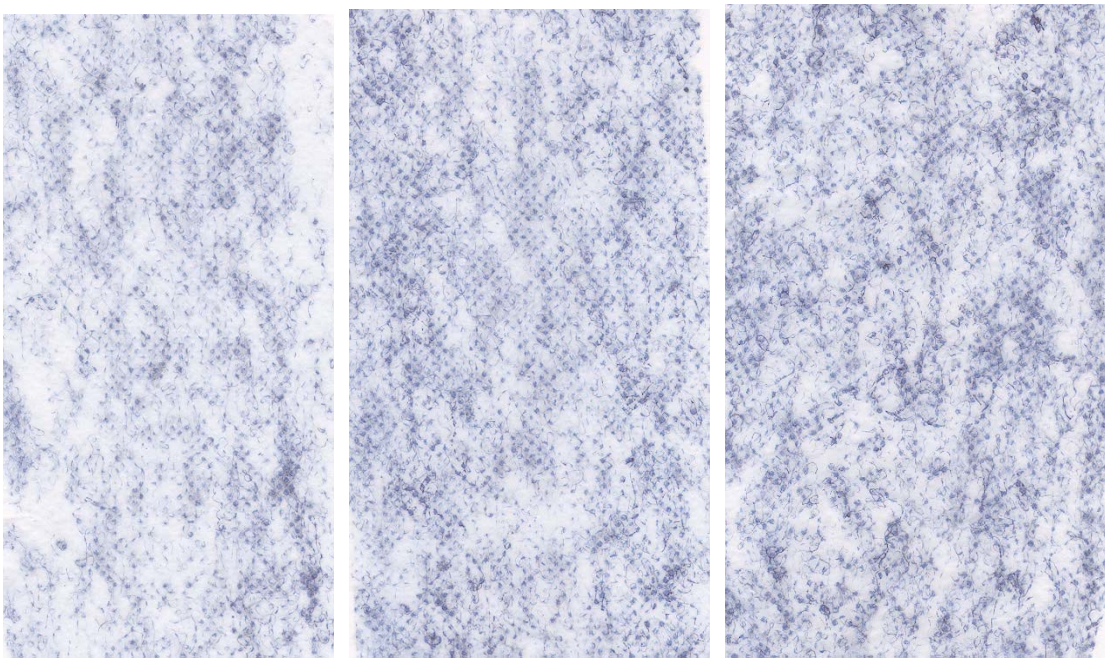

(a) 15% Eastar (b) 30% Eastar (c) 50% Eastar

Figure 4.14 Binder fiber distribution in low basis weight cotton/Eastar webs (40gsm).

Table 4.3 Weight loss during carding for high basis weight cotton/Eastar webs.

Blend ratio	Basis weight	Weight loss
Cotton/Eastar = 85/15	80g/m^2	18.1%
Cotton/Eastar = 70/30	80g/m^2	24.9%
Cotton/Eastar = 50/50	80g/m^2	32.3%

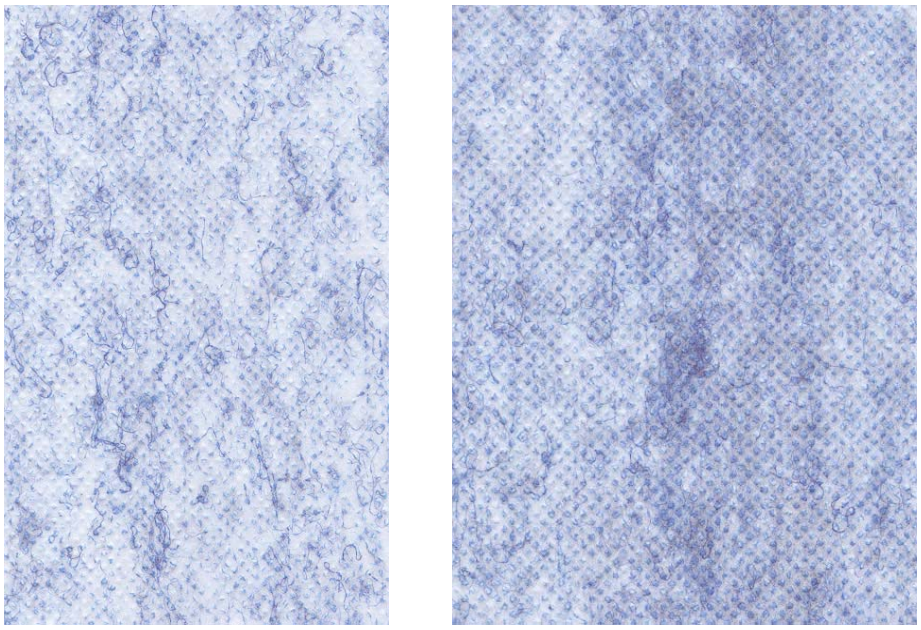

(a) 15% Eastar (b) 30% Eastar

Figure 4.15 Binder fiber distribution in high basis weight cotton/Eastar webs (80gsm).

can be seen from these pictures. These bundles of the binder filaments can be seen more clearly by SEM pictures, as shown in Figure 4.16. The round circular shaped fibers in the fiber bundles are Eastar binder fibers and the ribbon like structure is that of cotton fibers. Again, the results indicate that Eastar fiber is not suitable for the carding process.

As we know, stiffer fibers are preferred for the carding process. One disadvantage in using Eastar unicomponent as-spun fiber in the carding process is that it is hard to get the binder fibers well-distributed due to the high elasticity (high peak extension of 296% as shown in Table 4.1) and low crimps of the binder fiber, thereby leading to low tensile properties of the final nonwoven fabrics.

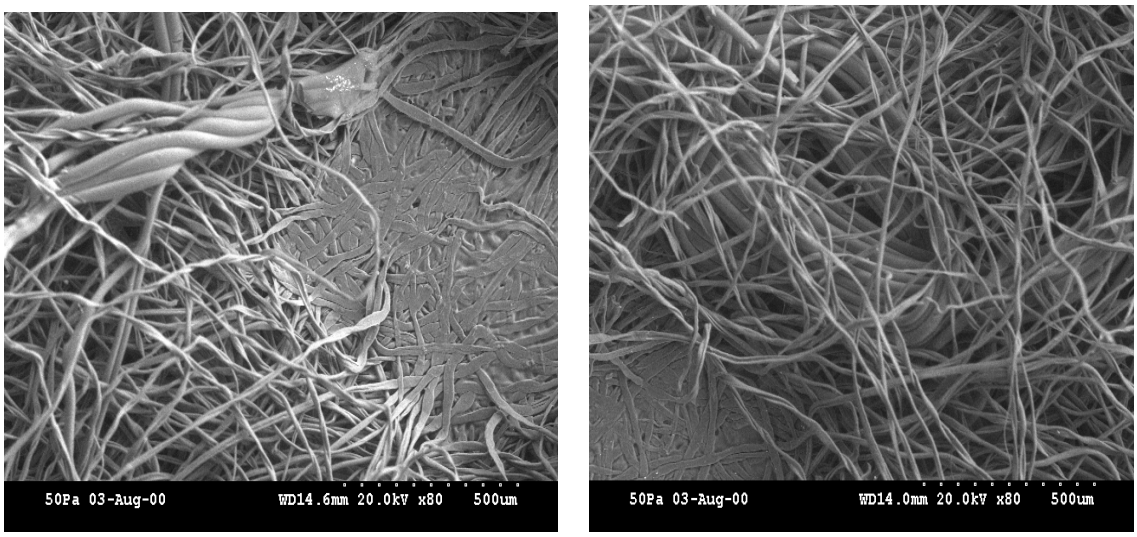

Figure 4.16 Binder fiber distribution in high basis weight cotton/Eastar=70/30 webs (80gsm).

4.2.3.1.3 Cotton/(Eastar/PP) low basis weight webs

Eastar/PP bicomponent fiber with Eastar *Bio*® GP copolyester as the sheath and polypropylene as the stiffer core was further selected as the binder fiber instead of Eastar unicomponent fiber to improve the stiffness of the fiber. This bicomponent binder fiber has higher tenacity, higher crimp, higher staple length, and lower peak extension compared to Eastar homopolymer binder fiber (Table 4.1). These properties are preferred for the carding process. Distribution of Eastar/PP binder fibers in the resulting webs was also observed under SEM. The round shape fiber is Eastar/PP binder fiber and the ribbon like structure denotes cotton fibers. It can be seen that the binder fibers are well-distributed in the webs, as shown in Figure 4.17.

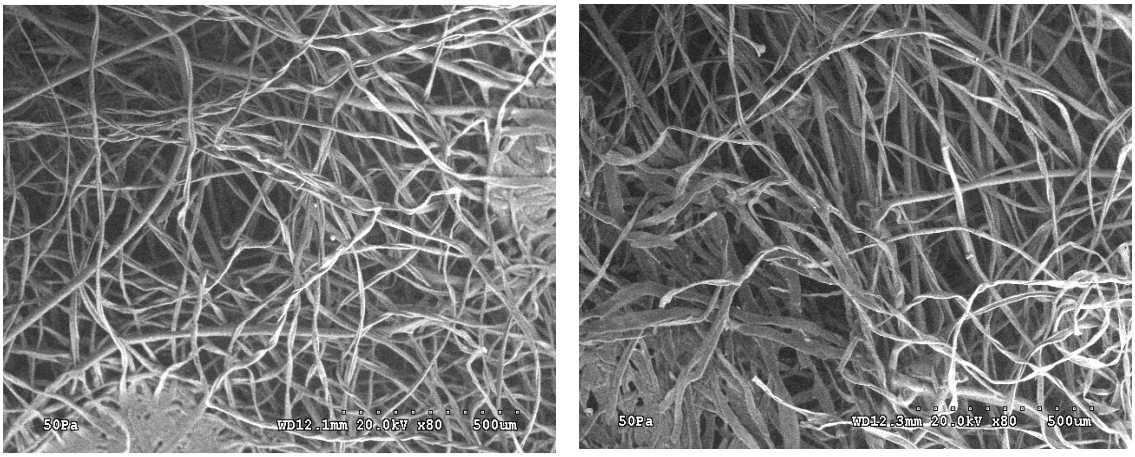

(a) Cotton/(Eastar/PP) = 70/30 (b) Cotton/(Eastar/PP) = 50/50

Figure 4.17 Binder fiber distribution in low basis weight cotton/(Easter/PP) webs (40gsm).

4.2.3.1.4 Cotton/(PE/PET) low basis weight webs

The binder fiber distribution in the control fabric was also observed under SEM. Figure 4.18 shows that PE/PET binder fiber is distributed more uniformly in the web. The round circular shapes are the PE/PET binder fibers, while the ribbon like fibers are cotton fibers. This is the combined result of the high crimps, high strength, and low elongation of the PE/PET binder fiber.

§4.2.3.2 Quantitative Description

Although the binder fiber distribution can be qualitatively determined by either dyeing the binder fibers and observing the fabrics under microscopy, or by observing the different shape of the binder fibers under scanning electronic microscopy (SEM), there is almost no reporting of a practical method that can be used to quantitatively characterize

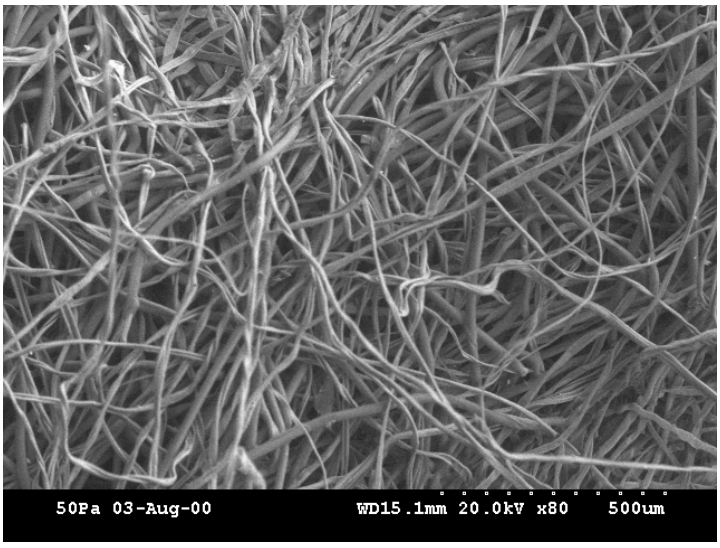

Figure 4.18 Binder fiber distribution in cotton/(PE/PET)=70/30 web (40gsm).

the binder fiber distribution of the webs. Differential scanning calorimetry (DSC) can be used to measure the heat flow to and from the sample as a function of temperature. Various material characteristics can be determined from these data, including oxidative stability, purity, and polymorphism. Chemical reactions, melting behavior, and the temperature evolution of the specific heat can also be investigated [61-63]. DSC was used to determine the weight/weight concentration of the binder fiber in the thermally point-bonded carded cotton/(Eastar/PP) and cotton/(PE/PET) webs. Thus, the uniformity of the binder fiber distribution of the carded webs was evaluated by taking several measurements of specific enthalpy of cooling across the width of the web.

The weight/weight concentration of the samples was obtained by calculating the ratio of the specific enthalpy of cooling for a certain web to the specific enthalpy of cooling for 100% binder fiber.

4.2.3.2.1 Evaluation Of DSC Characterization Method

To evaluate the accuracy and reliability of DSC measurement, first binder fiber and cotton fiber were manually blended at different weight percentages of 100%, 50%, 40%, 30%, 20%, and 10%. Each of the concentrations was studied at least three times under the same conditions so that the standard deviation (σ) and the coefficient of variation (C.V.) could be obtained. Figure 4.19 (a, b) illustrate the DSC traces of 100% contents of the two binder fibers, while Figure 4.20 (a, b) show the DSC traces of the blends at different binder fiber contents.

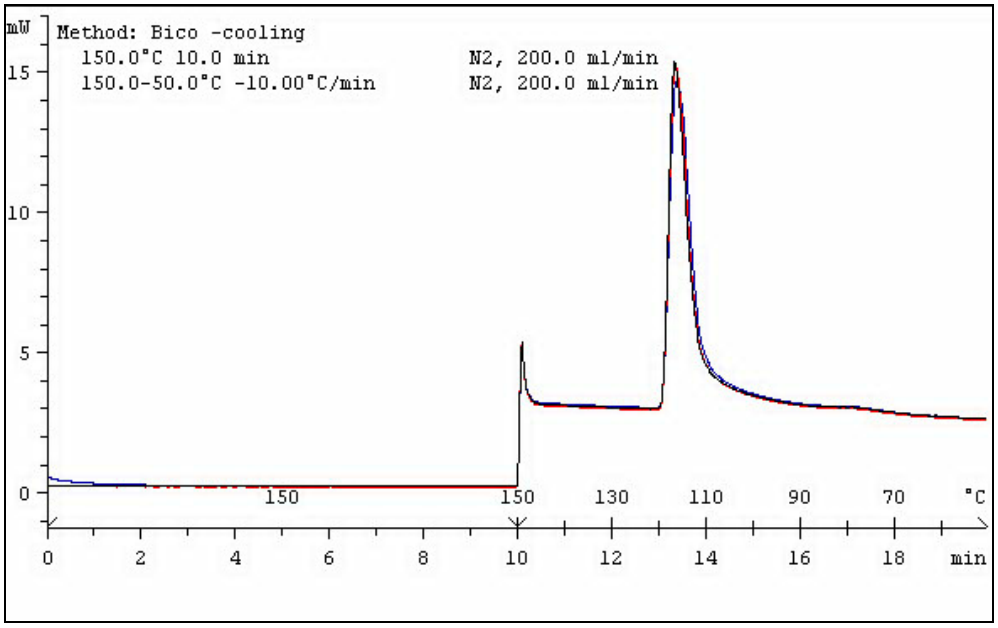

(a) PE/PET binder fiber

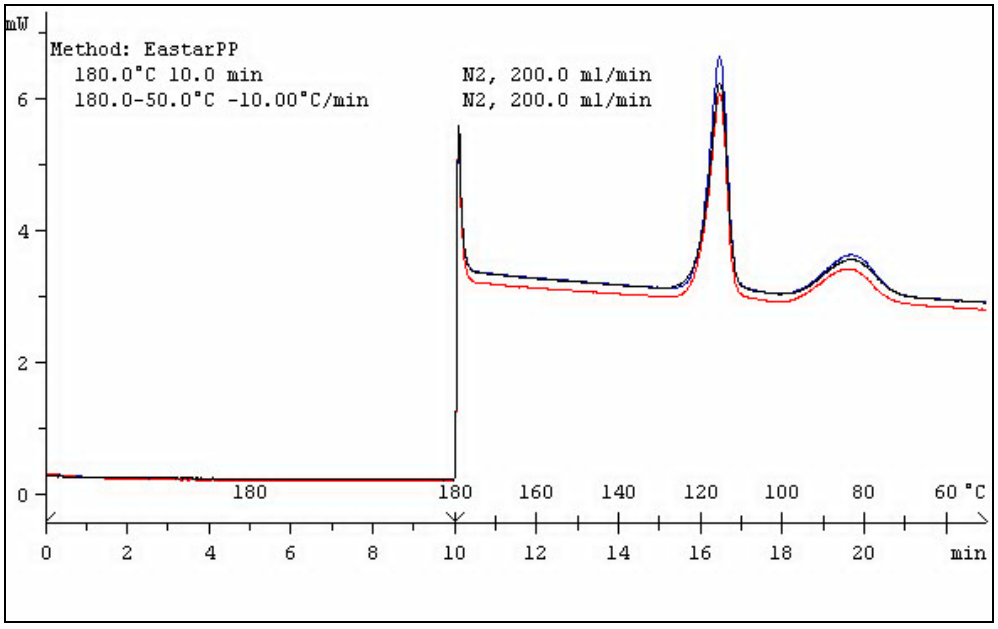

(b) Eastar/PP binder fiber

Figure 4.19 DSC traces of 100% binder fibers.

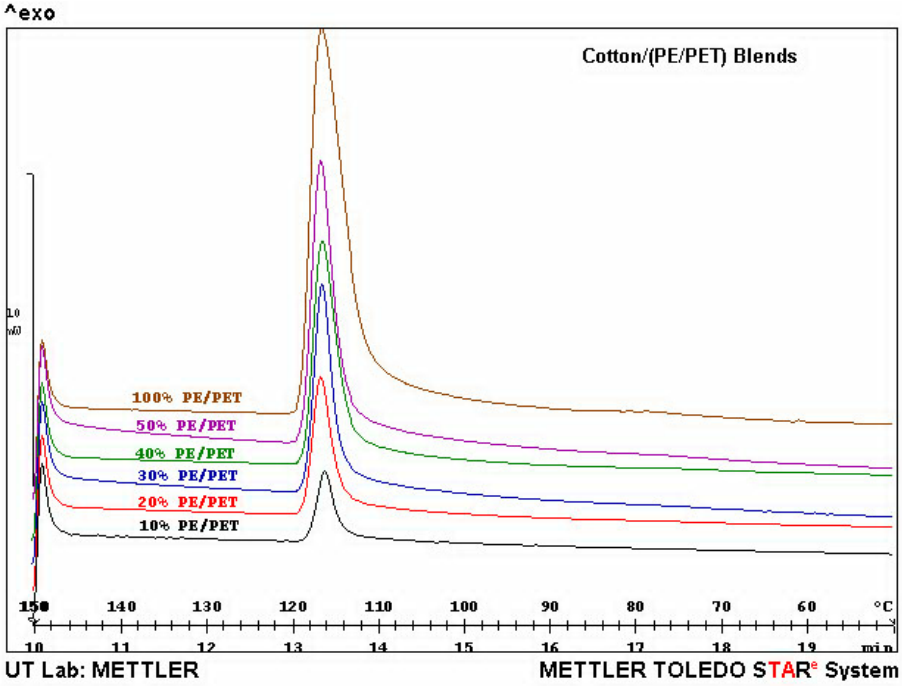

(a) Cotton/(PE/PET) Blends

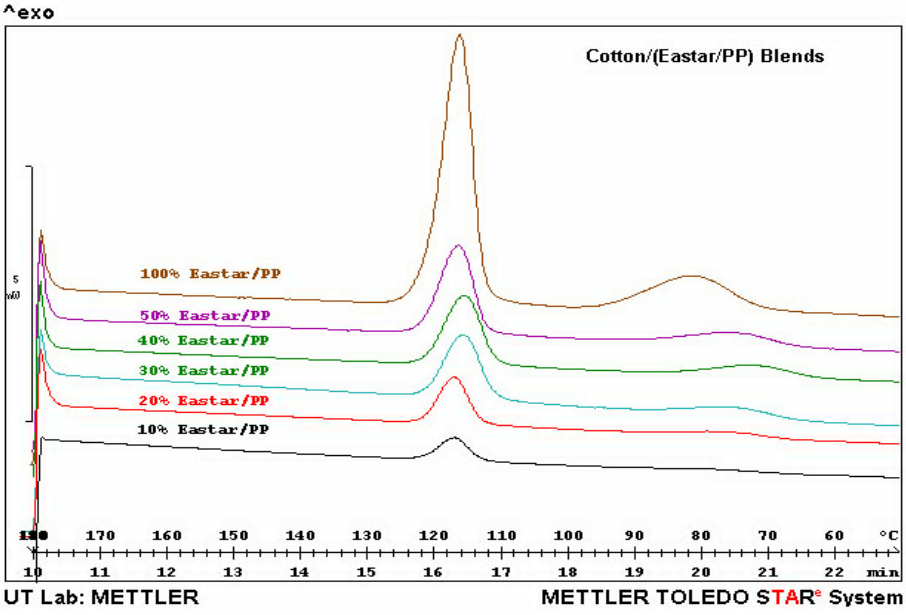

(b) Cotton/(Eastar/PP) Blends

Figure 4.20 DSC traces of the blends.

The specific heat (ΔH/g) for the samples with 100% binder fibers were considered here as "Actual" as well as "Observed" for the evaluation. Subsequently, the "Observed" specific heat for the other contents was calculated by the areas under the DSC exothermic peaks. Any error that occurred would be overcome by the conversion factor of gram (1000mg), because the sample was taken at the milligram level for the DSC study. Then the "Observed" weight/weight concentration of the samples was obtained by calculating the ratio of the specific heat at certain content with the specific heat for 100 % binder fiber. Parameters obtained from the DSC measurements for the two different binder fiber series are summarized in Tables 4.4 and 4.5.

Since PE is the only component melted and crystallized during the measurement of cotton/(PE/PET) blends, there is no obvious effect of the cotton component on the crystallization behavior of PE. This can be verified by the near constant onset crystallization temperatures and the peak crystallization temperatures under different PE/PET contents (Table 4.4). In the case of cotton/(Eastar/PP) blends where both the components (Eastar and PP) in the binder fiber melted and crystallized, the presence of Eastar component does not affect on the primary nucleation and crystallization of the PP component, since the onset and peak crystallization temperatures of PP are almost stable for different Eastar/PP contents of cotton/(Eastar/PP) blends as shown by the data in Table 4.5. Therefore, there is no miscibility problem for both the blend series. According to the data in Tables 4.4 and 4.5, the "observed" binder fiber contents fit well with the "actual" binder fiber contents, with a variation of ± 1%.

Table 4.4 Parameters obtained from DSC for cotton/(PE/PET) blends.

"Actual" PE/PET (%)	$T_{o,c}=T_c$ (°C)	$T_{p,c}$ (°C)	ΔH_c (J/g)	Ave. ΔH_c (J/g)	σ (ΔH_c)	C.V.	Observed PE/PET (%)
100	119.17	116.75	89.49	90.20	2.241	0.025	100
	119.14	117.11	92.71				
	119.15	117.28	88.40				
50	118.93	117.32	44.46	44.23	0.854	0.019	49.04
	119.04	117.30	43.28				
	118.93	117.26	44.94				
40	118.95	117.23	36.89	35.80	1.047	0.029	39.69
	118.71	117.06	34.80				
	118.73	117.05	35.72				
30	118.64	117.06	26.50	26.31	0.219	0.008	29.17
	118.69	117.05	26.07				
	118.55	117.04	26.36				
20	118.66	116.96	17.66	17.42	0.216	0.012	19.31
	118.78	117.12	17.24				
	118.69	116.39	17.36				
10	118.26	116.53	8.38	8.31	0.110	0.013	9.21
	118.08	116.18	8.36				
	118.29	116.39	8.18				

Note: "T" is temperature, "c" is cooling or crystallizing, "o" is onset, "p" is peak, "ΔH_c" is the specific enthalpy for PE exothermic peak.

Table 4.5 Parameters obtained from DSC for cotton/(Eastar/PP) blends.

Actual Eastar/PP (%)	$T_{o,c}=T_c$ (°C)	$T_{p,c}$ (°C)	ΔH_c (J/g)	Ave. ΔH_c (J/g)	σ (ΔH_c)	C.V.	Observed Eastar/PP (%)
100	121.69	116.68	28.09	27.95	0.997	0.036	100
	122.77	117.10	26.89				
	122.10	116.61	28.87				
50	123.28	117.86	13.20	13.69	0.595	0.043	48.98
	122.41	117.03	13.51				
	122.07	116.67	14.35				
40	121.81	116.68	11.39	11.15	0.490	0.044	39.89
	121.67	115.83	10.59				
	121.57	115.82	11.48				
30	121.51	116.00	8.34	8.33	0.38	0.046	29.79
	121.77	116.83	7.94				
	122.15	117.32	8.70				
20	121.83	117.30	6.13	5.70	0.373	0.065	20.39
	122.55	117.46	5.54				
	122.79	117.62	5.44				
10	121.93	117.18	2.66	2.81	0.216	0.077	10.05
	120.47	115.44	3.06				
	121.71	116.76	2.72				

Note: "T" is temperature, "c" is cooling or crystallizing, "o" is onset, "p" is peak, "ΔH_c" is the specific enthalpy for PP exothermic peak.

The DSC measured specific enthalpy (ΔH_c) versus binder fiber weight concentration for the two binder fiber series are plotted in Figure 4.21(a) and 4.21(b), respectively. The regression lines fit both the binder fibers almost perfectly, with regression coefficients of 0.99997 and 0.99987 for PE/PET binder fiber and Eastar/PP binder fiber, respectively. Based on this analysis, it is clear that DSC specific enthalpy from crystallization of one of the binder fiber components in the cotton/binder blend series can be used to estimate binder fiber content in the samples.

4.2.3.2.3 Binder Fiber Distribution Of Carded Nonwovens

In order to describe the binder distribution in the webs, five different positions across the webs were selected as shown in Figure 4.22 at each binder content/composition. Parameters obtained from the DSC measurements for the two different carded nonwoven fabric series are summarized in Tables 4.6 and 4.7. Although the "observed" average binder fiber content is close to the "actual" binder fiber content along cross direction for both the nonwoven series, high variation and C.V. of the binder fiber contents existed in some of the webs for both the carded nonwoven series as shown in Figure 4.23 (a, b). Therefore, we can say that binder fibers were not well-distributed in those nonwoven fabrics. Apparently, the variation is much higher for nonwovens of the lower(est) binder fiber contents.

Since high variation and C.V. of the binder fiber contents existed in both of the carded nonwoven series according to DSC measurement results, we can conclude that binder fibers were poorly distributed in the webs.

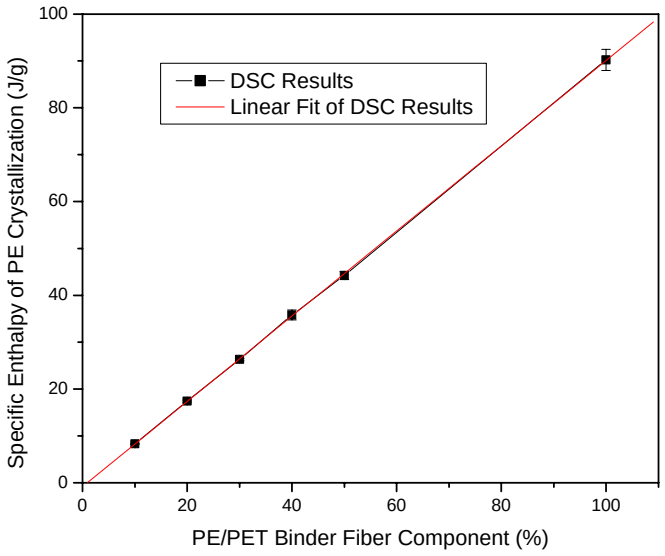

(a) PE/PET binder fiber

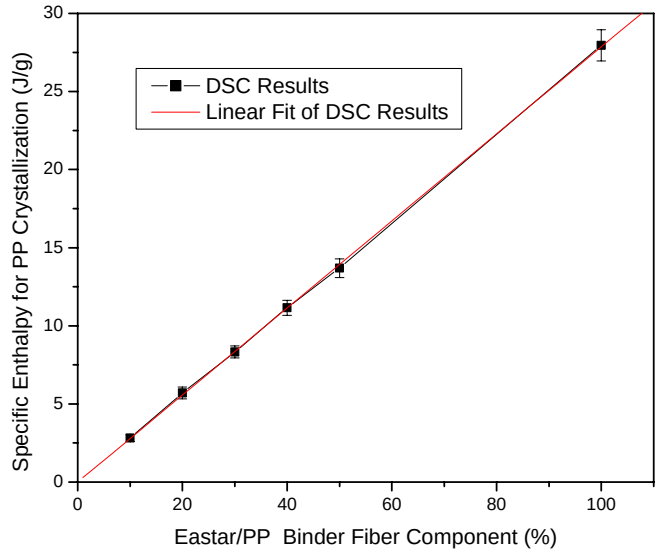

(b) Eastar/PP binder fiber

Figure 4.21 DSC measured enthalpy vs. binder fiber weight content.

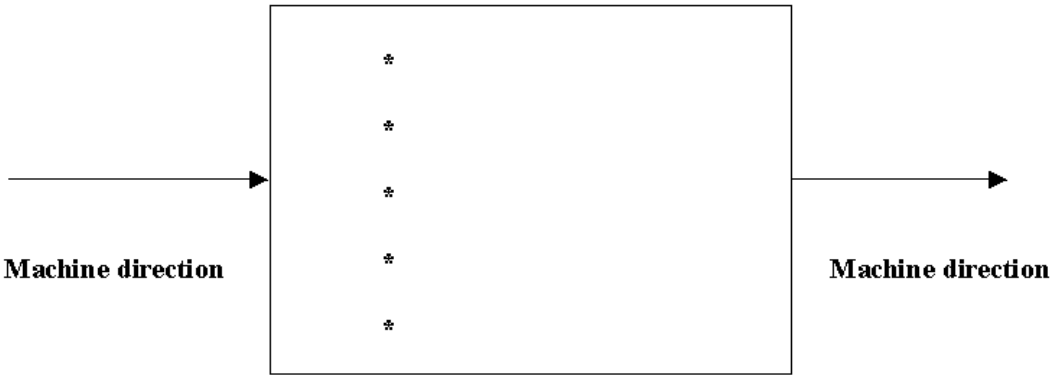

Figure 4.22 Schematic illustration of sample selection for nonwoven fabrics.

Table 4.6 Parameters obtained from DSC for cotton/(PE/PET) nonwovens.

Actual PE/PET (%)	$T_{o,c}=T_c$ (°C)	$T_{p,c}$ (°C)	ΔH_c (J/g)	Observed PE/PET (%)	Average PE/PET (%)	σ	C.V.
50	118.84	117.24	59.00	65.41	51.83	11.9	0.230
	118.82	117.15	52.45	58.15			
	118.80	117.28	42.29	46.88			
	118.68	116.92	49.17	54.51			
	118.64	116.83	30.86	34.21			
30	118.71	117.19	28.23	31.30	27.85	7.02	0.252
	118.68	117.17	26.82	29.73			
	118.73	117.21	33.15	36.75			
	118.49	116.94	18.00	19.96			
	118.58	116.94	19.40	21.51			
15	118.65	117.01	20.63	22.87	14.42	6.64	0.460
	118.46	116.82	17.82	19.76			
	118.40	116.87	6.87	7.62			
	118.56	117.06	11.37	12.61			
	118.51	117.01	8.33	9.24			

Note: "Actual" PE/PET (%) is the input % for the carding process, "T" is temperature, "c" is cooling or crystallizing, "o" is onset, "p" is peak, "ΔH_c" is the specific enthalpy for PE exothermic peak.

Table 4.7 Parameters obtained from DSC for cotton/(Eastar/PP) nonwovens.

Actual Eastar/PP (%)	$T_{o,c}=T_c$ (°C)	$T_{p,c}$ (°C)	ΔH_c (J/g)	Observed Eastar/PP (%)	Average Eastar/PP (%)	σ	C.V.
50	121.50	117.06	13.87	49.62	47.52	3.97	0.083
	121.33	116.88	13.98	50.02			
	121.14	116.71	14.26	51.02			
	121.23	116.31	12.65	45.26			
	120.64	115.95	11.65	41.68			
30	120.71	116.52	10.67	38.18	31.09	4.61	0.148
	120.65	116.50	7.60	27.19			
	121.27	116.84	8.55	30.59			
	120.21	116.29	7.53	26.94			
	120.74	116.62	9.10	32.56			
15	123.02	118.80	5.47	19.57	13.98	4.81	0.344
	123.16	119.13	4.35	15.56			
	122.89	118.79	3.30	11.81			
	122.93	118.75	4.48	16.03			
	122.99	118.89	1.93	6.91			

Note: "Actual" Eastar/PP (%) is the input % for the carding process, "T" is temperature, "c" is cooling or crystallizing, "o" is onset, "p" is peak, "ΔH_c" is the specific enthalpy for PP exothermic peak.

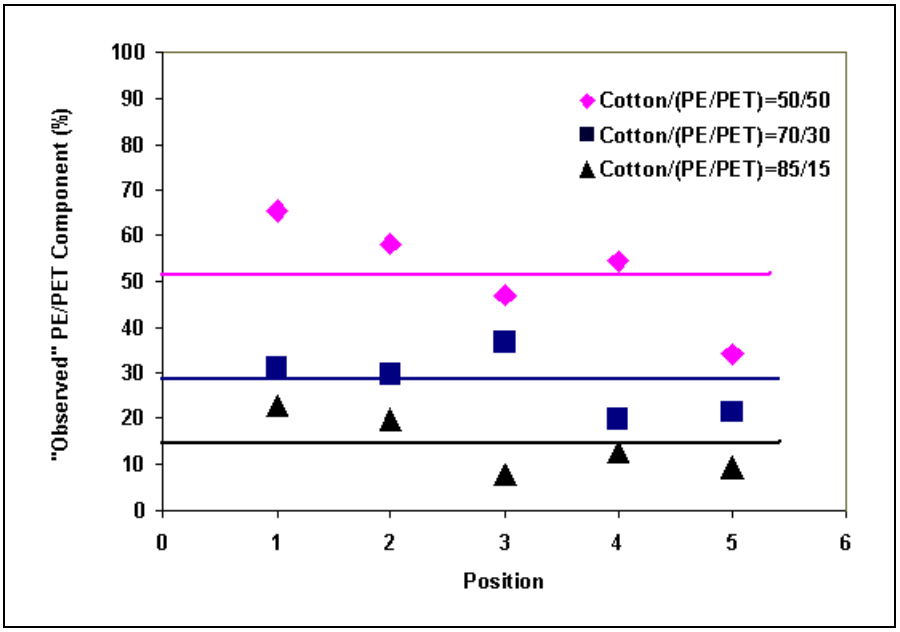

(a) Cotton/(PE/PET) nonwovens

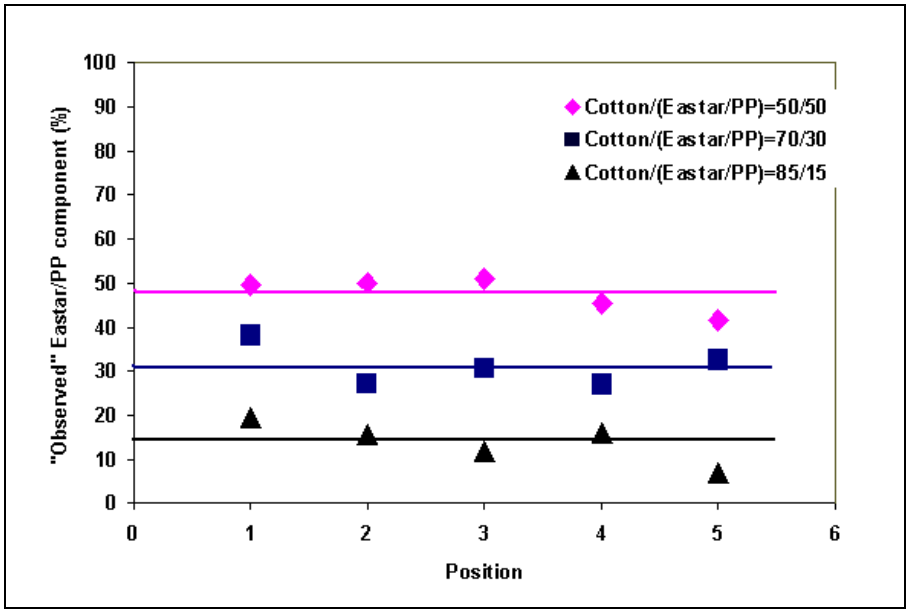

(b) Cotton/(Eastar/PP) nonwovens

Figure 4.23 Binder fiber distribution along cross direction.

§4.3 PROPERTIES OF THE BIODEGRADABLE NONWOVENS

§4.3.1 Tensile Strength

§4.3.1.1 Cotton/CA Nonwovens

In this part of the research, water and/or plasticized cellulose acetate were used instead of acetone solvent pre-treatment used in the previous study [11] for cotton/cellulose acetate nonwovens to decrease the softening temperature and to further lower the calendering temperature. The effect of water dip-nip treatment, plasticizer (binder type), binder fiber content, and bonding temperature on the tensile strength of the fabrics was studied. The peak load values for all the combinations are listed in Table 4.8.

The effect of water dip-nip treatment can be clearly observed. The peak loads of cotton/OCA webs at the two different blend ratios are increased to different degrees compared with those without treatment. Therefore, water dip-nip treatment can be applied to cotton/OCA webs to improve the fabric strength. Comparing the effect of water dip-nip treatment with acetone solvent treatment, it can be found that there is no significant difference between water dip-nip treatment and 20% acetone solvent treatment, and peak loads of cotton/cellulose acetate thermally bonded webs are increased by both the treatments. Thus, there is conclusive evidence that water can be used as the external plasticizer instead of 20% acetone solvent without compromising web strength, and the process is environmentally friendly.

From the point of energy concern, it is better to make the whole process as simple as possible. This is the purpose of selecting plasticized cellulose acetate fiber, in which an

Table 4.8 Peak loads for cotton/cellulose nonwovens (40gsm) (kg).

	Bonding Temperature (°C)	Binder content 25%	Binder content 50%
Cotton/OCA (No treatment)	150	0.10	0.03
	170	0.09	0.03
	190	0.09	0.09
Cotton/OCA (With water dip-nip treatment)	150	0.21	0.25
	170	0.37	0.44
	190	0.81	0.77
Cotton/OCA (With 20% acetone solvent treatment)	150	0.21	0.20
	170	0.34	0.47
	190	0.69	0.65
Cotton/PCA (No treatment)	150	0.17	0.25
	170	0.33	0.42
	190	0.63	0.90
Cotton/PCA (With water dip-nip treatment)	150	0.52	0.57
	170	0.80	0.86
	190	0.81	0.87

internal plasticizer was added during fiber manufacture to lower the softening temperature of ordinary cellulose acetate fiber and to further lower the bonding temperature during the thermal calendering process is a good alternative. It can be clearly seen from Table 4.8 that peak loads have been improved by using PCA instead of OCA, especially at higher bonding temperatures. Further comparison of external plasticizer (water) and internal plasticizer shows that there is no significant difference between the two plasticizers. Thus, it is clear that internal plasticizer (PCA) can be used in place of the external plasticizer (water) without compromising web strength and the process is more economical. Based on the above analysis, it seems that the optimal bonding temperature is 190°C either for cotton/OCA with water dip-nip treatment at both blend ratios.

The combination effect of both the external plasticizer (water) and the internal plasticizer can also be observed based on the data in Table 4.8. The peak loads of the fabrics can be improved for both the contents under the three bonding temperatures. In this case, the peak loads at the lowest bonding temperature 150°C is close to those of the fabrics using internal or external plasticizer separately. However, we need to consider the energy cost at higher bonding temperature with the more extensive processing procedure at a lower bonding temperature to make the best choice of processing implementation.

The overall strengths of cotton/cellulose acetate webs are lower in comparison with those of the control cotton/(PE/PET) webs in the next section. The low strength may come from the low strength of the cellulose acetate fibers and the elongation variability of the cellulose binder fibers and the carrier fibers (cotton fibers) as shown in Table 4.1.

§4.3.1.2 Cotton/(PE/PET) Nonwovens

Bicomponent PE/PET fiber was selected as the binder fiber for the control group since the resulting fabrics have excellent tensile strength. The peak loads of the cotton/(PE/PET) nonwovens are shown in Table 4.9 and Figure 4.24. All the tested fabrics had the same basis weight around 40g/m^2.

The graph shows that the optimal peak load of cotton/(PE/PET) nonwovens is as high as 2.29kg at the PE/PET binder fiber content of 50% and bonding temperature around 130°C. It can be clearly seen that 110°C is too low to get the webs bonded effectively since the strength of the fabrics bonded at that temperature is too low and does not change much with the increase of the binder fiber content. The high strength of cotton/(PE/PET) fabrics may be the result of the high strength of PE/PET binder fiber as shown in Table 4.1, good adhesion between the binder fiber and carrier fiber (cotton fiber) as shown in Figure 4.6(a), and the excellent load sharing properties as shown in Figure 4.11.

§4.3.1.3 Cotton/Eastar Nonwovens

In this segment, the effects of bonding temperature and blend ratio on fabric strength of contton/Eastar nonwovens were studied. And effect of binder fiber distribution on the web strength was also analyzed.

Table 4.9 Peak loads for cotton/(PE/PET) nonwovens (40gsm) (kg).

Bonding Temperature (°C)	Binder content 15%	Binder content 30%	Binder content 50%
110	0.12	0.11	0.09
120	0.21	0.29	0.54
130	0.28	0.85	2.29
140	0.39	0.57	1.56

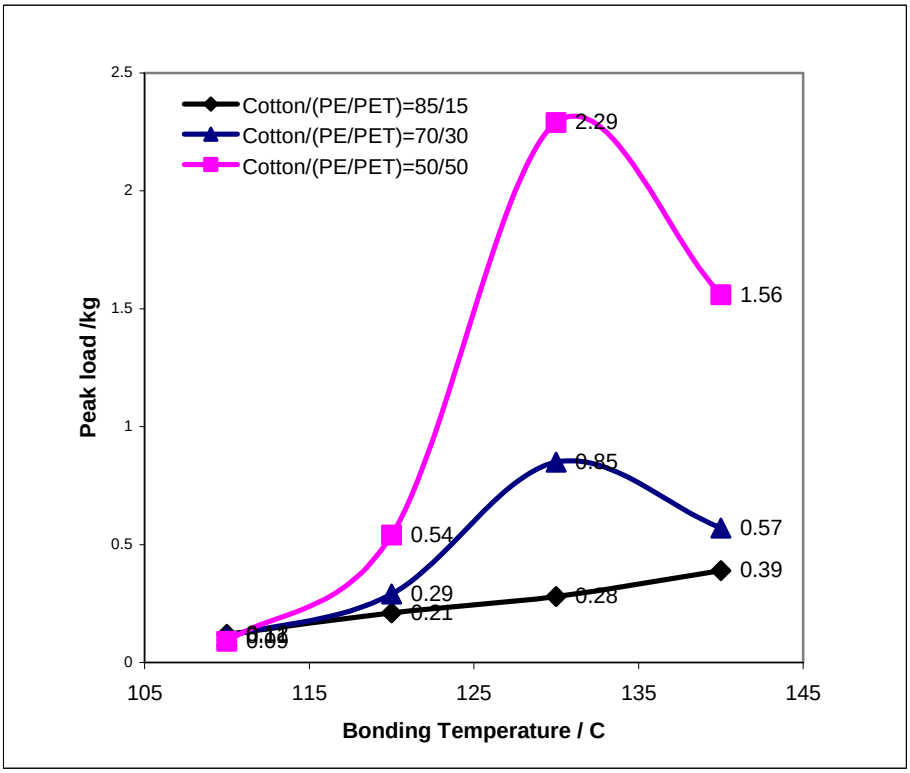

Figure 4.24 Peak loads of cotton/(PE/PET) nonwovens (40gsm).

4.3.1.3.1 Low basis weight cotton/Eastar nonwovens

To achieve good properties with the retention of optimum hand/feel in the final fabric, it is essential that the surface temperature of the calender rolls be selected appropriately. The effect of the Eastar fiber content and bonding temperature on the fabric peak load along the machine direction for the 40g/m^2 webs can be seen from the data in Figure 4.25. The graph shows that 90°C is too low to get the webs bonded effectively. The optimal bonding temperature is around 110°C for Eastar binder fiber content of 50% with peak load around 0.36kg. It also shows that the overall peak loads of cotton/Eastar webs are much lower compared to the cotton/(PE/PET) control nonwovens.

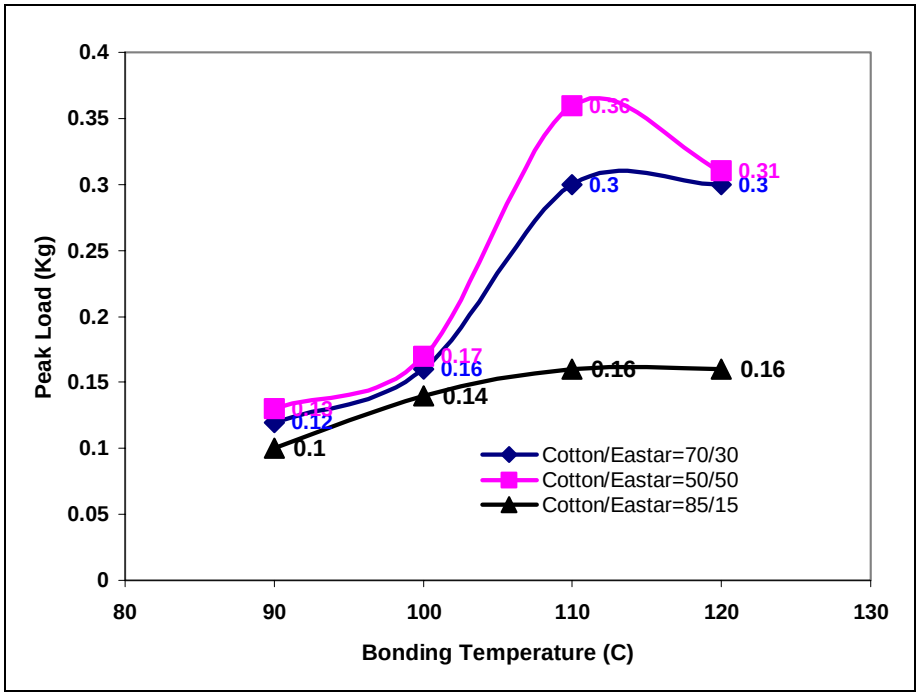

Figure 4.25 Peak loads of cotton/Eastar nonwovens (40gsm).

The properties of the bonded fabrics are dependent on the properties of the constituent fibers (carrier fibers and binder fibers), processing factors and the method of bonding. Previous researchers [43, 64] indicated that the fiber properties determined the mechanical behavior of the bonded fabric. They observed a similarity in the load-elongation behavior between bonded fabrics and their constituent fibers. Other researcher [33] found that the length of the fiber affect the strength of the bonded fabrics, since the longer fibers provide more cross over points and better anchoring of individual fibers and thus produce stronger fabrics. Binder concentration influences the tensile strength of the bonded fabrics as well as the flexural rigidity. Two main factors are involved in the determination of fabric strength, fiber load bearing behavior and the quantity of the polymer contributing to bonding at the points of embossing. At higher binder concentration, an increase in the binder content causes an increase in the strength.

The low strength of cotton/Eastar fabrics is the result of the low strength and high elongation of the Eastar binder fiber as shown in Table 4.1, which causes the nonhomogeneous load sharing during the break, combining with the poor distribution of the binder fibers in the webs which decreases web uniformity. The fracture structures of cotton/Eastar with 30% binder fiber as shown in Figure 4.9 illustrated the nearly brittle fracture of the fabrics, which indicates the poor load sharing of the fabrics.

4.3.1.3.2 High basis weight cotton/Eastar nonwovens

High basis weight cotton/Eastar nonwovens ($80g/m^2$) were also investigated to improve the web uniformity and further improve the resulting fabric strength. The effect

of the Eastar fiber content on fabric peak load along the machine direction is shown in Figure 4.26. With the increase of Eastar binder fiber content, the peak load increases at the lower thermal bonding temperature. This is the result of the increase of Eastar fiber content, which increases the number of bond points and the effective bond area. However, at higher bonding temperature (120°C) and higher Eastar binder fiber content (above 30%), the peak load decreases with increase in Eastar binder fiber content. This may be caused by the different failure mechanism of the fabrics bonded at higher temperature as shown in Figure 4.12. At low bonding temperatures, the bond failure mechanism was found to be the loss of interfacial adhesion at the bond site, leading to bond disintegration. At higher bonding temperatures, the failure mechanism was cohesive failure of the fibers in the bond point and/or at bond periphery due to the loss of fiber

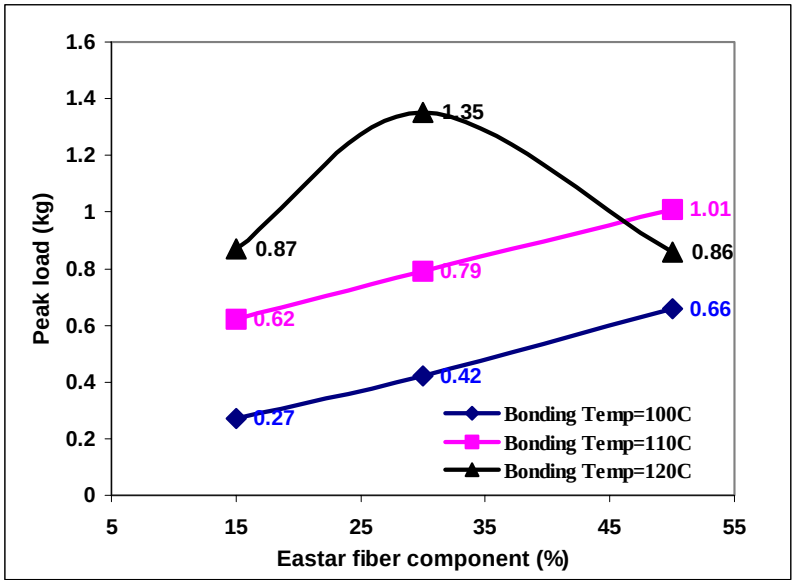

Figure 4.26 Effect of Eastar binder fiber content (80gsm).

integrity and formation of film-like spots at high temperatures, as well as the reduction in load transfer from fibers to film [43, 44].

The effect of bonding temperature on fabric peak load along the machine direction is shown Figure 4.27. Generally, an increase in bonding temperature improves the individual bond strength but can be detrimental to the base fiber strength [65]. It can be clearly seen that with the increase in calendering temperature, the peak load increases for lower binder fiber content (≤ 30%). With the increase in bonding temperature at lower binder fiber content, the increase in strength of the fabrics is the result of the increased penetration of the binder. At higher temperature, the binder fiber exhibits more of its fluid nature and incorporates more carrier fibers into the bonded network [66], resulting in the formation of better-developed bond structure. Again, the decrease of peak load at higher

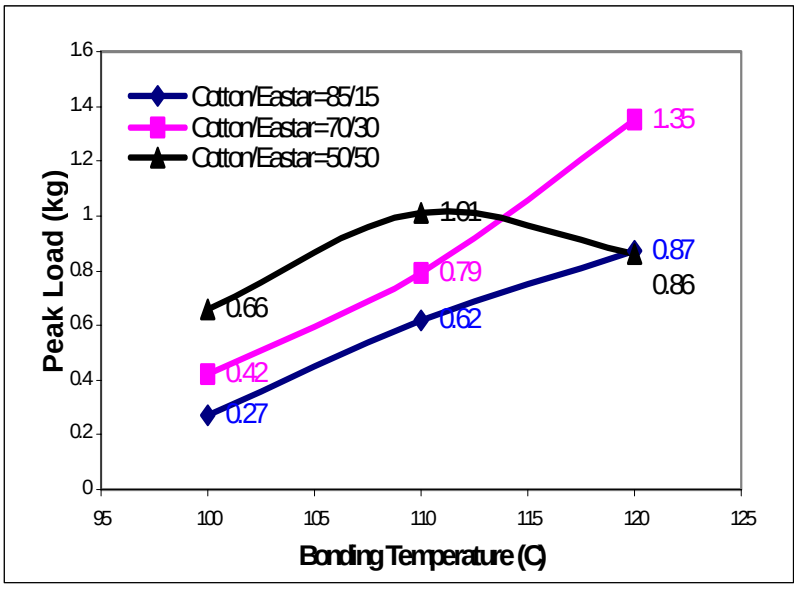

Figure 4.27 Effect of bonding temperature (80gsm).

binder fiber content and higher bonding temperature is due to a different failure mechanism of the nonwoven fabrics.

The overall peak loads of the high basis weight cotton/Eastar nonwovens are not very high, when we compare the peak loads of the high basis weight cotton/Eastar nonwovens with the low basis weight cotton/(PE/PET) nonwovens. The optimal peak load is only 1.35kg, much lower than the optimal peak load for cotton/(PE/PET) low basis weight nonwovens, which showed a peak load value of 2.29kg. The low strength of the high basis weight cotton/Eastar nonwovens may still be attributed to the non-uniformity of the webs. These results again indicate that the Eastar unicomponent fiber is not a good choice for the cotton-based nonwovens.

4.3.1.3.3 Cotton/(Eastar/PP) nonwovens

In this section, a bicomponent fiber, Eastar/PP, with Eastar *Bio*® GP copolyester as the sheath and polypropylene as the stiffer core was selected as the binder fiber instead of Eastar unicomponent fiber to improve the stiffness of the fiber. This bicomponent binder fiber has higher tenacity, higher crimps, and lower peak extension compared to the Eastar unicomponent binder fiber. These properties are preferred for carding process, which may contribute to the uniform distribution of the binder fibers as discussed earlier.

The peak loads of cotton/(Eastar/PP) nonwovens are shown in Figure 4.28. All the tested webs have a basis weight around 40g/m^2. The optimal cotton/(Eastar/PP) web has a peak load value of 1.21kg or 1.15kg for the binder fiber content of 50% at bonding temperatures of 110°C or 100°C, respectively. Although the optimal peak load is not as

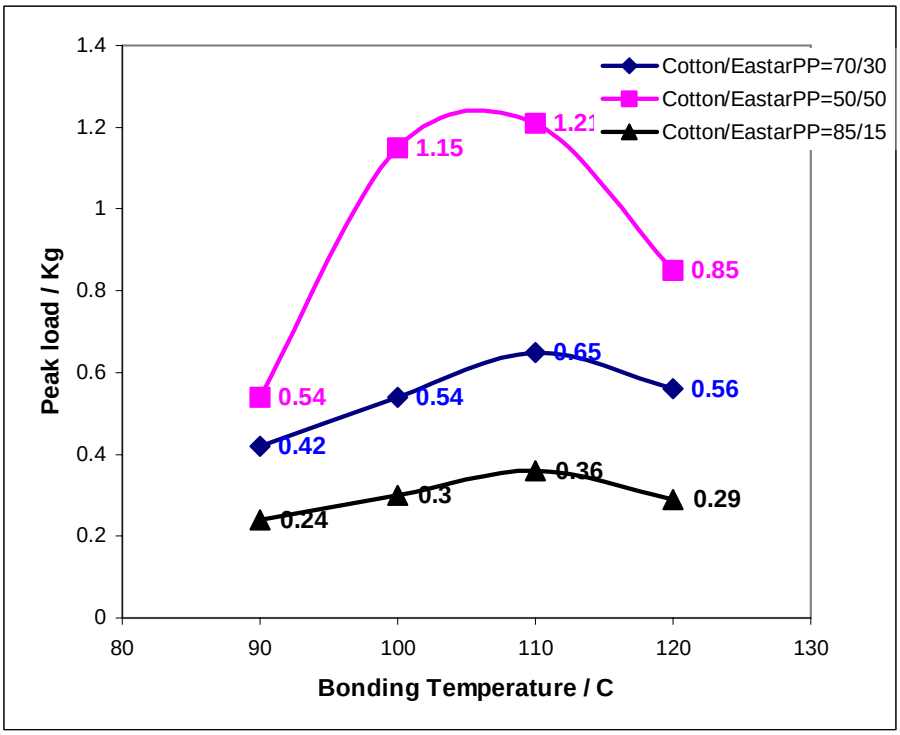

Figure 4.28 Peak loads of cotton/(Eastar/PP) nonwovens (40gsm).

high as that for the cotton/(PE/PET) control webs as shown in Figure 4.24, the peak load is much higher than those of cotton/CA webs and cotton/Eastar webs.

It was found that the peak loads first increase with increase of bonding temperature. Then with further increase in bonding temperature, the peak load decreases. Again, this may be caused by the different failure mechanism of the fabrics bonded at higher temperatures, as shown in Figure 4.13. At low bonding temperatures, the bond failure mechanism was found to be due to the loss of interfacial adhesion at the bond site leading to bond disintegration. At higher bonding temperatures, the failure mechanism was cohesive failure of the fibers near the bond periphery.

The comparison of the effect of the two Eastar binder fibers, Eastar unicomponent as-spun fiber and Eastar/PP bicomponent fiber, is demonstrated in Figure 4.29. At the three binder contents around 15%, 30%, and 50% under the four bonding temperatures (90°C, 100°C, 110°C, and 120°C), the peak loads of cotton/(Eastar/PP) nonwoven fabrics are much higher than those of cotton/Eastar nonwovens. Therefore, using Eastar/PP bicomponent fiber as a binder fiber can improve the tensile properties of cotton/Eastar nonwoven fabrics.

The strength comparison of cotton/cellulose acetate nonwovens vs. cotton/Eastar nonwovens is illustrated in Figure 4.30. The graph shows that the peak loads of cotton/(Eastar/PP) webs are higher than or comparable to those of cotton/Eastar, cotton/OCA, and cotton/PCA webs. The advantage of using Eastar/PP as a binder fiber can be obviously seen. That is, the cotton/(Eastar/PP) webs have higher strength and at relatively lower thermal calendering temperature comparing with cotton/CA webs, which means that the process cost can be greatly reduced by using Eastar/PP bicomponent fiber as the binder fiber for cotton-based biodegradable nonwovens. Based on this research, high strength cotton/(Eastar/PP) nonwoven fabrics with a basis weight of 40gsm can be produced by using cotton/(Eastar/PP) at a blend ratio of 50/50, and thermal calendered at 100°C or 110°C under a constant calendering speed of 10m/min and calendering pressure of 0.33MPa.

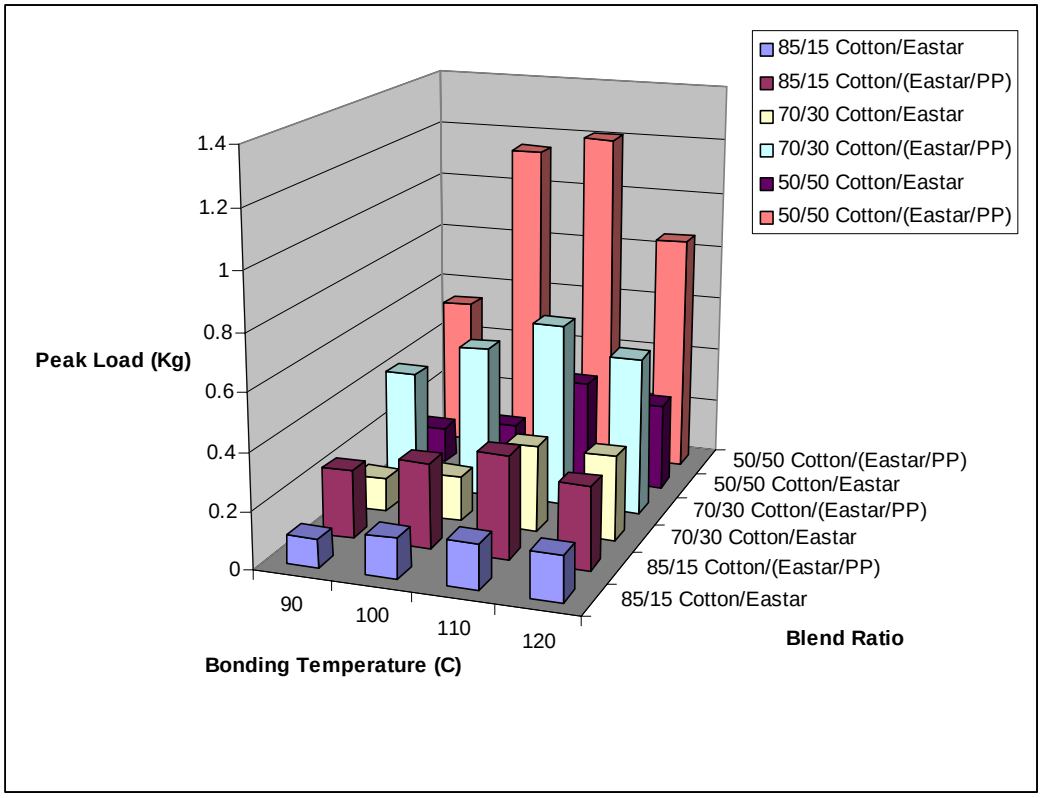

Figure 4.29 Peak loads comparison: cotton/Eastar vs. cotton/(Eastar/PP) (40gsm).

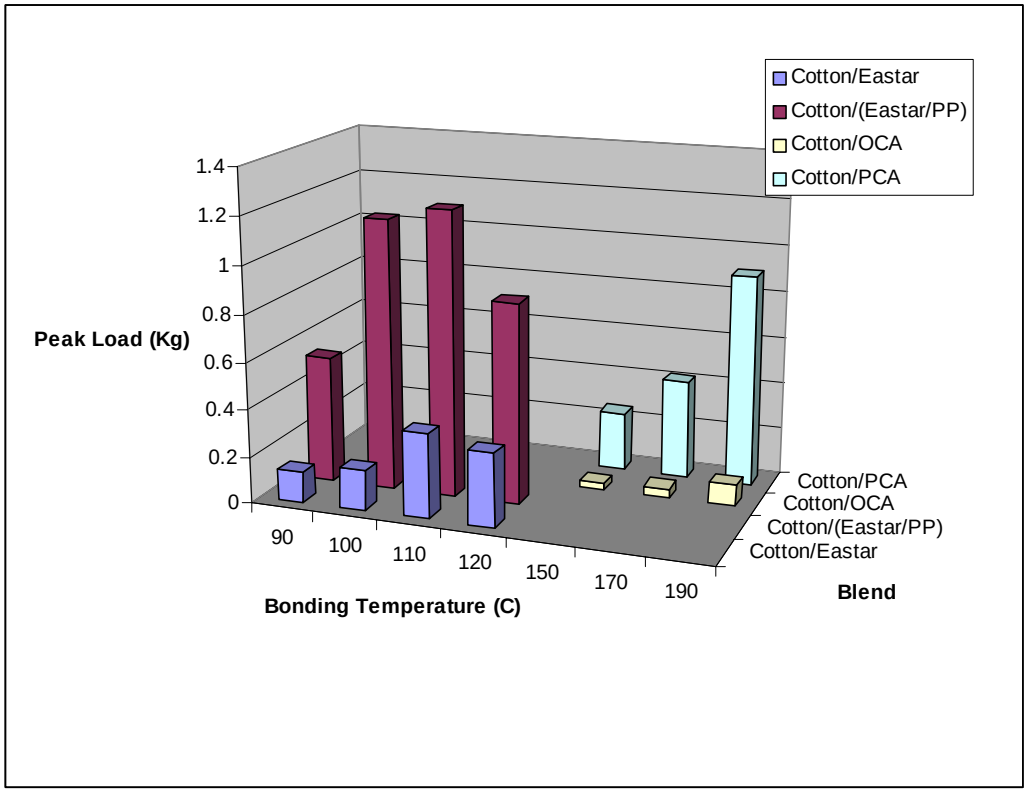

Figure 4.30 Peak loads comparison: cotton/CA vs. cotton/Eastar (40gsm).

§4.3.2 Single Bond Tensile Strength

To further analyze the strength of the fabrics, single bond strip tensile tests were carried out on the cotton/(PE/PET) and cotton/(Eastar/PP) webs. This test was done in order to estimate the bond strength and the degree of load sharing between fibers during the tensile deformation of the webs. The idea is that if the binder fibers were well-distributed in the nonwoven fabrics, the tensile data of the strip fabrics should be consistent with those of the single bond strips.

The results of the single bond strip tensile tests for the cotton/(PE/PET) nonwovens with basis weight of 40g/m^2 are shown in Figure 4.31. When comparing the tensile data for the single bond in Figure 4.31 with the tensile data for the strip test in Figure 4.24, it is obvious that the effects of temperature and binder content on the peak strength for the fabric strips is not exactly the same as those for the single bond strips. At the binder fiber contents of 15% and 30%, the trends of the curves for the strip tests are the same as those for the single bond strip tests while for the binder fiber content of 50% the trend of the peak loads for the strip test does not follow the same trend of the single bond strip test. Whereas strength drops after optimum bonding temperature for one-inch strips, single bond strength continues to increase with increase in bonding temperature. This indicates that the PE/PET binder fiber may not be well-distributed in the nonwoven fabrics. The result is consistent with what was observed from the DSC quantitative analysis in section 4.2.3.2. That is, there was high variation of binder fiber distribution along the cross direction of the fabrics. The standard deviation of the fabric with 50%

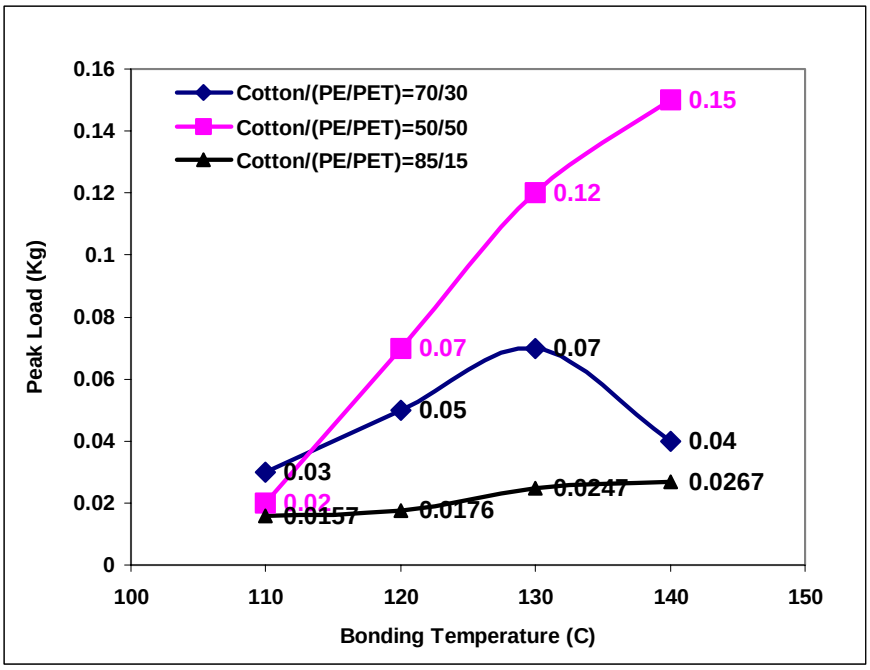

Figure 4.31 Single bond peak loads of cotton/(PE/PET) nonwovens (40gsm).

PE/PET binder fiber is 11.90, listed in Table 4.6, which is much higher than those of the fabrics with 15% PE/PET binder fiber (6.64) and 30% PE/PET binder fiber (7.02).

The single bond strength results for cotton/(Eastar/PP) webs with a basis weight of 40g/m^2 are shown in Figure 4.32. On comparing the tensile data for the single bond in Figure 4.32 with the tensile data for the strip test in Figure 4.28, it becomes clear that the effects of temperature and binder content on the peak strength for the fabric strip are also not exactly the same as for the single bond strip. At binder fiber content of 50%, the trend of the peak load for the strip test is almost the same as that for the single bond strip test. For the binder fiber content of 15% and 30% the trends of the peak loads for strip tests do not follow the same trends of single bond strip tests. This indicates that the Eastar/PP

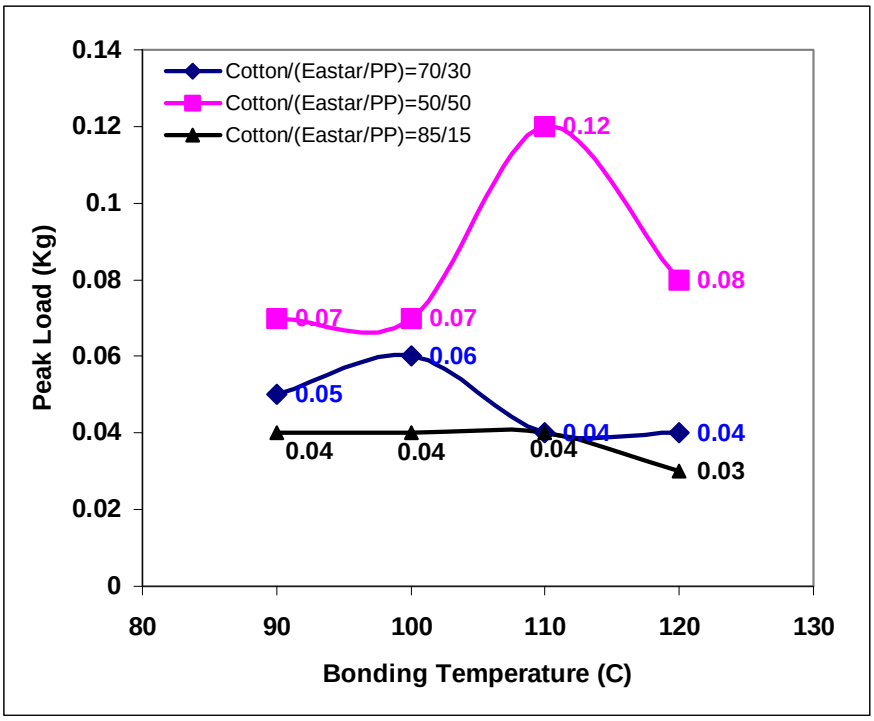

Figure 4.32 Single bond peak loads of cotton/(Eastar/PP) nonwovens (40gsm).

binder fiber may not be well-distributed in the nonwoven fabrics. These results are consistent with what was observed from the DSC quantitative analysis in section 4.2.3.2; that is, there is high variation of binder fiber distribution along the cross direction of the fabrics with binder fiber content of 15% and 30%. The C.V. and standard deviation of the fabrics with 15% and 30% Eastar/PP binder fiber are higher than those of the fabric with 50% Eastar/PP binder fiber (Table 4.7).

Since the effect of bonding temperature on tensile property of strip fabric is not consistent with that of single bond strip for both the cotton/(PE/PET) and cotton/(Eastar/PP) nonwovens, it can be concluded that the binder fibers were not

uniformly distributed in those carded nonwoven fabrics, especially for certain compositions. These results further demonstrate that DSC is a useful and reliable method for studying the binder fiber distribution in these carded cotton-based nonwovens by analyzing the specific enthalpy from crystallization of one of the binder fiber components in the fabrics.

§4.3.3 Flexural Rigidity

Strength, softness, and absorbency are the three most important properties of an absorbent web. These properties are determined by the manufacturing process, raw material selection, and the post processing treatment [67].

The effects of bonding temperature and binder fiber contents on flexural rigidity of cotton/(Eastar/PP) and cotton/(PE/PET) nonwoven webs are shown in Figure 4.33 and Figure 4.34, respectively. All the fabrics have a basis weight of around 40gsm. For both the nonwoven webs, flexural rigidity increases with the increase of bonding temperature and binder fiber content. That is, the fabrics become stiffer with increase in bonding temperature due to the melting of the sheath of the binder fiber at the bond points and formation of film like structures as shown in Figures 4.5 – 4.8.

The overall flexural rigidity of cotton/(PE/PET) webs is lower than that of cotton/(Eastar/PP) webs except for the fabric bonded at 140°C at the blend ratio of 50/50. This may be the result of the high crimps in PE/PET binder fibers (18 crimps/inch as listed in Table 4.1) compared to those in Eastar/PP binder fibers (11 crimps/inch as listed in Table 4.1). Allan and Ingalls [68] have suggested that the use of helically crimped

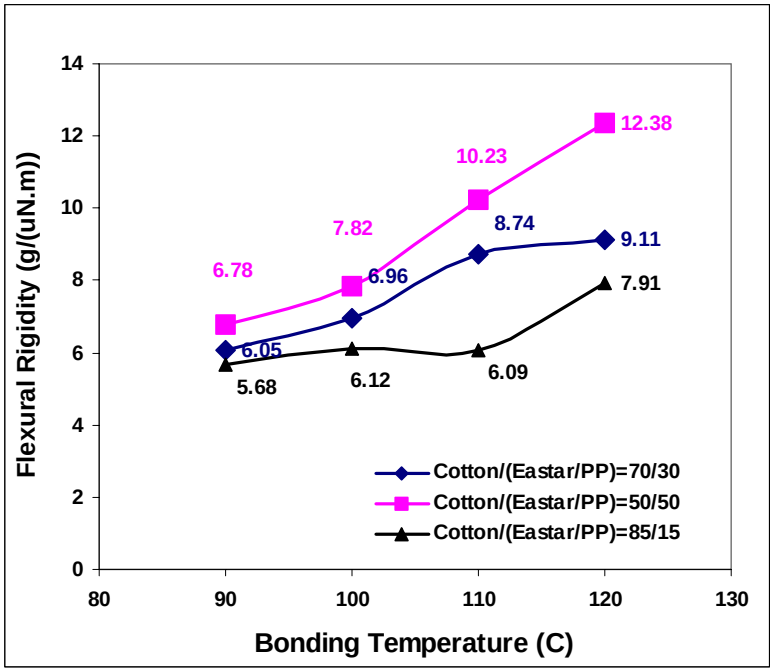

Figure 4.33 Flexural rigidity of cotton/(Eastar/PP) nonwovens (40gsm).

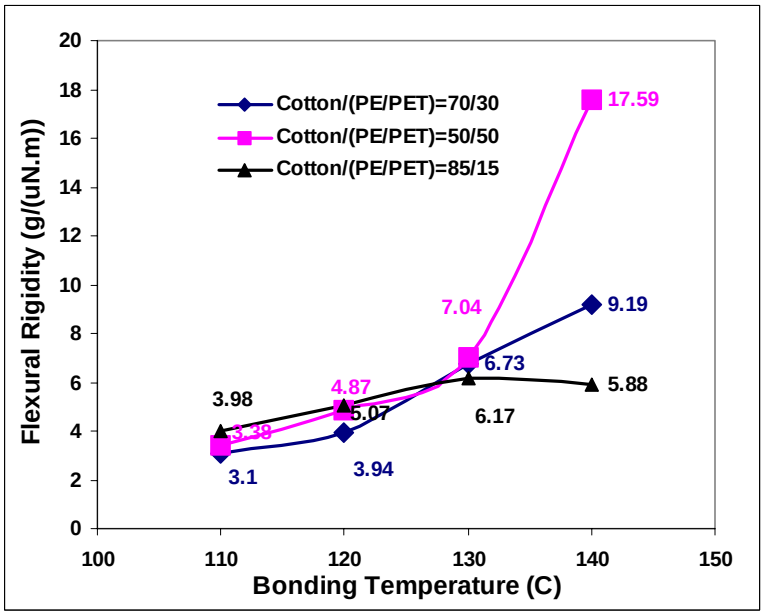

Figure 4.34 Flexural rigidity of cotton/(PE/PET) nonwovens (40gsm).

fiber segments between the bond points. The improvement in the flexibility of the fabric has been attributed to the actual increase in length of unbonded fiber segments, which lessen fiber interactions and, for this reason, make bending and shear deformation easier.

§4.3.4 Absorbency

Absorbency is another important property for an absorbent web. Absorbency rate and absorbent capacity are the two most important performance parameters to be considered for absorbent applications of nonwovens.

The absorption curves of cotton/(Eastar/PP) nonwoven webs with binder fiber contents of 30% and 50% are demonstrated in Figure 4.35 and Figure 4.36, respectively. All the fabrics have a basis weight around 40gsm. The maximum amount of absorption for the blend ratio of 70/30 can get as high as 13 grams/gram. Even for the stronger fabrics at a blend ratio of 50/50 the absorption can reach 11 grams/gram, indicating that the fabrics have potential applications as absorbent materials.

It can be clearly seen from these figures that the total amount of absorption and absorption rate decrease with increase in bonding temperature and binder fiber content, while the time needed to obtain the balanced absorption increases with increase in bonding temperature and binder fiber content. The sheath of the Eastar/PP binder fiber melts at higher bonding temperature and penetrates into some capillaries at the bond points, causing the total amount of absorption and absorption rate to decrease. Moreover, the more the binder fiber in content, the larger the decrease of the number of capillaries at the bond points.

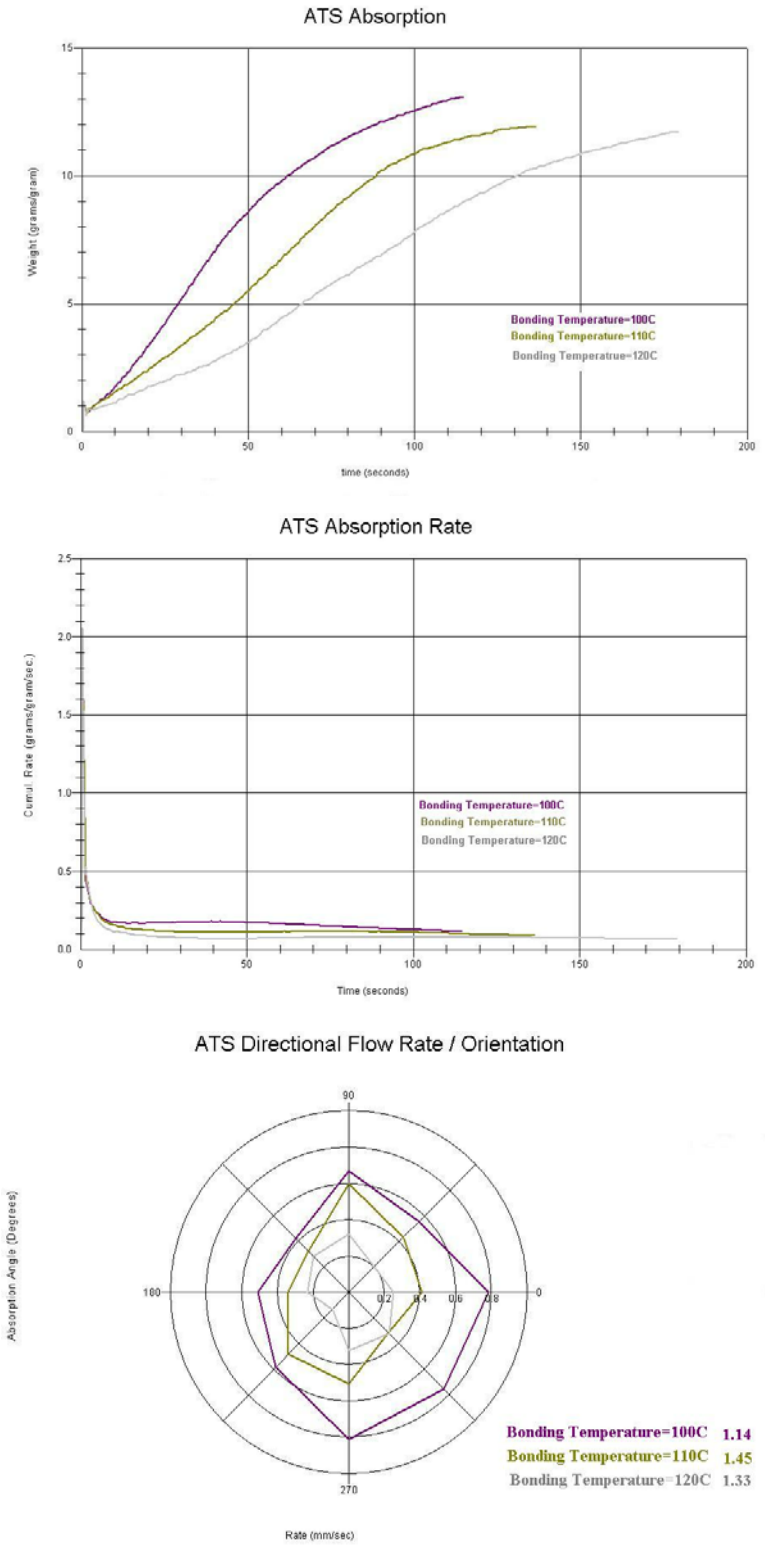

Figure 4.35 Absorption behavior of cotton/(Eastar/PP)=70/30 webs (40gsm).

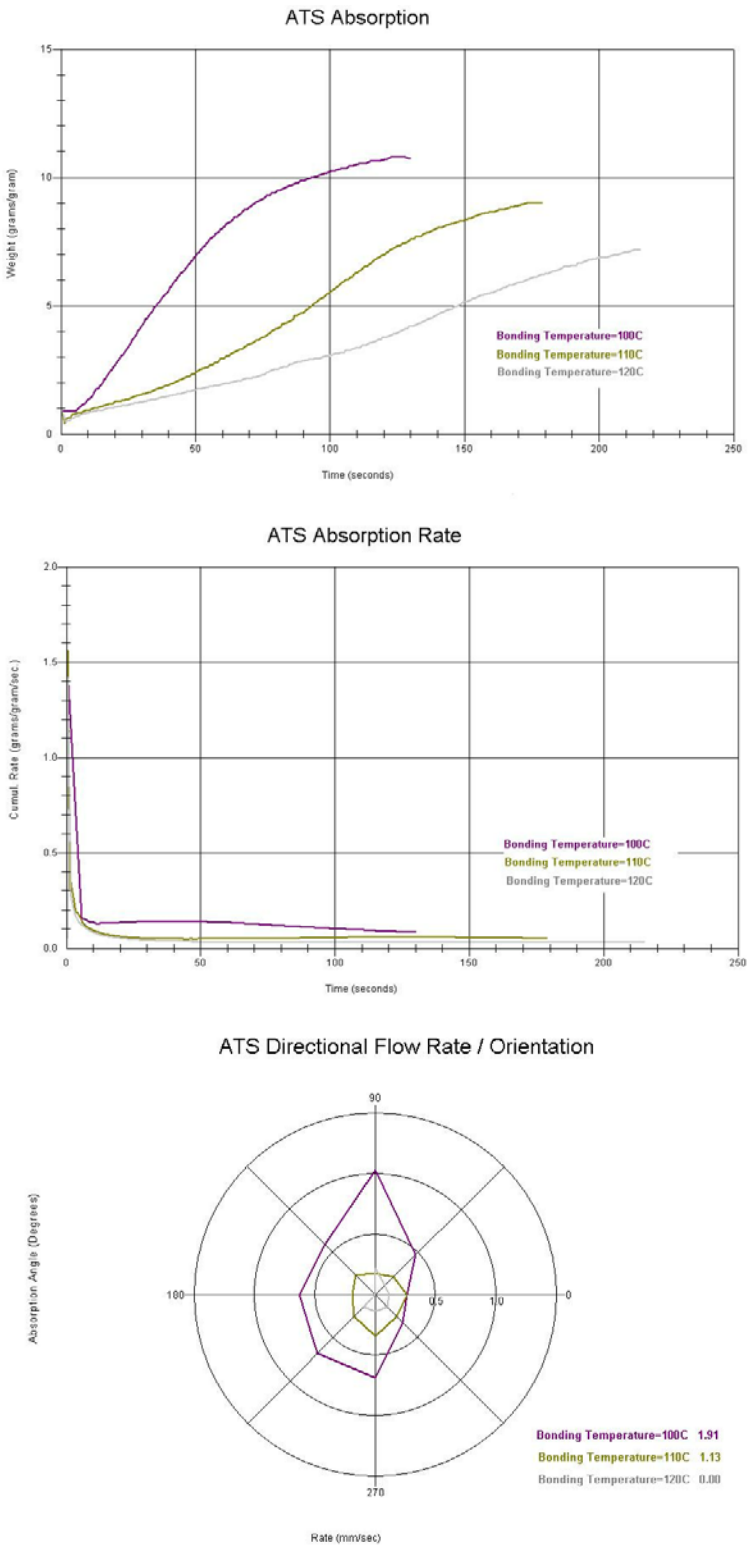

Figure 4.36 Absorption behavior of cotton/(Eastar/PP)=50/50 webs (40gsm).

The directional flow charts in these figures indicate that flow rates along machine direction (90° and 270° line) are higher than those along cross direction (0° and 180° line) for all the samples. The numbers on the right bottom of the charts show the ratio of the flow rate along the machine direction versus the flow rate in the cross direction. These ratios are larger than 1, which means that the flow rate in the machine direction is higher than that of the cross direction. This aspect ratio indicates that fibers and capillaries are more orientated along the machine direction for the carded nonwovens.

The absorption curves of 40gsm cotton/(PE/PET) webs are illustrated in Figure 4.37. An absorption slope of 0.005 grams per 20 seconds was used for the webs due to the lower flow rate of the fabrics. Comparison of Figure 4.37 with Figure 4.35 and 4.36 indicates that the maximum amount of absorption for cotton/(PE/PET) webs is much lower than that for cotton/(Eastar/PP) webs. The highest absorption for cotton/(PE/PET) was only 7 grams/gram for the blend ratio of 70/30 bonded at 120ºC. This is due to the lower wettability of PE/PET binder fibers shown by the high contact angle of 85.43º in Table 4.1. It is difficult to obtain any readings for the blend ratio of 50/50 even under the low absorption slope, indicating the low absorbency of the materials.

Thus, the cotton/(Eastar/PP) nonwoven fabrics have good water absorbency and, even for the better strength fabrics at blend ratio of 50/50, the absorption can reach 11 grams/gram, indicating that the fabrics have potential applications as absorbent materials.

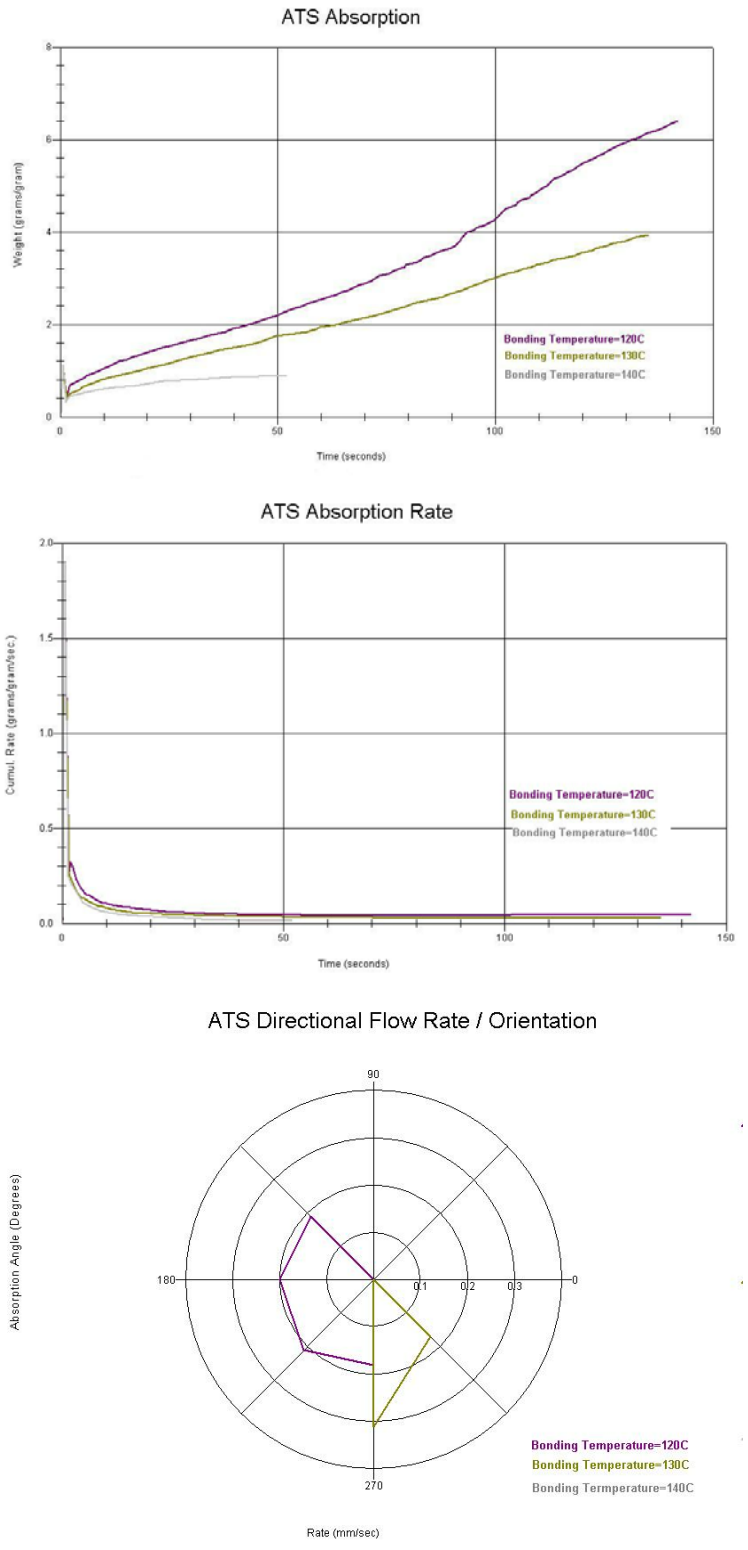

Figure 4.37 Absorption behavior of cotton/(PE/PET)=70/30 webs (40gsm).

§4.4 STATISTIC MODELING OF THE TENSILE PROPERTY OF THE BIODEGRADABLE NONWOVENS

In this section, the experimental results for 40gsm cotton/Eastar(/PP) webs were statistically analyzed using the General Linear Model Procedures (GLM) in JMP 5.0 to determine the significance of the effects of the parameters (variables) on the peak load (LOAD) (response) of the resulting biodegradable nonwovens and further fit the parameters to proper models. These parameters are thermal calendering temperature (TEMP), binder fiber forms (TYPE), and binder fiber contents or blend ratio (COMP). The experimental design is shown in Table 3.1 as TEMP at 4 levels, TYPE at 2 levels, and COMP at 3 levels. Since five strips were tested for each specimen, so each treatment has 5 measurements. This is not a full factorial design but a split plot design due to the restrictions of experimental conditions. The parameter, bonding temperature, does not have true replications. The mean values, standard deviation (σ), and coefficient of variation (C.V.) of the peak loads of the resulting nonwoven fabrics are listed in Table 4.10.

§4.4.1 Fit Model Considering All Variables Nominal – Model (1)

It is better to consider all the three variables nominal to fit model due to the special experimental design. Fit model platform was used to investigate whether the effect of the three variables are significant at α level of 0.05. The interactions among the three variables were also considered in the model. The added parameters were: TEMP,

Table 4.10 Peak loads of cotton/Eastar(/PP) nonwovens (40gsm) (kg).

Binder Content (%)	Bonding Temperature (°C)	Cotton/Eastar			Cotton/(Eastar/PP)		
		Mean	σ	C.V.	Mean	σ	C.V.
15	90	0.10	0.03	0.27	0.24	0.04	0.16
	100	0.14	0.03	0.24	0.30	0.05	0.15
	110	0.17	0.02	0.12	0.36	0.05	0.13
	120	0.17	0.03	0.19	0.29	0.06	0.20
30	90	0.12	0.03	0.26	0.42	0.04	0.10
	100	0.15	0.02	0.15	0.54	0.20	0.38
	110	0.30	0.12	0.41	0.65	0.15	0.23
	120	0.30	0.06	0.19	0.56	0.36	0.64
50	90	0.13	0.04	0.34	0.54	0.14	0.26
	100	0.15	0.03	0.21	1.15	0.36	0.32
	110	0.36	0.05	0.15	1.21	0.27	0.22
	120	0.31	0.05	0.16	0.85	0.26	0.31

TYPE, TEMP*TYPE, COMP, TEMP*COMP, TYPE*COMP, and TEMP*TYPE*COMP. The first part of the JMP outputs in Table 4.11 is the summary of the fit. R-square of the fit is 0.838, which represents the proportion of variability in peak load accounted by the model. The second part is the significance level of the model as a whole for the response variable, which is the peak load of the fabrics. The last part lists the significance levels for each of the independent variables, which are the parameters and their interactions. The term DF in the last two parts of the table is the degrees of freedom for each variable in the design. It is one less than the total number of observations. Thus, in the second part of the table, the value in column DF in the last row is 119 which is one less than the total number of the combinations multiplied by the five replicated measurements of each combination. In the last part of the table, the DF for each variable is obtained by subtracting one from the respective number of levels.

The sum of squares is an indication of the variation in the observed data and is calculated by using the standard procedure. The mean square is obtained by dividing the sum of squares value by the corresponding degree of freedom [69]. The F-value is calculated by dividing the mean square by the mean error in the second part. The F-values are used to obtain the corresponding p-level (the significance level) for each independent variable. The p-value of TEMP*TYPE*COMP is 0.0532, which is greater than $\alpha = 0.05$, indicating the interaction is not significant at $\alpha = 0.05$; while for variables TYPE, COMP, and TYPE*COMP are very significant with p-values lower than 0.001. That is, the effect of binder type, binder fiber content and their mutual interactions is very important to fabric strength, which is represented by the peak load value. Therefore, TEMP, TYPE,

Table 4.11 Fit model with all variables and their interactions – Model (1).

Summary of Fit

RSquare	0.837571
RSquare Adj	0.798656
Root Mean Square Error	0.148304
Mean of Response	0.396417
Observations (or Sum Wgts)	120

Analysis of Variance

Source	DF	Sum of Squares	Mean Square	F Ratio
Model	23	10.887719	0.473379	21.5229
Error	96	2.111440	0.021994	Prob > F
C. Total	119	12.999159		<.0001

Effect Tests

Source	Nparm	DF	Sum of Squares	F Ratio	Prob > F
TYPE	1	1	4.6374008	210.8469	<.0001
COMP	2	2	2.7251517	61.9517	<.0001
TYPE*COMP	2	2	1.5829217	35.9850	<.0001
TEMP	3	3	0.9507025	14.4084	<.0001
TYPE*TEMP	3	3	0.2998292	4.5441	0.0051
COMP*TEMP	6	6	0.4062350	3.0784	0.0085
TYPE*COMP*TEMP	6	6	0.2854783	2.1633	0.0532

TEMP*TYPE, COMP, TEMP*COMP, and TYPE*COMP should be kept while TEMP*TYPE*COMP could be deleted in the model for further study.

§4.4.2 Reduced Model Considering All Variables Nominal – Model (2)

Based on the above analysis, the reduced model was fitted by TYPE, COMP, and their interaction TYPE*COMP. The JMP outputs are shown as follows in Table 4.12. R-square of the reduced fitted model is 0.816, which represents the proportion of variability in peak load accounted by the reduced model. It is close to that of the larger model, which is 0.838. This indicates the excluded variables do not contribute much to the larger model, so it could be excluded. The p-values of all the parameters are smaller than α = 0.05, indicating all of them are significant at α = 0.05. The predicted profiles of the reduced model are shown in Figure 4.38 (a, b) by using the effect screening method. It can be clearly seen from these profiles again that the better binder type is Eastar/PP and the better binder fiber content is 0.5 (50%), and the optimal bonding temperature is around 110°C.

§4.4.3 Fit Model Considering Both TEMP And COMP As Continuous Variables – Model (3)

We fitted a model considering TEMP and COMP as continuous variables while TYPE as the only nominal variables where temperature was fitted to the third degree since it had four levels and composition to the second degree since it had three levels and

Table 4.12 Reduced model – Model (2).

Summary of Fit

RSquare	0.81561
RSquare Adj	0.784878
Root Mean Square Error	0.153294
Mean of Response	0.396417
Observations (or Sum Wgts)	120

Analysis of Variance

Source	DF	Sum of Squares	Mean Square	F Ratio
Model	17	10.602241	0.623661	26.5397
Error	102	2.396918	0.023499	Prob > F
C. Total	119	12.999159		<.0001

Effect Tests

Source	Nparm	DF	Sum of Squares	F Ratio	Prob > F
TYPE	1	1	4.6374008	197.3429	<.0001
COMP	2	2	2.7251517	57.9839	<.0001
TYPE*COMP	2	2	1.5829217	33.6803	<.0001
TEMP	3	3	0.9507025	13.4856	<.0001
TYPE*TEMP	3	3	0.2998292	4.2530	0.0071
COMP*TEMP	6	6	0.4062350	2.8812	0.0123

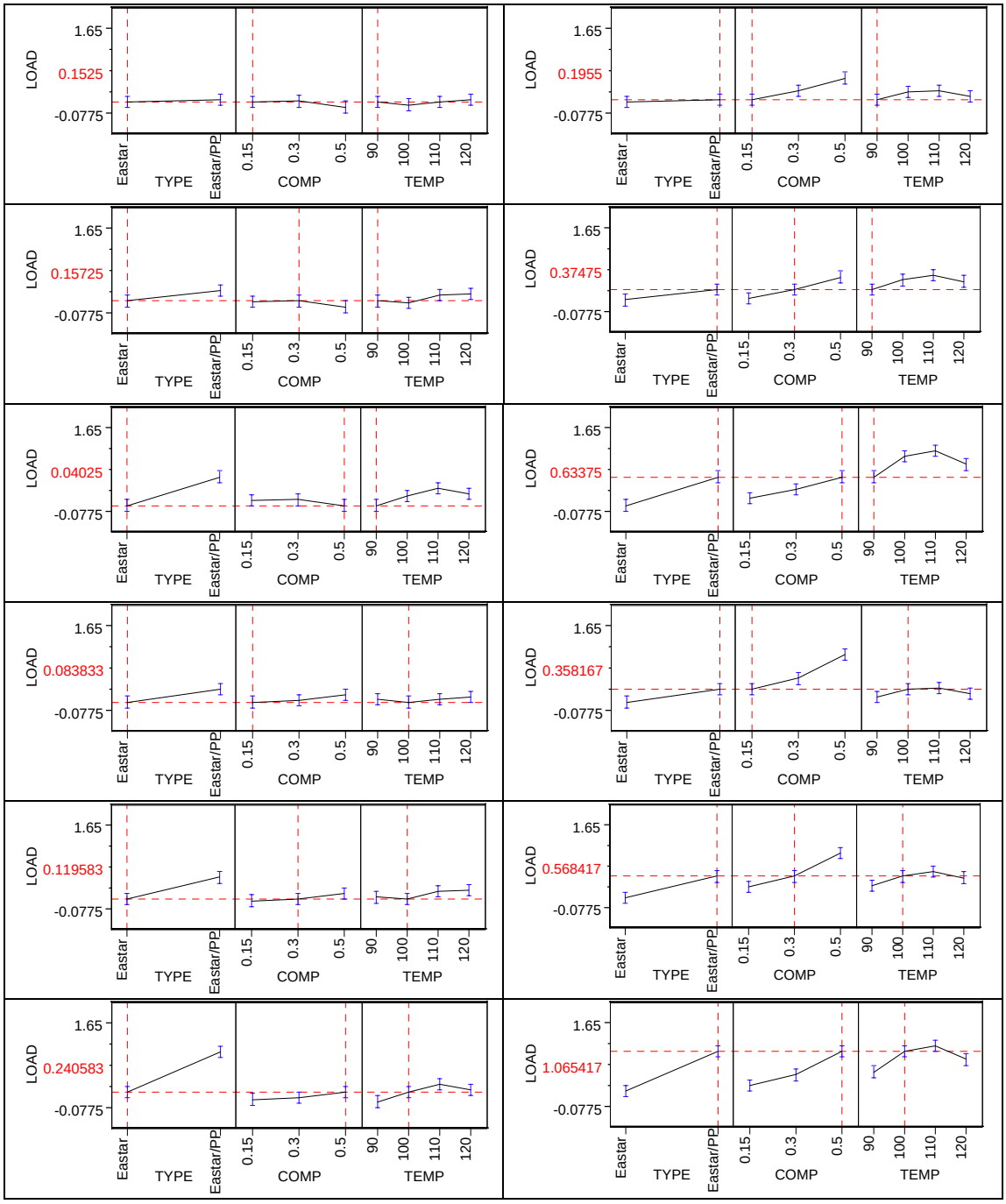

Figure 4.38 (a) Predicted profiles.

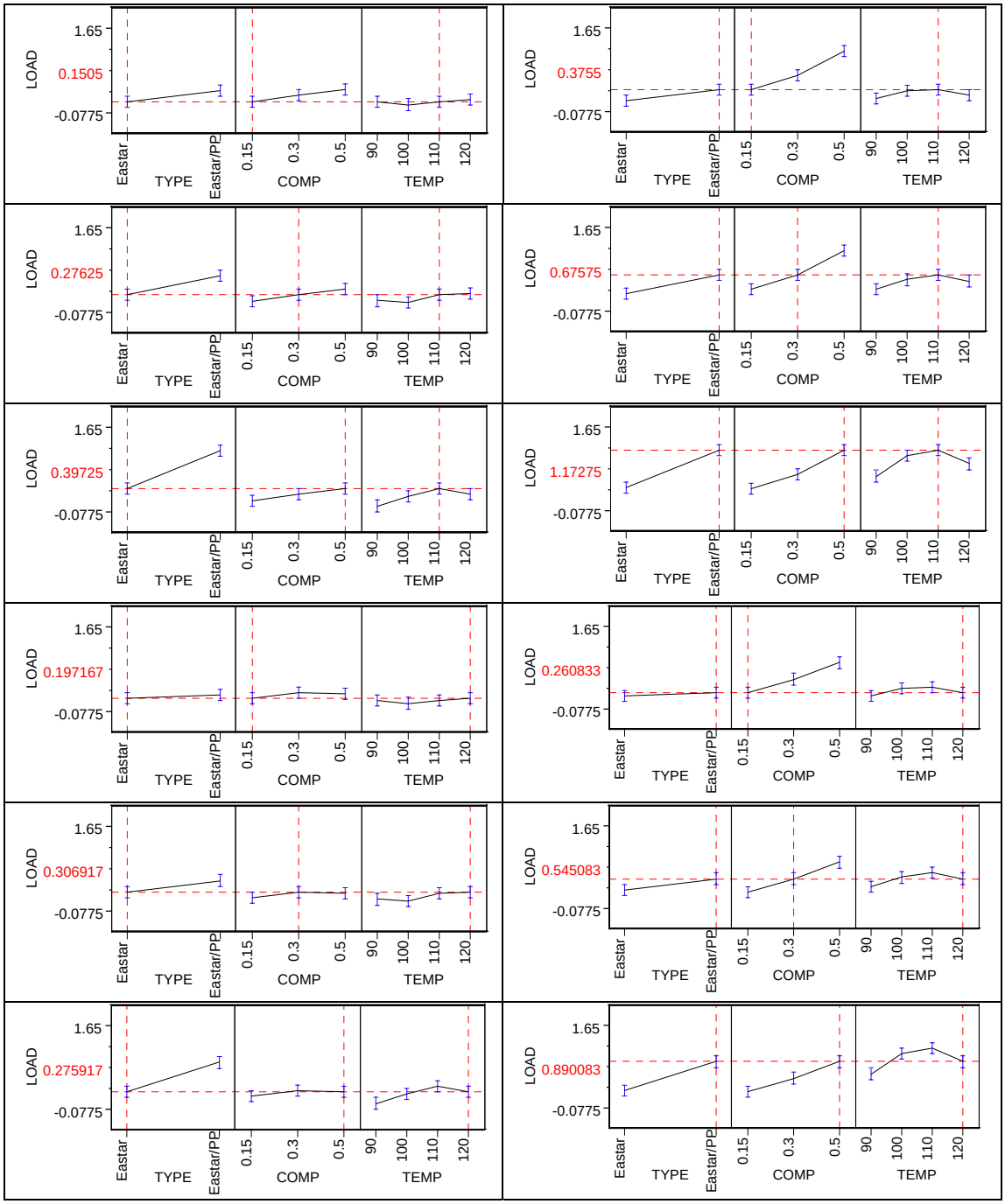

Figure 4.38 continued (b) Predicted profiles.

binder type was considered as the only nominal variable. All interactions were included. See Table 4.13 for the estimated values of the model coefficients.

According to the JMP output in Table 4.13, R-square of the fit is 0.813, which represents the proportion of variability in peak load accounted by the new model. It is worth noticing that the R-square value in this model is close to those previous models considering all variables nominal, as shown Table 4.11 and Table 4.12, indicating that this new model fits as well as the original ones.

Based on Table 4.13 the model was simplified to include only the following effects: TYPE, COMP, TYPE*COMP, TEMP, TEMP*TEMP, TEMP*COMP, TEMP*TEMP*COMP, TEMP*TYPE, TEMP*TEMP*TYPE. The practice of including lower level terms that are not significant if higher level terms are significant was followed. For example, TEMP*COMP was included in the model because TEMP*TEMP*COMP was significant. Similarly, TEMP*TYPE was included because TEMP*TEMP*TYPE was significant. The terms not included in the model were not significant even though the experimental variation was less in this split plot design than would have been in the case of true replication. This fact gives confidence in the non-significance of the dropped terms.

§4.4.4 Simplified Model – Model (4)

Based on above analysis, the simplified model was fitted by TYPE, COMP, TYPE*COMP, TEMP, TEMP*TEMP, TEMP*COMP, TEMP*TEMP*COMP, TEMP*TYPE, TEMP*TEMP*TYPE. The JMP results are given in the Table 4.14. The

Table 4.13 Fit model with all variables and their interactions – Model (3).

Summary of Fit

RSquare	0.812666
RSquare Adj	0.785646
Root Mean Square Error	0.153021
Mean of Response	0.396417
Observations (or Sum Wgts)	120

Analysis of Variance

Source	DF	Sum of Squares	Mean Square	F Ratio
Model	15	10.563968	0.704265	30.0771
Error	104	2.435191	0.023415	Prob > F
C. Total	119	12.999159		<.0001

Parameter Estimates

Term	Estimate	Std Error	t Ratio	Prob>|t|
Intercept	-1.213176	0.50776	-2.39	0.0187
TYPE[Eastar]	-0.236893	0.03025	-7.83	<.0001
COMP	1.4519873	0.157886	9.20	<.0001
TYPE[Eastar]*(COMP-0.31667)	-0.769365	0.100477	-7.66	<.0001
TEMP	0.0116628	0.004807	2.43	0.0170
TYPE[Eastar]*(TEMP-105)	0.0028181	0.004448	0.63	0.5278
(COMP-0.31667)*(TEMP-105)	0.0261152	0.031101	0.84	0.4030
(TEMP-105)*(TEMP-105)	-0.000606	0.00014	-4.34	<.0001
(TEMP-105)*(TEMP-105)*(TEMP-105)	-0.000025	0.000021	-1.22	0.2255
(COMP-0.31667)*(COMP-0.31667)	0.0452381	0.991098	0.05	0.9637
(TEMP-105)*(TEMP-105)*(COMP-0.31667)	-0.003216	0.000974	-3.30	0.0013
(TEMP-105)*(TEMP-105)*(TEMP-105)*(COMP-0.31667)	-0.000032	0.000145	-0.22	0.8276
(COMP-0.31667)*(COMP-0.31667)*(TEMP-105)	-0.040286	0.088646	-0.45	0.6504
(TEMP-105)*(TEMP-105)*TYPE[Eastar]	0.0004908	0.00014	3.51	0.0007
(TEMP-105)*(TEMP-105)*(TEMP-105)*TYPE[Eastar]	-0.000014	0.000021	-0.67	0.5012
(COMP-0.31667)*(COMP-0.31667)*TYPE[Eastar]	-1.02381	0.991098	-1.03	0.3040

Effect Tests

Source	Nparm	DF	Sum of Squares	F Ratio	Prob > F
TYPE	1	1	1.4360019	61.3275	<.0001
COMP	1	1	1.9803377	84.5745	<.0001
TYPE*COMP	1	1	1.3728800	58.6318	<.0001
TEMP	1	1	0.1378535	5.8873	0.0170
TYPE*TEMP	1	1	0.0093992	0.4014	0.5278
COMP*TEMP	1	1	0.0165096	0.7051	0.4030
TEMP*TEMP	1	1	0.4404408	18.8100	<.0001
TEMP*TEMP*TEMP	1	1	0.0348082	1.4866	0.2255
COMP*COMP	1	1	0.0000488	0.0021	0.9637
TEMP*TEMP*COMP	1	1	0.2551532	10.8969	0.0013
TEMP*TEMP*TEMP*COMP	1	1	0.0011163	0.0477	0.8276
COMP*COMP*TEMP	1	1	0.0048359	0.2065	0.6504
TEMP*TEMP*TYPE	1	1	0.2891008	12.3467	0.0007
TEMP*TEMP*TEMP*TYPE	1	1	0.0106682	0.4556	0.5012
COMP*COMP*TYPE	1	1	0.0249865	1.0671	0.3040

Table 4.14 Simplified model – Model (4).

Summary of Fit

RSquare	0.806783
RSquare Adj	0.790975
Root Mean Square Error	0.151107
Mean of Response	0.396417
Observations (or Sum Wgts)	120

Analysis of Variance

Source	DF	Sum of Squares	Mean Square	F Ratio
Model	9	10.487504	1.16528	51.0343
Error	110	2.511655	0.02283	Prob > F
C. Total	119	12.999159		<.0001

Parameter Estimates

Term	Estimate	Std Error	t Ratio	Prob>|t|
Intercept	-0.579155	0.140174	-4.13	<.0001
TYPE[Eastar]	-0.257938	0.022081	-11.68	<.0001
COMP	1.4531081	0.154014	9.43	<.0001
TYPE[Eastar]*(COMP-0.31667)	-0.79473	0.096212	-8.26	<.0001
TEMP	0.00563	0.001234	4.56	<.0001
(TEMP-105)*(TEMP-105)	-0.000606	0.000138	-4.39	<.0001
(TEMP-105)*(COMP-0.31667)	0.0186162	0.008605	2.16	0.0327
(TEMP-105)*(TEMP-105)*(COMP-0.31667)	-0.003216	0.000962	-3.34	0.0011
(TEMP-105)*TYPE[Eastar]	-0.000063	0.001234	-0.05	0.9592
(TEMP-105)*(TEMP-105)*TYPE[Eastar]	0.0004908	0.000138	3.56	0.0006

Effect Tests

Source	Nparm	DF	Sum of Squares	F Ratio	Prob > F
TYPE	1	1	3.1156334	136.4517	<.0001
COMP	1	1	2.0325556	89.0175	<.0001
TYPE*COMP	1	1	1.5579352	68.2311	<.0001
TEMP	1	1	0.4754535	20.8229	<.0001
TEMP*TEMP	1	1	0.4404408	19.2895	<.0001
TEMP*COMP	1	1	0.1068571	4.6799	0.0327
TEMP*TEMP*COMP	1	1	0.2551532	11.1746	0.0011
TEMP*TYPE	1	1	0.0000602	0.0026	0.9592
TEMP*TEMP*TYPE	1	1	0.2891008	12.6614	0.0006

model has an R^2 of 0.8068 versus 0.8127 for the full model (Model (3)) so we have not lost much prediction power by simplifying the model as we have done.

The new fitted model is:

$$\begin{aligned} Load = & -0.5792 - 0.2579 \times z + 1.4531 \times COMP - 0.7947 \times z \times (COMP - 0.3167) \\ & + 0.0056 \times TEMP + 0.0186 \times (COMP - 0.3167)(TEMP - 105) \\ & - 0.0006 \times (TEMP - 105)(TEMP - 105) \\ & + 0.0005 \times z \times (TEMP - 105)(TEMP - 105) - 0.000063(TEMP - 105) \times z \\ & - 0.0032 \times (TEMP - 105)(TEMP - 105)(COMP - 0.3167) \end{aligned} \quad (4)$$

where, z = 1 for Eastar

z = -1 for Eastar/PP

Similar Predict Profiles can also be obtained based on Model (4). Figure 4.39 shows the predicted profiles for Eastar and Eastar/PP binders respectively according to above Model (4). The model predicts that the highest strength for 40gsm cotton/Eastar nonwoven is given when we use binder content of 0.5 (50%) and a bonding temperature around 111°C; while the highest strength for 40gsm cotton/(Eastar/PP) nonwoven is given when we use binder content of 0.5 (50%) and a bonding temperature around 108°C. The optimal peak load of cotton/(Eastar/PP) nonwovens is much higher than that of cotton/Eastar nonwoven. Thus, Eastar/PP binder fiber is the better choice.

§4.4.5 Predicted Peak Loads And Their Prediction Intervals

For practical applications, a prediction interval (PI) was preferred. An interval estimate for an individual observation is called a PI, which is different from confidence

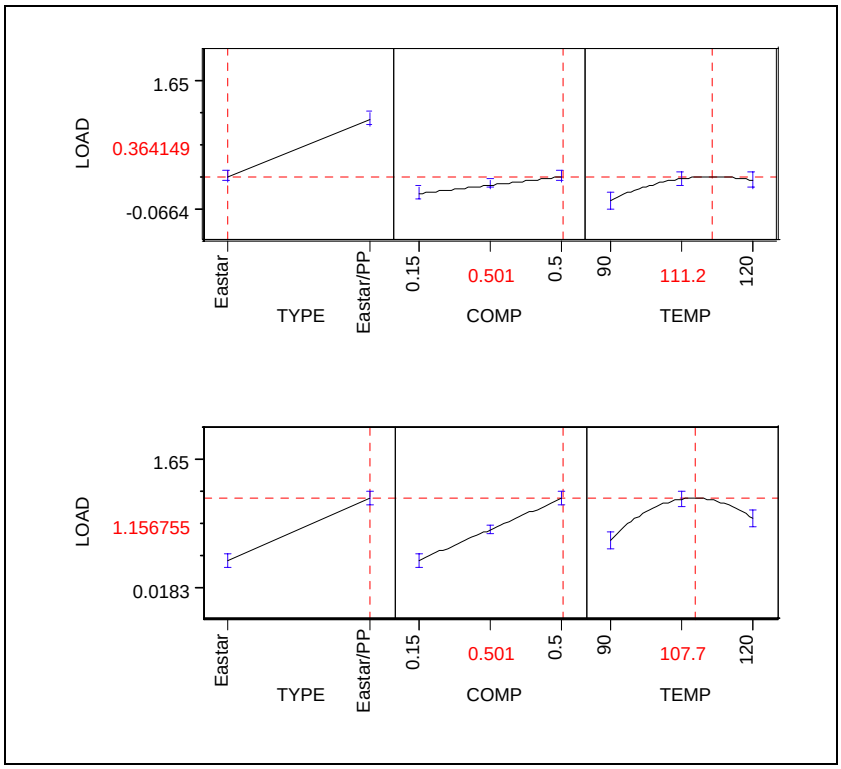

Figure 4.39 Prediction profiles based on Model (4).

interval of the mean of the population [69]. The predicted peak loads and their 95% prediction intervals are shown in Table 4.15, based on the simplified model (4). Here the prediction interval is the strength that a future observation will be in the interval with 95% confidence. The predicted optimal peak loads and their prediction intervals are also listed in Table 4.15. The optimal peak load for 40gsm cotton/Eastar nonwovens is only 0.3635kg, relatively lower compared with that for 40gsm cotton/(Eastar/PP) nonwovens, which is 1.154kg. Thus, Eastar/PP should be selected as the best binder fiber.

The optimal process conditions for obtaining high strength nonwoven fabrics are to select Eastar/PP as the binder fiber type, to choose binder fiber content at 50%, and to use 107.7°C as the best bonding temperature. The predicted peak load of the 40gsm nonwoven fabrics processed under the optimal condition is 1.154kg.

Table 4.15 Predicted peak loads and their prediction intervals (kg).

Binder (%)	Bonding Temp. (°C)	Cotton/Eastar			Cotton/(Eastar/PP)		
		Predicted Load	LPL	UPL	Predicted Load	LPL	UPL
15	90	0.162252	-0.15429	0.478799	0.190442	-0.1261	0.506989
	100	0.102685	-0.20747	0.412837	0.328475	0.018322	0.638627
	110	0.127324	-0.18283	0.437477	0.354381	0.044228	0.664534
	120	0.236171	-0.08038	0.552718	0.268161	-0.04839	0.584708
30	90	0.110575	-0.1983	0.419449	0.377184	0.068311	0.686058
	100	0.175418	-0.12953	0.48037	0.639627	0.334676	0.944579
	110	0.227982	-0.07697	0.532934	0.693458	0.388507	0.99841
	120	0.268267	-0.04061	0.577141	0.538676	0.229802	0.84755
50	90	0.041673	-0.27648	0.359823	0.626173	0.308023	0.944324
	100	0.272397	-0.03885	0.583642	1.054498	0.743253	1.365743
	110	0.362193	0.050948	0.673438	1.145561	0.834316	1.456806
	120	0.311062	-0.00709	0.629212	0.899363	0.581212	1.217513
*50	111.2	0.363498	0.022088	0.647734			
*50	107.7				1.154481	0.829364	1.45501

* predicted values for optimal processing conditions.

Chapter 5

CONCLUSIONS AND FUTURE WORK

§5.1 CONCLUSIONS

High strength cotton-based biodegradable nonwoven fabrics can be produced by using cotton/(Eastar/PP) at the blend ratio of 50/50 under the lower thermal calendering temperature around 108°C (peak strength is around 1.154kg) at the calendering pressure of 0.33MPa and the calendering speed of 10m/min with a basis weight of 40gsm.

Both bonding temperature and binder fiber content affect bond morphology. The shape of the bond becomes well-developed and the surface of the bond points becomes smoother with the increase of bonding temperature. The regular shape of the bond point and the smooth surface of the fabrics bonded at high bonding temperature show the well-developed bond structure. The carrier fibers and the cores of the binder fibers were deformed by the thermal bonding process. When the bonding temperature is sufficient, the shape of the bond becomes well-developed and the bond point becomes more film-like with the increase of binder fiber content.

The fractures for cotton/Eastar webs are generally brittle while the fractures for cotton/(PE/PET) webs are ductile. The fractures for cotton/(Eastar/PP) webs are between the two.

The failure mechanism of the fabrics with lower binder fiber content bonded at lower temperature is found to be due to the loss of interfacial adhesion at the bond site, leading to bond disintegration. The failure mechanism of the fabric with higher binder fiber content bonded at higher temperature is the result of the cohesive failure of the fibers in the bond point and/or near the bond periphery due to the loss of fiber integrity and formation of film-like spots at high temperatures, as well as the reduction in load transfer from fibers to film.

High weight loss was observed in the carding process for both low and high basis weight cotton/Eastar webs. Eastar binder fibers are not uniformly distributed in the webs and Eastar binder fiber bundles were observed in these webs. Binder fibers are better distributed in cotton/(Eastar/PP) webs and cotton/(PE/PET) webs.

DSC is a useful method to quantitatively characterize the binder fiber distribution in the carded cotton-based nonwovens by analyzing the specific enthalpy from crystallization of one of the binder fiber components in the fabrics. Binder fibers were not well-distributed in either cotton/(Eastar/PP) or cotton/(PE/PET) nonwovens since high variation and C.V. of the binder fiber content existed in both of the carded nonwoven series, according to the DSC quantitative measurement results. This result is further verified by the different trends of the effect of bonding temperature on tensile loads for strip tests and single bond tests for both the nonwoven series.

The strength of cotton/OCA can be improved by using either an external (water) or internal plasticizer or both of them. Water dip-nip treatment can replace a 20% acetone solvent treatment. The optimal processing conditions are either for cotton/OCA with water dip-nip treatment or cotton/PCA without treatment bonded at 190°C for both the blend ratios of 75/25 and 50/50. However, the optimal bonding temperature is relatively high and the overall strength of cotton/cellulose acetate nonwovens is lower compared to the control cotton/(PE/PET) nonwovens when using external and internal plasticizers.

Strengths of cotton/Eastar nonwovens are very low due to the low strength and high elongation of the Eastar binder fiber, which causes an unbalanced load sharing during tensile deformation. To this is added the binder fiber distribution problem during the carding process. The peak loads of cotton/(Eastar/PP) nonwoven fabrics are much higher than those of cotton/Eastar nonwoven fabrics. The peak strengths of cotton/(Eastar/PP) nonwoven fabrics are higher than or comparable to those of cotton/Cellulose Acetate nonwovens.

Empirical models have been developed to predict the breaking load of the webs based on the interactions of binder fiber composition and bonding temperature using the General Linear Models Procedure in JMP 5.0.

Binder fiber type and content and thermal calendering temperature are the main variables which determine the properties of thermal bonded nonwovens. With the increase in binder fiber content, peak load increases at a lower thermal bonding temperature. With the increase of calendering temperature, peak load increases at lower binder fiber content. However, at higher bonding temperatures and higher binder fiber

contents, the peak load decreases. This observed trend may be attributed to the different failure mechanism of the fabrics bonded at higher temperature.

The flexural rigidity increases with the increase of bonding temperature and binder fiber content for cotton/(Eastar/PP) nonwovens. That is, the fabrics become stiffer with an increase in bonding temperature.

Cotton/(Eastar/PP) nonwoven fabrics have good water absorbency and, even for the high strength fabrics at a blend ratio of 50/50, the absorption can reach 11 grams/gram, indicating that the fabrics have potential applications as absorbent materials. The total amount of absorption and the absorption rate decrease with the increase in bonding temperature and binder fiber content. Also the absorption of the fabrics is found to be directional, higher along the machine direction than that along the cross direction, indicating that fibers and capillaries are orientated more along the machine direction for the carded nonwovens.

§5.2 FUTURE WORK

The future work can be directed toward the following areas. First, there should be further development of 100% biodegradable nonwoven materials. The optimal combination obtained for this research is cotton/(Eastar/PP) in which the PP part cannot be biodegradable. Biodegradable substitutes such as PLA might be used for further study. A bicomponenet binder fiber with Eastar as the sheath is recommended because of its lower thermal calendering process temperature.

Secondly, studies should continue on the relationship of the fabric tensile strength and single bond tensile strength, and factors which affect the tensile property of both the fabric and the single bond are recommended. A computer-modeling program may be used to do the calculation and prediction.

The third recommendation is to theoretically characterize absorption properties of the resulting thermally-calendered nonwoven fabrics. Models may be developed based on the properties of the penetrated liquid and the physical properties of the constituent fibers and fabrics, which include fiber diameter, surface tension of the constituent fibers, crimps of the fiber, fiber linear density, pore size, pore distribution in the fabrics, bonded area, fabric thickness, fabric basis weight, and so on.

LIST OF REFERENCES

References

1. http://www.inda.org/category/nwn_index.html.
2. Bornhoeft, J.W., The Development of Nonwoven Fabrics and Products that are Friendly to the Environment, "Proc. TAPPI Nonwoven Conference," 1990, pp. 1-3.

3. Suh, H., Duckett, K.E. and Bhat, G.S., Biodegradable and Tensile Properties of Cotton/Cellulose Acetate Nonwovens, *Textile Res. J.* 66, 230-237 (1996).

4. Lichstein, B. M., "The Nonwovens Handbook," INDA, Association of the Nonwoven Fabrics Industry, New York, 1988.

5. Amass, W., Amass, A., and Tighe, B., A Review of Biodegradable Polymers: Uses, Current Developments in the Synthesis and Characterization of Biodegradable Polyesters, Blends of Biodegradable Polymers and Recent Advances in Biodegradation Studies, *Polym. Int.* 47, 89-144 (1998).

6. Ikada, Y., Tsuji, H., Biodegradable Polyesters for Medical and Ecological Applications, *Macromol. Rapid Commun.* 21, 117-132 (2000).

7. Duckett, K.E., Wadsworth, L.C., Tensile Properties of Cotton/Polyester Staple Fiber Nonwovens, "Proc. TAPPI Nonwoven Conference," 1987, pp. 121-127.

8. Duckett, K.E., Wadsworth, L.C., Physical Characterization of Thermally Point-Bonded Cotton/Polyester Nonwovens, "Proc. TAPPI Nonwoven Conference," 1988, pp. 99-107.

9. Moreau, J.P., Cotton Fiber for Nonwovens, *Tappi J.* 73, 179-184 (1990).

10. Duckett, K.E., Wadsworth, L.C., and Sharma, V., Comparison of Layered and Homogeneously Blended Cotton and Thermally Bonding Bicomponent Fiber Webs, *Tappi J.*, 78, 169-174 (1995).

11. Larson, G., "Biodegradable Staple Fiber Nonwovens Calendered with the Assistance of an Aqueous Solvent: Their Fabrication, Properties, and Structural Characteristics", Thesis, The University of Tennessee, 1997.

12. http://www.eastman.com/Brands/Eastar_Bio/Eastar_Bio_products.asp

13. http://www.inda.org/category/nwn_index.html

14. http://www.nonwovens.com/technology/mb/fiber_index.shtml

15. Karlsson, S., and Albertsson, A-C, Biodegradable Polymers and Environmental Interaction, *Polym. Engr. Sci.* 38(8), 1251-1253 (1998).

16. Haile, W.A., Tincher, M.E., Tanner, C.M., New Biodegradable Copolyester for Fiber and Nonwoven Applications, "Proceedings of EDANA Nonwovens Symposium," 2001.

17. Duckett, K.E., Bhat, G.S., Suh, H., Compostable and Biodegradable Compositions of A Blend of Natural Cellulosic and Thermoplastic Biodegradable Fibers, U.S. patent 5783505, 1998.

18. Nakagawa, M., Nakagawa, Y., Nishida, M., Hosokawa, J., Nishiyama, M., Kubo, T., Yoshihara, K., Biodegradable Nonwoven Fabric and its Molding Vessel, U.S. patent 5308663, 1994.

19. Wadsworth, L. et al, Melt Processing of PLA Resin into Nonwovens, "Proc. Of 3rd Annual TANDEC Conference," Knoxville, 1993.

20. Woodings, C., New Developments in Biodegradable nonwovens, *New Fibers*, February 9, 2001. http://www.technica.net/NF/NF3/biodegradable.htm

21. Muller, D.H., Krobjilowski, A., Meltblown Fabrics from Biodegradable Polymers, *Int. Nonwovens J.*, 10(1), 11-17 (2001).

22. Wnuk, A.J., Young, D.H., Alan, T., Biodegradable Polymeric Compositions and Products Thereof, U.S. patent 5939467, 1999.

23. Lunt, J., Polylactic Acid Polymers for Fibers and Nonwovens, *Int. Fiber J.* June 2000, 48-52.

24. Ramkumar, D.H.S., and Bhattacharya, M., Steady Shear and Dynamic Properties of Biodegradable Polyesters, *Polym. Engr. Sci.* 38(9), 1426-1435 (1998).

25. Potts, J.E., Clendinning, R.A., Ackart, W.B., Niegisch, W.D., *Polym. Sci. Technol.* 61, 3 (1973).

26. Tokiwa, Y., Suzuki, T., *Nature*, 76, 270 (1977).

27. http://www.eastman.com/Product_Information/ProductHome.asp?Product=1469

28. Meng, J., Seyam, A. M., and Batra, S. K., Carding Dynamics, Part I: Previous Studies of Fiber Distribution and Movement in Carding, *Textile Res. J.* 69, 90-

96 (1999).

29. http://www.nonwovens.com/technology/mb/bond_thermal.shtml

30. Hoyle, A.G., Thermal Bonding of Nonwoven Fabrics, *Tappi J.* 73, 85-88 (1990).

31. http://trcs.he.utk.edu/textile/nonwovens, 1999.

32. Dharmadhikary, R.K., Gilmore, T.F., Davis, H.A., and Batra, S.K., Thermal Bonding of Nonwoven Fabrics, *Textile Prog.* 26 (2), 1-37 (1995).

33. Shimalla, C.J., and Whitwell, J.C., Thermomechanical Behavior of Nonwovens, Part I: Responses to Changes in Processing and Post-Bonding, *Textile Res. J.* 46, 513-518 (1976).

34. De Angelis, V., Digiaoacchino, T., and Olivieri, P. Hot Calenderd Polypropylene Nonwoven Fabrics, "Proceedings of 2nd International Conference on Polypropylene Fibers and Textiles, Plastics and Rubber Institute," Univeristy of York, England, 1979, pp. 52.1-52.13.

35. Bastioli, C., Properties and Applications of Mater-Bi Starch-based Materials, *Polym. Degradation and Stability*, 59, 263-272 (1998).

36. Bechter, D., Kurz, G., Maag, E., and Schutz, J., Thermobonding of Nonwovens, *Textil-Prax.* 46, 1236-1240 (1991).

37. Malkan, S.R., Wadsworth, L.C., and Devis, C., Parametric Studies of the Reicofil Spunbonding Process, "Proc. Of 3rd TANDEC Conference," Knoxville, 1993.

38. Warner, S.B., Thermal Bonding of Polypropylene Fibers, *Textile Res. J.* 59, 151-159 (1989).

39. Dipl.-Ing., Krćma, R., "Manual of Nonwovens," The Textile Trade Press, Manchester, England, 1971,p. 107-144.

40. Kim, J.K., and Mai, Y.W., "Engineered Interfaces in Fiber Reinforced Composites," Elsevier Science Ltd., 1998, p. 6-38.

41. Childambaram, A., "Fundamentals of Fiber Bonding in Thermally Point Bonded Nonwovens", Thesis, North Carolina State University, 1998.

42. Turbak, A. F., "Nonwoven Engineering Principles, Nonwovens---Theory,

Process, Performance & Testing", Edited by TAPPI Press, GA, 1993.

43. Kwok, W. K., Crane, J.P., Gorrafa A. A-M., et al., Polyester Staple for Thermally Bonded Nonwovens, *Nonwovens Ind.* 19(6), 30-33 (1988).

44. Muller, D.H., How to Improve the Thermal Bonding of Heavy Webs, *INDA J. Nonwovens Res.* 1(1), 35-43 (1989).

45. Gibson, P.E., and McGill, R.L. Thermally Bondable Polyester Fiber: The Effect of Calender Temperature, *Tappi J.* 70, 82-86 (1987).

46. Bechter, D., Roth, A., Schaut, G., Ceballos, R., Kleinmann, K., and Schafer, K., Thermal Bonding of Nonwovens, *Melliand Textilberichte*, No.3, E39- 40 (1997).

47. Mi, Z.X., Batra, S.K., and Gilmore, T.F., "Computational Model for Mechanical Behavior of Point-Bonded Webs," First Annual Report, NCRC, 1992.

48. Wei, K.Y., Vigo, T.L., and Goswami, B.C. Structure-Property Relationships of Thermally Bonded Polypropylene Nonwovens, *J. Appl. Polym. Sci.* 30, 1523-1534 (1985).

49. Akai, M., and Aspin, A.F., Properties, Structure and Applications of Embossed Polypropylene Tapes, *Plast. & Rubber Process. & Appl.* 1, 327-329 (1981).

50. Chand, S., Bhat, G.S., Role of Fiber Morphology In Thermal Bonding, *Int. Nonwovens J.* 11(3), 12-20 (2002).

51. Wang, X., Michielsen, S., Morphology Gradients in Thermally Point-bonded Polypropylene Nonwovens, *Textile Res. J.* 71(6), 475-480 (2001).

52. L. F. Fryer, B. S. Gupta, Determination of Pore Size Distribution in Fibrous Webs and Its Impact on Absorbency, "Proceedings of 1996 Nonwovens Conference," 1996, pp. 321-327.

53. Chatterjee, P. K., "Absorbency," Elsevier, New York, 1985.

54. Gupta, B. S., The Effect of Structural Factors on Absorbent Characteristics of Nonwovens, *Tappi J.* 71, 147-152 (1988).

55. Gupta, B. S., and Crews, A. L., Nonwoven: An Advanced Tutorial, "The Effect of Fluid Characteristics in Nonwovens," TAPPI Press, Atlanta, GA, 1989.

56. Gupta, B. S., and Hong, C. J., Changes in Dimensions of Web During Fluid

Uptake and its Impact on Absorbency, *Tappi J.* 77, 181-188 (1994).

57. Gupta, B. S., Whang, H. S., Capillary Absorption Behaviors of Hydroentangled and Needlepunched Webs of Cellulosic Fibers, "Proceedings of INDA-TEC 96: International nonwovens conference," September 11-13, 1996, Hyatt Regency Crystal City, Crystal City, Virginia, USA.

58. Gupta, B.S., and Smith, D. K., Nonwovens in Absorbent Materials, *Textile Sci. and Technol.* 13, 349-388 (2002).

59. Lucas, R., Kolloid Z., "Ueber das Zeitgesetz des Kapillaren Aufstiegs von Flussigkeiten," 23, 15 (1918).

60. Washburn, E.W., The Dynamics of Capillary Flow, *Phys. Rev.* 17(3), 273 (1921).

61. Pagella, C., De Faveri, D. M., DSC Evaluation of Binder Content in Latex Paints, *Prog. in Organic Coatings*, 33, 211-217 (1998).

62. Zhao, M., Shen, B., and Liu, F., Analysis of Paraffin Wax Fraction in Asphalt by DSC, "Proceedings of International Symposium on Heavy Oil and Residue Upgrading and Utilization," 63-65 (1992).

63. Tripathy, A. R., Patra, P. K., Sinha, J. K., and Banerji, M. S., Application of Differential Scanning Calorimetry and Differential Thermogravimetry Techniques to Determine the Ratio of Blend Components in Reactive Chlorinated Elastomer Blends, *J. Appl. Polym. Sci.* 83, 937-948 (2002).

64. Hearle, J. W. S., A. Newton, *Textile Res. J.* 38, 343-351 (1968).

65. Muller, D.H., "Carding and Thermobonding of Nonwovens" Nonwovens Workshop, The University of Tennessee, Knoxville, 1988.

66. Hertel, K. L., and R. Lawson, *J. Textile Inst.* 70, 439-451 (1979).

67. Makoui, K.B., Performance Evaluation of Gravimetric Absorbency Tester (GAT), "Proceedings of 1996 Nonwovens Conference", 1996, pp. 199-203.

68. Allan, G. G., Ingalls, C.W., *Cellulose Chemistry and Technology*, 10, 801 (1976).

69. Tamhane, A. C., and Dunlop, D. D., "Statistics and Data Analysis: From Elementary to Intermediate," Prentice-Hall Inc., New Jersey, 2000.

APPENDIX

REFEREED PUBLICATIONS FROM THIS WORK

LIST OF PAPERS PUBLISHED

Binder Fiber Distribution and Tensile Properties of Thermally Point Bonded Cotton-Based Nonwovens

Haoming Rong, Gajanan S. Bhat

University of Tennessee, Knoxville, Tennessee 37996

Received 10 February 2003; accepted 1 August 2003

ABSTRACT: Cotton-based nonwovens are generally produced by carding and then bonding. One of the most important characteristics of nonwoven materials is the uniformity of their structure and properties. However, the carded webs always have irregularities caused by processing and material variables. The binder fiber distribution in carded cotton-based nonwoven fabrics was analyzed based on the crystallization behavior of one of the components of the binder fibers by DSC. The effects of process parameters, such as bonding temperature and binder fiber component, on the uniformity were discussed in detail in this article. Also, the relationship of binder fiber distribution and the strip tensile property and single-bond tensile strength were investigated. The results showed that if the binder fibers were not well distributed in the fabric, it would be hard to get the same trend of temperature effect on tensile property for the strip and single-bond tests. © 2004 Wiley Periodicals, Inc. J Appl Polym Sci 91: 3148–3155, 2004

Key words: nonwovens; thermal calendering; differential scanning calorimetry (DSC); specific heat; bicomponent binder fiber

INTRODUCTION

Carding is the most common process used to produce nonwoven fabrics from staple fibers. The objective of carding is to disentangle the fiber stock into individual fibers with minimum fiber breakage. Thus the carding process consists of opening and thoroughly blending different species of fibers. For cotton-based thermally point bonded nonwovens, it is important that the low-melting binder fiber be distributed evenly throughout to ensure uniformity of fabric properties. However, the carded webs always have area irregularities of mass distribution caused by machine variables (the nature and conditions of card clothing, the relative speeds and settings of the carding elements), fiber properties, and area irregularities of the fed fiber mat.[1] For any application, the most important characteristic of a carded web is uniformity of fiber areal density.

The mechanical properties of nonwoven fabrics depend on three groups of variables: the mechanical properties of the constituent fibers, which are the principal load carrying elements: the arrangement of the fibers in the web, which principally determines the web anisotropy, and the bonds that bind the fibers and transfer stresses.[2] Because strength is an extrinsic property, if some parts of a whole fabric sample are weakly bonded, such as regions with low binder fiber distribution, they may affect fabric strength significantly.

Correspondence to: H. Rong (hrong@utk.edu).

Journal of Applied Polymer Science, Vol. 91, 3148–3155 (2004)

Although binder fiber distribution can be qualitatively determined by either dyeing the binder fiber, then observing the fabrics under microscopy, or by observing the different shapes of binder fiber under scanning electronic microscopy (SEM), there is hardly any report on any method used to quantitatively characterize the binder fiber distribution of the carded webs. Differential scanning calorimetry (DSC) can be used to measure the heat flow to and from the sample as a function of temperature. Various materials characteristics can be determined from these data, including oxidative stability, purity, and polymorphism. Chemical reactions, melting behavior, and the temperature evolution of the specific heat can also be investigated.[3–5] In this article, DSC was used to determine the weight/weight concentration of the binder fiber in the thermally point bonded carded webs. Thus, the uniformity of the binder fiber distribution of the carded webs was evaluated by taking several measurements of specific enthalpy of cooling across the width of the web.

The objective of this study was to investigate the effect of binder fiber distribution on the mechanical properties of thermally bonded cotton-based nonwoven fabrics.

EXPERIMENTAL

Fibers

The fibers used in this study were cotton fiber, polyethylene/poly(ethylene terephthalate) (PE/PET) bicomponent binder fiber, and Eastar/polypropylene (PP) bicomponent binder fiber. The cotton fiber was supplied by Cotton Incorporated (Raleigh, NC). The

1

[1] Reprint permitted by JAP.

TABLE I
Properties of Selected Fibers (Single Filament)

Property	Cotton	PE/PET	Eastar/PP
Filament density (g/cm^3)	1.5	1.38	1.1
Filament tex (tex)	0.244	0.333	0.444
Peak strength (mN/tex)	152.2	264.8	269.6
Peak extension (%)	5.4	42.9	96.0
Initial modulus (mN/tex)	360.9	—	392.5
Staple length (in.)	0.96[a]	1.5	1.5

[a] Upper-half-mean fiber length.

scoured and bleached commodity cotton fiber had a moisture content of 5.2%, a micronaire value of 5.4, and an upper-half-mean fiber length of 24.4 mm (0.96 in.). The PE/PET bicomponent binder fiber was provided by Kosa, Inc. (Kingsport, TN). The Eastar *Bio* GP copolyester bicomponent (Eastar/PP) staple fibers were produced by Eastman Chemical Co. (Kingsport, TN). Both the bicomponent fibers have a sheath/core structure, with PE and Eastar *Bio* GP copolyester as the sheaths, and PET and PP as the stiffer cores. Properties of the three different fibers are listed in Table I. The two binder fibers have similar peak strength values, but Eastar/PP has an extension value twice that of PE/PET.

Nonwoven web processing procedures

The important steps in processing are shown in Figure 1. Fibers were first opened by hand and then weighed according to the desired blend ratio and fabric weight. The blend of fiber was then carded to form a web using a modified Hollingsworth card. The resulting carded fabric weights were about 40 g/m^2. The carded webs were then thermally point-bonded using a Ramisch Kleinewefers 60 cm (23.6 in.) wide calender with a bonded area of 16.6%. Three blend ratios (85/15, 70/30, and 50/50 of cotton/binder fiber), and two sets of calendering temperatures (100, 110, and 120°C; and 120, 130, and 140°C) were used for cotton/(Eastar/PP) series and cotton/(PE/PET) series, respectively. All the webs were calendered under the same nip pressure (0.33 MPa) at a constant speed of 10 m/min.

Characterizations

Tensile properties

The tensile properties of single-filament and nonwoven fabrics were tested using a united tensile tester according to ASTM D 3822-91 (Standard Test Method for Testing for Fiber/Filament) and ASTM D 1117-80 (Standard Test Method for Tensile Testing of Nonwoven Fabrics), respectively. All the tensile tests were carried out under the standard atmosphere for testing textiles, with temperature of 21 ± 1°C and relative humidity of 65 ± 2%.

Fabric weight

Basis weights of nonwoven fabrics were determined according to INDA Standard Test 130.1-92 (Standard Test Method for the Mass Per Unit Area of Nonwoven Fabrics).

Thermal analysis

The thermal properties of all the samples were analyzed using a Mettler differential scanning calorimeter (Model DSC-821, Mettler, Greifensee, Switzerland). Temperature calibration was performed using indium with the melting temperature of 156.56°C and heat of fusion (ΔH_f) of 28.54 J/g. To eliminate the effect of different heat histories of the two binder fibers during processing, the crystallization behavior of one of the binder fiber components was measured. For the cotton and PE/PET binder fiber series, the crystallization behavior of PE was measured. Samples (~ 5 mg) were first heated under nitrogen atmosphere (at a flow rate of 200 mL/min) at 150°C for 10 min to make sure the PE component of the binder fiber was fully melted, and then cooled to 50°C at a cooling rate of 10°C/min, whereas for the cotton and Eastar/PP binder fiber series, the crystallization behavior of PP was recorded. Samples (~ 5 mg) were first heated under a nitrogen atmosphere (at a flow rate of 200 mL/min) at 180°C for 10 min to make sure the PP component of the binder fiber was fully melted, and then cooled to 50°C at a cooling rate of 10°C/min.

The weight/weight concentration of the samples was obtained by calculating the ratio of the specific enthalpy of cooling for a certain web with the specific enthalpy of cooling for 100% binder fiber.

RESULTS AND DISCUSSION

Evaluation of DSC characterization method

To evaluate the accuracy of DSC measurement, first binder fiber and cotton fiber were manually blended

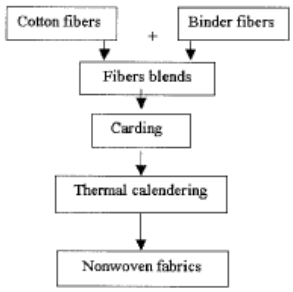

Figure 1 Flow chart of nonwoven web processing procedures.

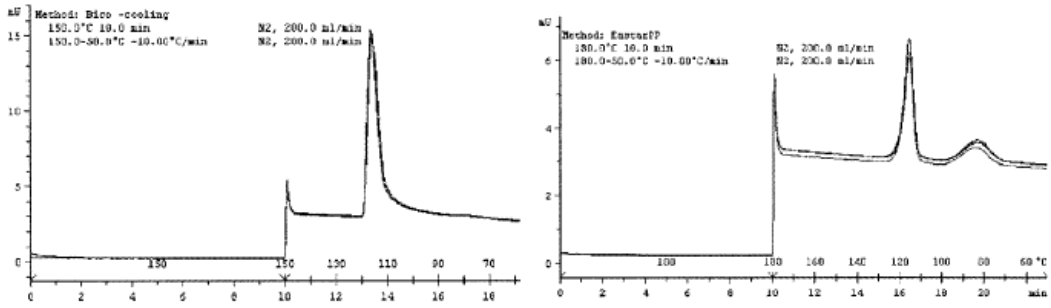

Figure 2 DSC traces of 100% binder fibers.

at different weight percentages, that is, binder fiber component of 100, 50, 40, 30, 20, and 10%. Each of the components was studied at least three times under the same conditions so that the standard deviation (σ) and the coefficient of variation (C.V.) could be measured. Figure 2(a) and (b) illustrates the DSC traces of 100% component of the two binder fibers.

Specific heat ($\Delta H/g$) values for the samples with 100% binder fibers were considered here as "Actual" as well as "Observed" for the sake of calculation. Subsequently, the "Observed" specific heats for the other components were calculated by the areas under the DSC exothermic peaks. Any error that occurred will be overcome by the conversion factor of gram (1000 mg) because the sample is taken at the milligram level for the DSC study. Then the "Observed" weight/weight concentration of the samples can be obtained by calculating the ratio of the specific heat at a certain component with the specific heat for 100% binder fiber. Parameters obtained from the DSC measurements for the two different binder fiber series are summarized in Tables II and III.

Because PE is the only component melted and crystallized during the measurement of cotton/(PE/PET) blends, there is no obvious effect of cotton component on the crystallization behavior of PE. This can be verified by the near constant onset crystallization temperatures and the peak crystallization temperatures under different PE/PET components in Table II. In the case of cotton/(Eastar/PP) blends, although both the components (Eastar and PP) in the binder fiber melted and crystallized, the presence of the Eastar component has no significant effect on the primary nucleation and crystallization of the PP component because the onset

TABLE II
Parameters Obtained from DSC Measurements for Cotton/(PE/PET) Blends[a]

"Actual" PE/PET (%)	$T_{o,c} = T_c$ (°C)	$T_{p,c}$ (°C)	ΔH_c (J/g)	Average ΔH_c (J/g)	σ (ΔH_c)	C.V.	"Observed" PE/PET (%)
100	119.17	116.75	89.49	90.20	2.241	0.025	100
	119.14	117.11	92.71				
	119.15	117.28	88.40				
50	118.93	117.32	44.46	44.23	0.854	0.019	49.04
	119.04	117.30	43.28				
	118.93	117.26	44.94				
40	118.95	117.23	36.89	35.80	1.047	0.029	39.69
	118.71	117.06	34.80				
	118.73	117.05	35.72				
30	118.64	117.06	26.50	26.31	0.219	0.008	29.17
	118.69	117.05	26.07				
	118.55	117.04	26.36				
20	118.66	116.96	17.66	17.42	0.216	0.012	19.31
	118.78	117.12	17.24				
	118.69	116.39	17.36				
10	118.26	116.53	8.38	8.31	0.110	0.013	9.21
	118.08	116.18	8.36				
	118.29	116.39	8.18				

[a] T, temperature; c, cooling or crystallizing; o, onset; p, peak; ΔH_c, the specific enthalpy for PE exothermic peak.

TABLE III
Parameters Obtained from DSC Measurements for Cotton/(Eastar/PP) Blends[a]

"Actual" Eastar/PP (%)	$T_{oc} = T_c$ (°C)	T_{pc} (°C)	ΔH_c (J/g)	Average ΔH_c (J/g)	σ (ΔH_c)	C.V.	"Observed" Eastar/PP (%)
100	121.69	116.68	28.09	27.95	0.997	0.036	100
	122.77	117.10	26.89				
	122.10	116.61	28.87				
50	123.28	117.86	13.20	13.69	0.595	0.043	48.98
	122.41	117.03	13.51				
	122.07	116.67	14.35				
40	121.81	116.68	11.39	11.15	0.490	0.044	39.89
	121.67	115.83	10.59				
	121.57	115.82	11.48				
30	121.51	116.00	8.34	8.33	0.38	0.046	29.79
	121.77	116.83	7.94				
	122.15	117.32	8.70				
20	121.83	117.30	6.13	5.70	0.373	0.065	20.39
	122.55	117.46	5.54				
	122.79	117.62	5.44				
10	121.93	117.18	2.66	2.81	0.216	0.077	10.05
	120.47	115.44	3.06				
	121.71	116.76	2.72				

[a] T, temperature; c, cooling or crystallizing; o, onset; p, peak; ΔH_c, the specific enthalpy for PP exothermic peak.

and peak crystallization temperatures of PP are almost stable for different Eastar/PP components of cotton/(Eastar/PP) blends (Table III). Therefore, there is no miscibility problem for both blend series. According to the data in Tables II and III, the "observed" binder fiber components are well fitted with the "actual" binder fiber components, with a variation of ±1%.

Results of the DSC measurements of specific enthalpy (ΔH_c) versus binder fiber weight concentration for the two binder fiber series are plotted in Figure 3(a) and (b). The regression lines fit both the binder fibers perfectly with regression coefficients of 0.99997 and 0.99987 for PE/PET binder fiber and Eastar/PP binder fiber, respectively.

Based on the preceding analysis, it appears that DSC specific enthalpy from crystallization of one of the binder fiber components in the cotton/binder blend series can be used to estimate binder fiber components in the samples.

Binder fiber distribution of carded nonwovens

To describe the binder distribution in the web, five different positions along the cross-direction were selected (as shown in Fig. 4) at each binder component. Parameters obtained from the DSC measurements for the two different carded nonwoven fabric series are summarized in Tables IV and V.

It may be observed from the data in Tables IV and V that, although the "observed" average binder fiber content is close to the "actual" binder fiber content along the cross direction for both the nonwoven series, high variation and C.V. of the binder fiber component existed in some of the webs for both the carded nonwoven series. Therefore, we can say that binder fibers were not well distributed in those nonwoven fabrics. Apparently, the variation is much higher for the nonwovens of lower(est) binder fiber component.

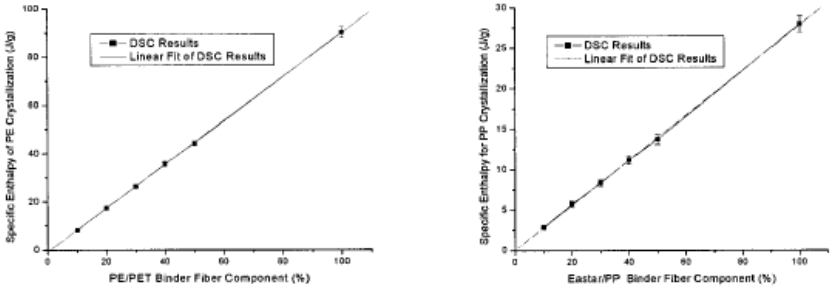

(a) PE/PET binder fiber (b) Eastar/PP binder fiber

Figure 3 DSC measured enthalpy versus binder fiber weight component.

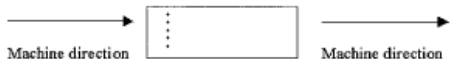

Figure 4 Schematic illustration of sample selection for nonwoven fabrics.

Effect of binder fiber component on peak load of cotton-based nonwovens

The effect of bonding temperature under different binder fiber components on fabric peak load along the machine direction (MD) can be seen from the data in Figure 5(a) and (b). It can be clearly seen that with the increase in binder fiber component, peak load increases at all the bonding temperatures. This is the result of the increase of binder fiber, which causes an increase in the number of bond points and the effective bond area.

With an increase in thermal bonding temperature, the peak load first increases and then decreases at higher bonding temperatures. The first increase in strength of the fabrics is the result of the formation of a better-developed bonding structure. This can be verified by observing the SEM micrographs of the bond points (Fig. 6). The regular shape of the bonding points and smooth surface of the fabrics bonded at relatively high bonding temperature show the well-developed bond structure. However, with a further increase in bonding temperature the peak load decreases. This may be caused by a different failure mechanism of the fabrics bonded at higher temperatures.[6]

Failure of nonwoven fabrics can occur by failure of the fiber (fiber breakage), failure within the bond (adhesive breakage or cohesive failure) or at the fiber–binder bonding interface, or by a combination of these

TABLE IV
Parameters Obtained from DSC Measurements for Cotton/(PE/PET) Nonwovens[a]

"Actual" PE/PET (%)	$T_{o,c} = T_c$ (°C)	$T_{p,c}$ (°C)	ΔH_c (J/g)	"Observed" PE/PET (%)	Average PE/PET (%)	σ	C.V.
50	118.84	117.24	59.00	65.41	51.83	11.9	0.230
	118.82	117.15	52.45	58.15			
	118.80	117.28	42.29	46.88			
	118.68	116.92	49.17	54.51			
	118.64	116.83	30.86	34.21			
30	118.71	117.19	28.23	31.30	27.85	7.02	0.252
	118.68	117.17	26.82	29.73			
	118.73	117.21	33.15	36.75			
	118.49	116.94	18.00	19.96			
	118.58	116.94	19.40	21.51			
15	118.65	117.01	20.63	22.87	14.42	6.64	0.460
	118.46	116.82	17.82	19.76			
	118.40	116.87	6.87	7.62			
	118.56	117.06	11.37	12.61			
	118.51	117.01	8.33	9.24			

[a] "Actual" PE/PET (%) is the input % for the carding process; T, temperature; c, cooling or crystallizing; o, onset; p, peak; ΔH_c, the specific enthalpy for PE exothermic peak.

TABLE V
Parameters Obtained from DSC Measurements for Cotton/(Eastar/PP) Nonwovens[a]

"Actual" Eastar/PP (%)	$T_{o,c} = T_c$ (°C)	$T_{p,c}$ (°C)	ΔH_c (J/g)	"Observed" Eastar/PP (%)	Average Eastar/PP (%)	σ	C.V.
50	121.50	117.06	13.87	49.62	47.52	3.97	0.083
	121.33	116.88	13.98	50.02			
	121.14	116.71	14.26	51.02			
	121.23	116.31	12.65	45.26			
	120.64	115.95	11.65	41.68			
30	120.71	116.52	10.67	38.18	31.09	4.61	0.148
	120.65	116.50	7.60	27.19			
	121.27	116.84	8.55	30.59			
	120.21	116.29	7.53	26.94			
	120.74	116.62	9.10	32.56			
15	123.02	118.80	5.47	19.57	13.98	4.81	0.344
	123.16	119.13	4.35	15.56			
	122.89	118.79	3.30	11.81			
	122.93	118.75	4.48	16.03			
	122.99	118.89	1.93	6.91			

[a] "Actual" Eastar/PP (%) is the input % for the carding process T, temperature; c, cooling or crystallizing; o, onset; p, peak; ΔH_c, the specific enthalpy for PP exothermic peak.

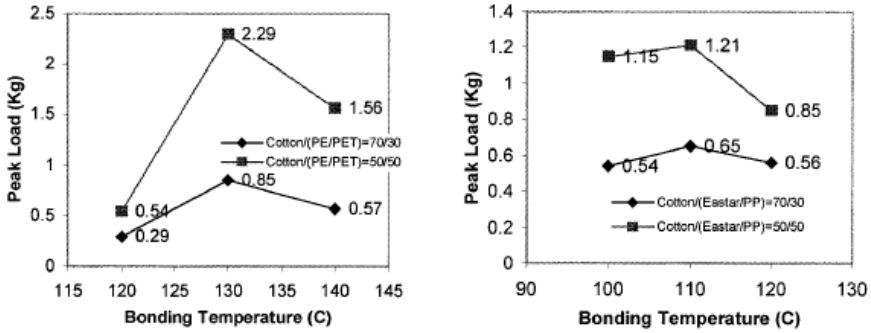

Figure 5 Effect of bonding temperature on peak load of cotton-based nonwovens (machine direction). Fabric weight: about 40 g/m^2; calendering pressure: 0.33 MPa; calendering speed: 10 m/min.

modes. The interaction of component properties, structure, and fabric deformation mechanisms can lead to a variety of unique failure mechanisms for nonwoven fabrics. The nonwoven fabric failure mechanism is influenced by fiber physical properties, adhesive properties, and structural properties including the relative frequency and structure of the bonding elements, fiber orientation, and the degree of liberty of movement of the fibers between the bond points. Physical properties of the nonwoven fabrics will be controlled by the first failure occurring in the fabric sample.[7] We can say that the failure mechanism of nonwoven fabrics bonded at higher temperature is different from that of the nonwoven fabrics bonded at a lower calendering temperature. This difference in failure mechanism can be confirmed by the SEM micrographs of the failure structures of the fabrics produced at different bonding temperatures (Fig. 7). These observations are consistent with those of Gibson and McGill,[8] who studied the failure mechanism of thermally point bonded polyester nonwovens as a function of bonding temperature. At low bonding temperatures, the bond failure mechanism was found to be attributed to loss of interfacial adhesion at the bond site leading to bond disintegration. At higher bonding temperatures, the failure mechanism was cohesive failure of the fibers near the bond site attachment point. Similar observations were made with PP thermally bonded and spunbonded nonwovens by Bhat et al.[9,10]

Single bond strip tensile test results of the cotton-based nonwoven fabrics

To further analyze the effect of binder fiber distribution on fabric strength, a single-bond strip tensile test

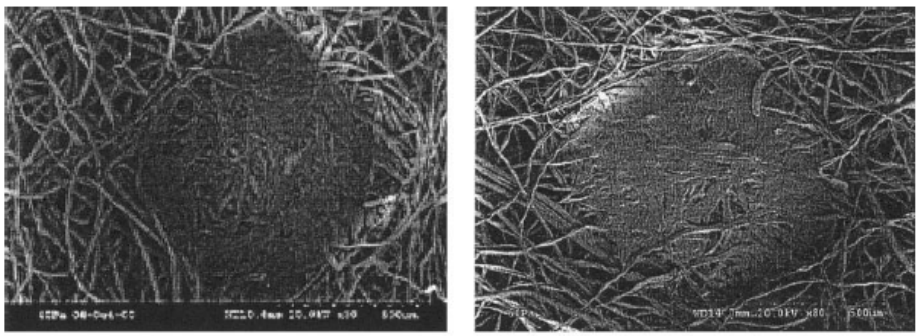

(a) Cotton/(PE/PET): 70/30
Bonding Temperature: 130°C
Calendering Pressure: 0.33MPa
Calendering speed: 10m/min
Fabric weight: ~ 40g/m^2

(b) Cotton/(Eastar/PP): 70/30
Bonding Temperature: 110°C
Calendering Pressure: 0.33MPa
Calendering speed: 10m/min
Fabric weight: ~ 40g/m^2

Figure 6 SEM micrographs of cotton-based nonwoven fabrics.

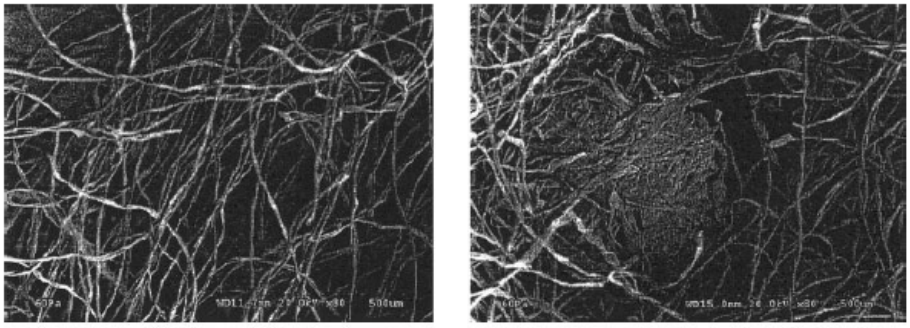

(a) Bond disintegration during break
Cotton/(Eastar/PP): 70/30
Bonding Temperature: 100°C
Calendering Pressure: 0.33MPa
Calendering speed: 10m/min
Fabric weight: ~ 40g/m^2

(b) Failure of the fibers near bond site
Cotton/(Eastar/PP): 70/30
Bonding Temperature: 120°C
Calendering Pressure: 0.33MPa
Calendering speed: 10m/min
Fabric weight: ~ 40g/m^2

Figure 7 SEM micrographs of failure structure after tensile testing for cotton/(Eastar/PP) nonwoven fabrics (machine direction).

was carried out for the two cotton-based nonwoven fabrics series. This test was done to estimate the bond strength and the degree of load sharing between fibers during the tensile deformation of the web. A schematic of this test is shown in Figure 8. A strip of size 80 × 5 mm was cut from the web. The strip was cut across the width direction from the two sides to leave only one bond uncut in the middle of the strip. The strip was then subjected to a conventional tensile test. The test was conducted on the United Tensile Tester with a gauge length of 1 in. (2.54 cm) and extension rate of 0.5 in./min (1.27 cm/min). A total of 20 tests were done for each sample.

Results of the single-bond strip tensile test for the two binder fiber series are shown in Figure 9(a) and (b). If the binder fibers were well distributed in the nonwoven fabrics, the effect of bonding temperature on the tensile strength of strip fabrics should be consistent with that of the single-bond strips.

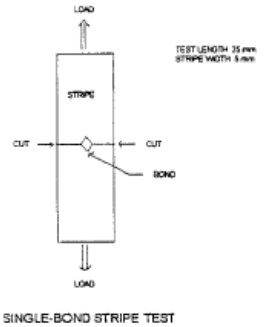

Figure 8 Schematic illustration of single-bond strip tensile test.

Comparing Figure 9 with Figure 5, we can see that the trends of the peak load data in the two figures are not exactly the same. In the case of cotton/(PE/PET) nonwovens, at a binder fiber component of 30%, the trend of the curve for the strip test is the same as that for the single-bond strip test, whereas for the binder fiber component of 50%, the trend of the peak load for the strip test does not follow the same trend as that of the single-bond strip test. This is the result of the high variation of binder fiber distribution along the cross-direction of the fabric. The standard deviation of the fabric with 50% PE/PET binder fiber is 11.90, listed in Table IV, which is much higher than that of the fabric with 30% PE/PET binder fiber (7.02), although the C.V. values of the two fabrics are close to each other.

However, in the case of cotton/(Eastar/PP) nonwovens, at the binder fiber component of 50%, the trend of the peak load for the strip test is the same as that for the single-bond strip test, whereas for the binder fiber component of 30%, the trend of the peak load for the strip test does not follow the same trend as that of the single-bond strip test. Again, it is the result of the high variation of binder fiber distribution along the cross-direction of the fabric with binder fiber component of 30%. The C.V. and standard deviation of the fabric with 30% Eastar/PP binder fiber are 14.8% and 4.61, respectively, listed in Table V, which are higher than those of the fabric with 50% Eastar/PP binder fiber, which are 8.3% and 3.94, respectively.

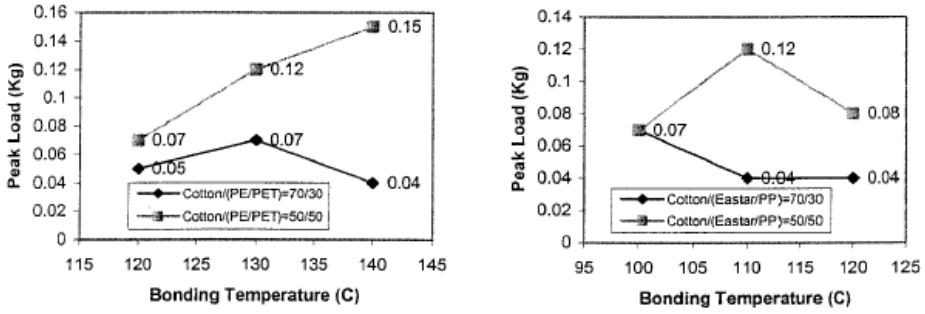

(a) Cotton/(PE/PET) nonwovens (b) Cotton/(Eastar/PP) nonwovens

Figure 9 Effect of bonding temperature on peak load of single-bond strips (machine direction). Fabric weight: about 40 g/m^2; calendering pressure: 0.33 MPa; calendering speed: 10 m/min.

CONCLUSIONS

The results show that DSC is a useful and a reliable method for studying the binder fiber distribution in the carded cotton-based nonwovens by analyzing the specific enthalpy from crystallization of one of the binder fiber components in the fabrics. Because a high standard deviation and C.V. of the binder fiber component existed in both of the carded nonwoven series according to DSC measurement results, we can conclude that binder fibers were not well distributed in those nonwoven fabrics series. This result is consistent with the comparison of tensile test results of fabric strips and single-bond strips. If the binder fibers were well distributed in the nonwoven fabrics, the effect of bonding temperature on the tensile property of strip fabric should be consistent with that of the single bond strip. In fact, the trends of the tensile curves under different bonding temperatures for the two binder fiber series are not exactly the same. This further verified that binder fibers were not well distributed on those carded nonwoven fabrics, especially for certain compositions.

Binder fiber component and bonding temperature are the two main variables that determine the properties of final thermal bonding nonwoven products. With the increase of binder fiber component, the peak load increases. With the increase of bonding temperature, the peak load first increases and then decreases with further bonding temperature increase. The initial increase in strength of the fabrics is the result of the formation of a better-developed bonding structure. The further decrease of peak load may be caused by the different failure mechanism of the fabrics bonded at higher temperature.

The authors thank Cotton Incorporated, Raleigh, NC and Tennessee Agricultural Experimental Station for the financial support; and Kosa Inc. and Eastman Chemical Company, Kingsport, TN for providing binder fibers for this study.

References

1. Meng, J.; Seyam, A. M.; Batra, S. K. Text Res J 1999, 69, 90.
2. Erel, S.; Warner, S. B. Text Res J 2001, 71, 22.
3. Pagella, C.; De Faveri D. M. Prog Org Coat 1998, 33, 211.
4. Zhao, M.; Shen, B.; Liu, F. In: Analysis of Paraffin Wax Fraction in Asphalt by DSC, Proceedings of the International Symposium on Heavy Oil and Residue Upgrading and Utilization, 1992; pp. 63–65.
5. Tripathy, A. R.; Patra, P. K.; Sinha, J. K.; Banerji, M. S. J Appl Polym Sci 2002, 83, 937.
6. Rong, H.; Bhat, G. S. Int Nonwovens J 2003, 12, 53.
7. Hansen, S. M. Nonwoven Engineering Principles: Nonwovens—Theory, Process, Performance, and Testing; Turbak, A. F., Ed.; TAPPI Press: Atlanta, GA, 1993; Chapter 5.
8. Gibson, P. E.; McGill, R. L. In: Proceedings of the 1987 TAPPI Nonwovens Conference; TAPPI Press: Atlanta, GA, 1987; p. 129.
9. Bhat, G. S.; Kotra, R.; Nanjundappa, R.; In Proceedings of INTC 2001, September 5–7, 2001, Baltimore, MD.
10. Bhat, G. S.; Chand, S.; Spruiell, J. E.; Malkan, S. R. Thermochim Acta 2001, 367/368, 155.

ORIGINAL PAPER/PEER-REVIEWED

Preparation and Properties Of Cotton-Eastar Nonwovens

By Haoming, Rong and Gajanan, S. Bhat, Department of Materials Science and Engineering, The University of Tennessee, Knoxville, TN 37996

Abstract

As biodegradable/compostable cotton-based nonwovens are sustainable materials, there is increasing interest in them, with the expansion of nonwovens into novel applications. Over the past few years, research has been done at the University of Tennessee, Knoxville to produce and evaluate nonwoven products containing cotton/cellulose acetate fibers. Nonwoven fabrics manufactured from cotton and Eastar, a biodegradable thermoplastic fiber have shown great promise. The production of nonwovens by the thermal bonding process from such compositions, and the structure and properties of the resulting products are investigated. The results have shown that, by appropriately selecting the combination of fibers and process conditions, nonwoven fabrics with good performance properties can be produced.

Keywords

Nonwovens, Cotton, Eastar Bio copolyester, Thermal Bonding, Compostable

Introduction

In recent years, nonwoven fabrics have been widely used in many applications including, home furnishings, automotive industry, civil engineering, geotextiles, industrial filters and medical sanitary materials. More than 50% of these nonwoven fabrics are disposable products [1]. Majority of these products are made of synthetic fibers, such as polypropylene, polyethylene, polyester and polyamide, which are not biodegradable and end up as solid waste. With the growing environmental awareness throughout the world, environmentally compatible nonwoven products have been receiving increasing attention in recent years [2, 3].

Cotton-based biodegradable/compostable nonwovens become a major choice, due to the good properties of cotton fibers, such as biodegradability, softness, absorbency and breathability. Cellulose Acetate (CA) fiber has shown to be a good binder fiber for cotton-based biodegradable/compostable thermal calendered nonwoven products by the University of Tennessee, because it is a thermoplastic, hydrophilic and a biodegradable fiber. However, the softening temperature of cellulose acetate fiber is relatively high (Ts: 180-205°C), even in the presence of some kinds of internal and/or external plasticisers [4,5]. Recently Eastman Chemical Co. developed the "Eastar Bio," GP copolyester (Eastar) unicomponent [6] fiber, which can be totally degraded into CO2, H2O and biomass. Eastar unicomponent fiber and an "Eastar Bio," GP copolyester bicomponent (Eastar/PP) fiber were selected as binder fibers instead of cellulose acetate, to make thermal calendered nonwoven products. Another advantage of these binder fibers is their relatively low melting temperature (110°C) of the Eastar component.

The effect of some key processing variables, such as blend ratio and bonding temperature, was studied. Preparation and the structure and properties of cotton/Eastar nonwoven fabrics are discussed in this paper.

Experimental

Fiber Selection and Properties

The cotton fiber used in this research was supplied by Cotton Incorporated. The scoured and bleached commodity cotton fiber had a moisture content of 5.2%, a micronaire value of 5.4 and an upper-half-mean fiber length of 24.4 mm (0.96 inch). The "Eastar Bio", GP copolyester (Eastar) unicomponent and bicomponent (Eastar/PP) staple fibers selected for this study were produced by Eastman Chemical Company. The bicomponent fiber has a sheath/core structure, with

[1] Reprint permitted by INJ.

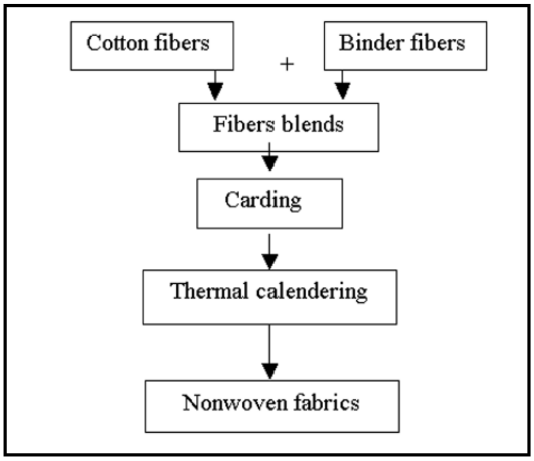

Figure 1
FLOW CHART OF PROCESSING PROCEDURES

"Eastar Bio," GP copolyester as the sheath on a stiffer core, in this case, polypropylene.

Processing

The important steps in processing are shown in *Figure 1*. Fibers were first opened by hand and then weighed according to the desired blend ratio and fabric weight. The blend of fiber was then carded to form a web using a modified Hollingsworth card. The resulting carded fabric weights varied from 40 grams/m² to 80 grams/m². The carded webs were then thermally point-bonded using a Ramisch Kleinewefers 60 cm (23.6 inches) wide calender with a bonded area of 16.6%. Three blend ratios (85/15, 70/30, and 50/50 of Cotton/Binder fiber), three calendering temperatures (100 °C, 110 °C, and 120 °C), and two nip pressures (0.33 MPa, and 0.4 MPa) were used. All the webs were calendered under the same speed of 10 m/min.

Characterization

Tensile properties of single filament and nonwoven fabrics were tested according to ASTM D 3822-91 Standard Test Method for Testing for Fiber/Filament and ASTM D 1117-80 Standeard Test Method for Tensile Testing of Nonwoven Fabrics respectively. All the tensile tests were carried out under the standard atmosphere for testing textiles, the temperature of 21 ± 1° C and the relative humidity of 65 ± 2%.

Thermal analysis of the binder fiber was done using the Mettler DSC25 machine at a scanning rate of 10°C/min.

Basis weight of nonwoven fabrics was determined according to INDA Standard Test 130.1-92 Standard Test Method for the Mass Per Unit Area of Nonwoven Fabrics.

Scanning Electron Microscopy (SEM) pictures were taken for bonding points and failure structure under a Hitachi S - 3500 N Scanning Electron Microscope. 20.0 KV electronic beam, 50 MPa vacuum, and a magnification of 80 were used for the images.

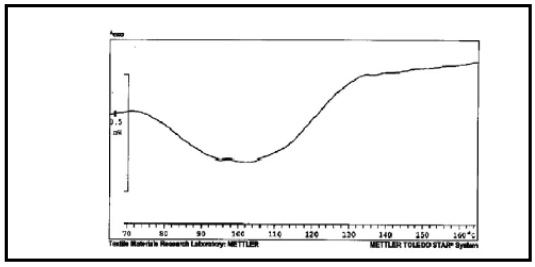

Figure 2
DSC SCAN OF EASTAR STAPLE FIBER
(HEATING RATE 10°C/MIN

Results and Discussion

Fiber Properties

Physical properties of all the fibers used in this research are listed in *Table 1*. The data show that the tenacity or peak strength of Eastar unicomponent fiber is comparable to that of cotton fiber, while the tenacity or peak strength of Eastar bicomponent (Eastar/PP) fiber is much higher than that of cotton fibers, for the peak extension of both Eastar unicomponent and bicomponent fiber are much higher than that of the cotton fibers.

A DSC scan of Eastar staple fiber is shown in *Figure 2*. The melting temperature of the fiber is around 110°C. This is much lower than that of the cellulose acetate fibers (which is around 250°C) that have been investigated as binder fibers. Based on this, thermal calendering temperatures to be used will be relatively lower.

Effect of Eastar Fiber Component on Peak Load of Cotton/Eastar Nonwovens

The effect of Eastar fiber component on fabric peak load along the machine direction can be seen from the data in

Table 1
PROPERTIES OF SELECTED FIBERS
(SINGLE FILAMENT).

	Cotton	Eastar	Eastar/PP
Filament density (g/cm³)	1.5	1.2	1.1
Filament tex (tex)	0.24	0.44	0.44
Peak extension (%)	5.4	144.0	96.0
Peak strength (mN/tex)	152.2	138.0	269.6
Initial modulus (mN/tex)	360.9	204.6	392.5
Staple length (inches)	0.96*	1.0	1.5
Crimps (/inch)	**	Not measurable	11

* upper-half-mean fiber length
** cotton has natural convolutions

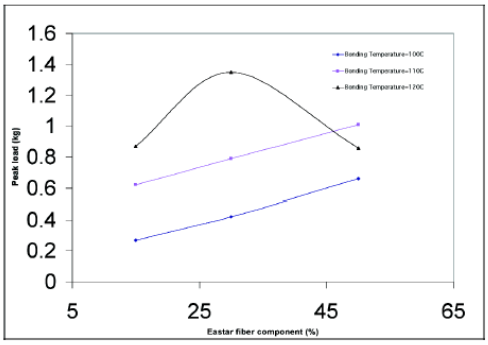

Figure 3
EFFECT OF EASTAR BINDER FIBER COMPONENT ON PEAK LOAD ALONG MACHINE DIRECTION OF COTTON/EASTAR NONWOVENS.
Fabric weight: ~ 80 g/m²
Calendering pressure: 0.33 MPa
Calendering speed: 10 m/min

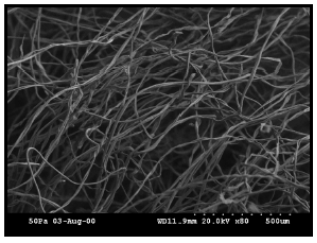

(a) Bond disintegration during break
Cotton/Eastar=70/30
Bonding Temperature=120°C
Calendering Pressure=0.33MPa
Calendering speed=10m/min
Fabric weight: ~ 80g/m²

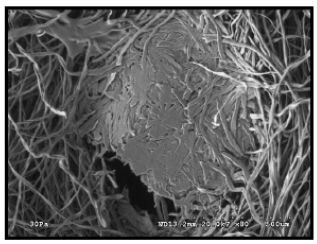

(b) Failure of the fibers near bond site
Cotton/Eastar=50/50
Bonding Temperature=120°C
Calendering Pressure=0.33MPa
Calendering speed=10m/min
Fabric weight: ~ 80g/m²

Figure 4
SEM PHOTOGRAPHS OF SAMPLES AFTER TENSILE TESTING FOR COTTON/EASTAR NONWOVEN FABRICS (ALONG MACHINE DIRECTION)

Figure 3. With the increase of Eastar binder fiber component, peak load increases at the lower thermal bonding temperature. This is the result of the increase in Eastar fiber, which causes increases in the number of bond points and the effective bond area. However, at a higher bonding temperature (120°C) and higher Eastar binder fiber component (Eastar component above 30%), the peak load decreases with the increase in Eastar binder fiber. This may be caused by the different failure mechanism of the fabrics bonded at higher temperature.

Failure of nonwoven fabrics can occur by the failure of the fiber (fiber breakage), failure within the bond (bond breakage or cohesive failure) or at the fiber-binder bonding interface, or by a combination of these modes [7-8]. The interaction of component properties, structure, and fabric deformation mechanisms can lead to a variety of unique failure mechanisms for nonwoven fabrics. The nonwoven fabric failure mechanism is influenced by fiber physical properties, adhesive properties, and structural properties including the relative frequency and structure of the bonding elements, fiber orientation and the degree of liberty of movement of the fibers between the bond points. Physical properties of the nonwoven will be controlled by the first failure occurring in the fabric sample [9]. Based on this, we can say that the failure mechanism of nonwoven fabrics of high Eastar binder fiber component bonded at a higher temperature is different from that of the nonwoven fabrics bonded at a low calendering temperature. This difference in failure mechanism can be clearly seen by the SEM pictures of the failed structures of the fabrics produced with different binder fiber compositions *(Figure 4)*. These observations are consistent with those of Gibson and McGill [10], who have studied the failure mechanism of thermal point-bonded polyester nonwovens as a function of the bonding temperature. At low binder fiber component and lower bonding temperatures, the bond failure mechanism was found to be the loss of interfacial adhesion at the bond site leading to bond disintegration; at higher binder fiber component and higher bonding temperatures, the failure mechanism was cohesive failure of the fibers near the bond periphery.

Effect of Bonding Temperature on Peak Load of Cotton/Eastar Nonwovens

The effect of bonding temperature on fabric peak load along the machine direction is shown in *Figure 5*. With the increase in calendering temperature, peak load increases at lower binder fiber component (≤ 30%). The observed increase in strength of the fabrics is the result of the formation of better-developed bonding structure. This phenomenon can be verified by observing the SEM pictures of the bonding point *(Figure 6)*. The regular shape of bond point and smooth surface of the fabrics bonded at high bonding temperature *(Figure 6(b))* show the well-developed bond structure. Again, the decrease of peak load at higher binder fiber component and higher bonding temperature is due to the different failure mechanism of the nonwoven fabrics. The decrease in peak load at higher bonding temperature was attributed to the loss of fiber integrity and formation of film-like spots at high temperature, as well as the reduction in load transfer from fibers to bond points [11,12].

Tensile Property Comparison of Cotton/Eastar and Cotton/(Eastar/PP) Nonwovens

One disadvantage in using Eastar unicomponent as-spun fiber as a binder fiber is that it is hard to get the binder fibers

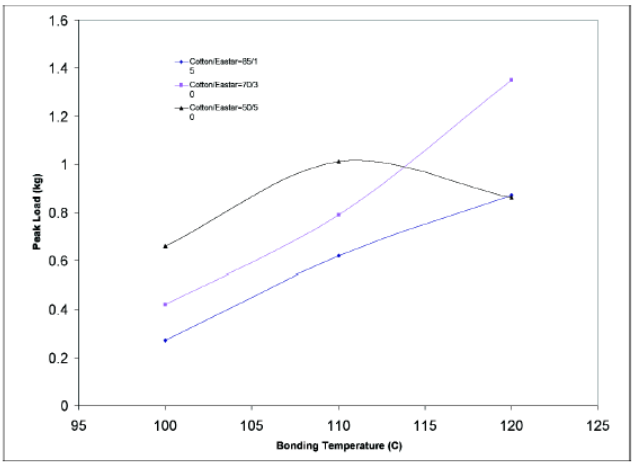

Figure 5
EFFECT OF BONDING TEMPERATURE ON PEAK LOAD ALONG MACHINE DIRECTION OF COTTON/EASTAR NONWOVENS.
Fabric weight: ~ 80 g/m²
Calendering pressure: 0.33 MPa
Calendering speed: 10 m/min

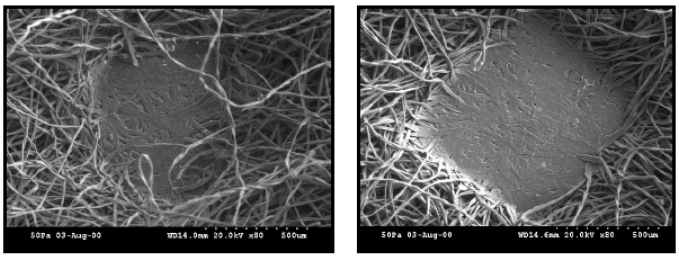

(a) Cotton/Eastar=70/30
Bonding Temperature=100°C
Calendering Pressure=0.33MPa
Calendering speed=10m/min
Fabric weight: ~ 80g/m²

(b) Cotton/Eastar=70/30
Bonding Temperature=120°C
Calendering Pressure=0.33MPa
Calendering speed=10m/min
Fabric weight: ~ 80g/m²

Figure 6
SEM PICTURES OF COTTON/EASTAR (70/30) FABRICS

well distributed due to the high elasticity of the fiber (high peak extension and low modulus), which leads to low tensile properties of the final nonwoven fabrics. So a bicomponent fiber, Eastar/PP, with Eastar Bio, GP copolyester as the sheath, and polypropylene as the stiffer core was selected as the binder fiber instead of Eastar unicomponent fiber. *Figure 7(a, b)* show that at the two blend ratios cotton/binder fiber around 70/30 and 50/50, and the three bonding temperatures (100°C, 110°C, 120°C), the peak loads of Cotton/(Eastar/PP) nonwoven fabrics are much higher than that of Cotton/Eastar nonwovens. Therefore, using Eastar/PP bicomponent fiber as a binder fiber can improve the tensile properties of Cotton/Eastar nonwoven fabrics. This improvement in tensile properties is the result of better binder properties as well as improved processing characteristics of the modified binder fiber.

Based on the above, high strength Cotton/(Eastar/PP) nonwoven fabrics can be produced by using Cotton/(Eastar/PP) at a blend ratio of 50/50, thermal calendered at 110°C under 0.33 MPa pressure. In fact the tensile properties of Cotton/(Eastar/PP) nonwoven fabrics were found to be comparable to, or better than that of Cotton/Cellulose Acetate nonwovens [13].

Conclusions

Binder fiber component and calendering temperature are the two main variables, which determine the properties of thermal bonded nonwovens. With the increase in Eastar (binder) fiber component, peak load increases at a lower thermal bonding temperature. However, at higher bonding temperatures (e.g. 120°C) and higher Eastar binder fiber components (Eastar > 30%), the peak load decreases. This may be caused by the different failure mechanism of the fabrics bonded at higher temperature. With the increase of calendering temperature, peak load increases at lower binder fiber component. With the increase of bonding temperature at lower binder fiber component, the increase in peak load of the fabrics is the result of the formation of better-developed bonding structure.

Good quality cotton-based nonwoven fabrics can be made using Eastar/PP bicomponent binder fiber under lower calendering temperature (around 110°C). Peak load of Cotton/(Eastar/PP) nonwoven fabrics are much higher than Cotton/Eastar nonwoven fabrics. Peak strength of Cotton/(Eastar/PP) nonwoven fabrics are higher than or comparable to that of Cotton/Cellulose Acetate nonwovens. High strength Cotton/Eastar nonwoven fabrics can be produced by using Cotton/(Eastar/PP) at a blend ratio of 50/50, thermal calendering at 110°C under the pressure of 0.33 MPa with a calendering speed of 10 m/min.

Acknowledgements

The authors thank Cotton Incorporated, Raleigh, NC and Tennessee Agricultural Experimental Station for the financial support, and Eastman Chemical Company, Kingsport, TN for providing fibers for this study.

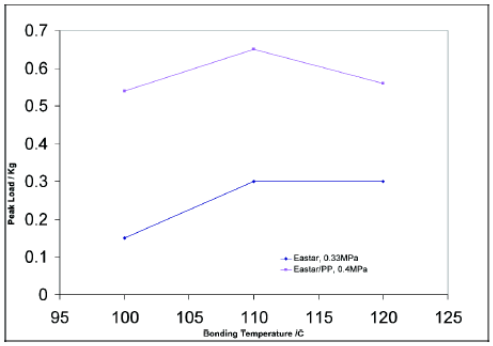

(a) Cotton/binder=70/30
Calendering Pressure=0.33 ~ 0.4 MPa
Calendering speed=10m/min
Fabric weight: ~ 40g/m²

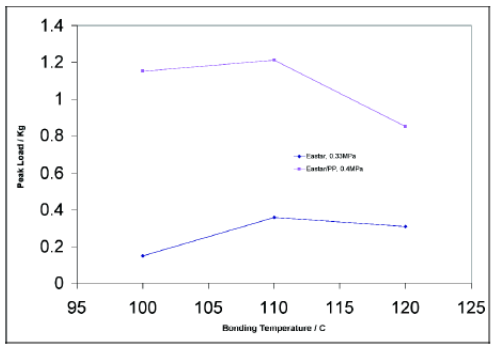

(b) Cotton/Eastar=50/50
Calendering Pressure=0.33 ~ 0.4 MPa
Calendering speed=10m/min
Fabric weight: ~ 40g/m²

Figure 7
EFFECT OF BINDER FIBER ON PEAK LOAD ALONG MACHINE DIRECTION OF COTTON/EASTAR NONWOVENS.

References

1. www.nonwovens.com/facts/markets/overview.htm.

2. John W. Bornhoeft, The Development of Nonwoven Fabrics and Products that are Friendly to the Environment, TAPPI Proceedings, 1990 Nonwovens Conference.

3. Suh, H., Duckett, K.E. and Bhat, G.S., Biodegradable and Tensile Properties of Cotton/Cellulose Acetate Nonwovens, *Textile Res. J.*, 66, 1996, 230-237.

4. Larson, G., Biodegradable Staple Fiber Nonwovens Calendered with the Assistance of an Aqueous Solvent: Their Fabrication, Properties, and Structural Characteristics, Thesis, The University of Tennessee, 1997.

5. Gao, X., Duckett, K. E., Ghat, G., Rong, H. M., Effects of Water on Processing and Properties of Thermally Bonded Cotton/Cellulose Acetate Nonwovens, *Int. Nonwovens J.*, 10(2), 21-25, 2001.

6. Haile, W. A., Bhat, G.S.,Williams F. W., Biodegradable copolyester for fibers and Nonwovens, *Int. Nonwovens J.*, summer 2002, 39-43.

7. Nanjundappa R., Bhat, G. S., Processing and Characterization of a PP Homopolymer in a Reicofil Spunbonding Process, Submitted to *International Nonwovens Journal*.

8. Bhat, G. S. and Nanjundappa, R., Structure and Properties of Spunbond Nonwovens from Propylene Polymers, Proceedings of the PP World Congress, Huddersfield, UK, July 2000.

9. S. M. Hansen, Nonwoven Engineering Principles, Nonwovens---Theory, Process, Performance & Testing, Edited by A. F. Turbak, TAPPI Press, GA, 1993, Chapter 5.

10. Gibson, P.E., McGill, R.L., 1987 TAPPI Nonwovens Conference Proceedings, TAPPI PRESS, Atlanta, p. 129.

11. Kwok, W. K., Crane, J.P., Gorrafa A. A-M., et al., Polyester Staple for Thermally Bonded Nonwovens, *Nonwovens Industry*, 19(6), 1988, 30-33.

12. Muller, D.H., How to Improve the Thermal Bonding of Heavy Webs, *INDA Journal of Nonwovens Research*, 1(1), 1989, 35-43.

13. Bhat, G., Rong, H. M., Effect of Binder Fiber on the Processing and Properties of Thermal Bonded Cotton-based Nonwovens, Proc. Nonwovens Conference Beltwide 2002, Atlanta, GA, January 11-12, 2002. — ***INJ***

Press to return to the Table of Contents

BIODEGRADABLE/COMPOSTABLE NONWOVENS FORM COTTON-BASED COMPOSITIONS

Gajanan S. Bhat and Haoming Rong
The University of Tennessee, Knoxville, TN 37996
And
Mac Mclean, Cotton Incorporated, Cary, NC 27513

ABSTRACT

There has been continuing research to produce and evaluate nonwoven products containing cotton with different binder fibers. Using a thermoplastic binder fiber is the best route to produce quality nonwovens using the most convenient and simple method of bonding, i.e., thermal calendering. The challenge is to find the right binder fiber that is biodegradable and works better with cotton. Several combinations of cotton and biodegradable thermoplastic fibers, traditionally available and new varieties, are being investigated. Whereas some of the newer polymers/fibers show a great deal of promise, having the right type of fiber, and in the right combination is important in achieving the desired properties. The production of nonwovens by the thermal bonding process from such compositions, and the structure and properties of the resulting products will be discussed.

INTRODUCTION

High waste disposal costs and tough environmental laws are forcing industrial manufacturers to consider making or using biodegradable/compostable nonwovens. Biodegradable means a material capable of being broken down into small chemical subunits which can be utilized in the food chain through naturally acting and/or environmentally safe enzymes, bacteria, spores and the like. Preferably, the material is capable of being broken down into water and CO_2. Compostable means a material that meets the following three requirements: First, the material is capable of being processed in a composting facility for solid waste. Second, if so processed, the material will end up in the final compost. And at last, if the compost is used in the soil, the material will ultimately biodegrade in the soil [1].

Cotton-based biodegradable/compostable nonwovens become a major choice, due to the superior properties of cotton fibers, such as biodegradability, softness, absorbency and breathability. Cellulose acetate (CA) fiber has been successfully used as a binder fiber for cotton-based biodegradable/compostable thermal calendered nonwoven products by the University of Tennessee, because it is a thermoplastic, hydrophilic and a biodegradable fiber. However, the softening temperature of cellulose acetate fiber is relatively high (T_s: 180-205˚C), even in the presence of some kinds of internal and/or external plasticisers [2,3]. Biodegradable copolyester *Bio*® GP copolyester fiber can be totally degraded into CO_2, H_2O and biomass [4]. The biodegradable copolyester fiber and a bicomponent of it with PP as core fiber were selected as binder fibers to make thermal calendered nonwoven products. Another advantage of these binder fibers is the relatively low melting temperature (110˚C) of biodegradable copolyester component.

[1] Reprint permitted by INDA.

The effect of various processing variables, such as blend ratio and bonding temperature, was studied. Preparation, and the structure and properties of the cotton-based nonwoven fabrics are reported in this paper.

EXPERIMENTAL

Fiber Selection and Properties

The cotton fiber used in this research was supplied by Cotton Incorporated. The scoured and bleached commodity cotton fiber had a moisture content of 5.2%, a micronaire value of 5.4 and an upper-half-mean fiber length of 24.4 mm (0.96inch). The biodegradable copolyester unicomponent and bicomponent staple fibers selected for this study were produced by Eastman Chemical Company. The bicomponent fiber has a sheath/core structure, with GP copolyester as the sheath on a stiffer polypropylene core.

Processing

Fibers were first opened by hand and then weighed according to the desired blend ratio and fabric weight. The blend of fiber was then carded to form a web using a modified Hollingsworth card. The resulting carded fabric weights were around 40 grams/m^2. The carded webs were then thermally point-bonded using a Ramisch Kleinewefers 60cm (23.6 inches) wide five-roll calender with a bonded area of 18%. Two blend ratios (70/30 and 50/50 of Cotton/Binder fiber), and three calendering temperatures (100°C, 110°C, and 120°C) were used for the processing. All the webs were calendered under the same nip pressure 0.33MPa at a constant speed of 10 m/min.

Characterization of Fiber and Nonwoven Fabrics

Tensile properties of single filament and nonwoven fabrics were tested according to *ASTM D 3822*-91 Standard Test Method for Testing for Fiber/Filament and ASTM D 1117-80 Standard Test Method for Tensile Testing of Nonwoven Fabrics respectively. All the tensile property tests were carried under the standard atmosphere for testing textiles, the temperature of 21 ± 1 °C and the relative humidity of 65 ± 2 %, using a United Tensile Tester. Samples were conditioned in the standard atmosphere before testing.

Thermal analysis of binder fiber was done using the Mettler DSC25 at a scanning rate of 20°C/min. Basis weight of nonwoven fabrics was determined according to *INDA Standard Test 130.1-92* Standard Test Method for the mass per unit area of nonwoven fabrics.

Scanning Electron Microscopy (SEM) pictures were taken for the surface and cross sections of the bonding points, and failure structure under a Hitachi S - 3500N scanning electron microscope. A 20KV electronic beam and 50MPa vacuum were used for the test. Magnification was varied depending on the sample.

RESULTS & DISCUSSIONS

Fiber Properties

The properties of the binder fibers used in this research are listed in Table 1. The data show that the tenacity or peak strength of unicomponent copolyester fiber is comparable to that of cotton fiber. The tenacity or peak strength of the bicomponent (copolyester/PP) fiber is much higher than that of cotton fibers. The peak extensions of both the unicomponent and the bicomponent binder fibers are much higher than that of cotton fibers.

Table 1. Properties of Binder Fibers.

	CA*	PCA*	Copolyester	Copolyester/PP
Filament density (g/cm^3)	1.3	1.3	1.2	1.1
Filament denier (denier)	1.1	2.9	4.0	4.0
Filament tenacity (g/denier)	1.2	-	1.6	3.0
Peak load (gram)	1.3	-	6.2	12.0
Peak extension (%)	25	-	144	96
Staple length (inches)	1.65	1.77	1.0	1.5
Crimps (/inch)	-	13	not measurable	11

* – CA – cellulose acetate; PCA- plasticized cellulose acetate

The DSC scans of biodegradable copolyester and biodegradable copolyester/PP staple fiber are shown in Figure 1. Biodegradable copolyester fiber shows a broad melting endotherm around 110°C. The biodegradable copolyester/PP shows a strong peak for PP, which is broad and double melting and different than typical PP. This is probably due to crystal size distribution in the PP component. Biodegradable copolyester component shows a broad endotherm with no well-defined melting peak.

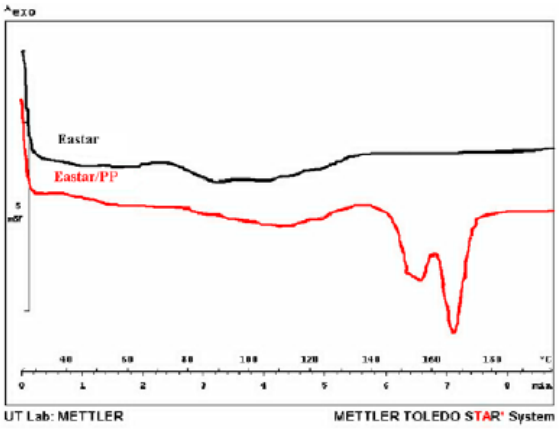

Figure 1. DSC Scans of Biodegradable Copolyester Binder Fibers (heating rate 20°C/min).

Cotton/Biodegradable Copolyester Nonwovens

The effect of bonding temperature and binder fiber component on fabric peak load along the machine direction is shown in Figure 2. The peak strengths of cotton/biodegradable copolyester nonwovens are relatively low, when compared with those of cotton/cellulose acetate nonwovens from our previous study [3], in which the highest peak load was around 0.8 kg.

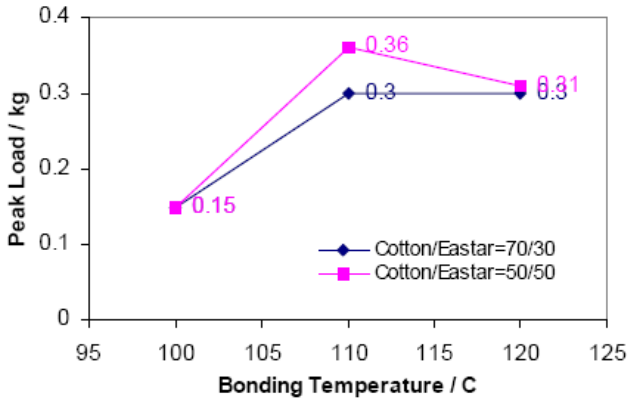

Figure 2. Peak Load of Cotton/Biodegradable Copolyester Nonwovens.

For cotton-based thermally point-bonded nonwovens, it is important that the low-melting binder fiber be distributed evenly throughout the web to ensure uniformity of fabric properties. However, the carded webs generally have area irregularities of mass distribution caused by machine variables (the nature and conditions of card clothing, the relative speeds and settings of the carding elements) and fiber properties, such as staple length, stiffness, crimps, fiber tensile properties, and fiber finishes etc. One disadvantage in using biodegradable copolyester unicomponent as-spun fiber as a binder fiber is that it is hard to get the binder fibers well distributed (Figure 3).

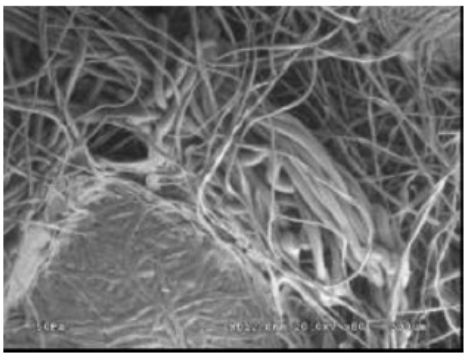

(a)Cotton/Biodegradable Copolyester=70/30

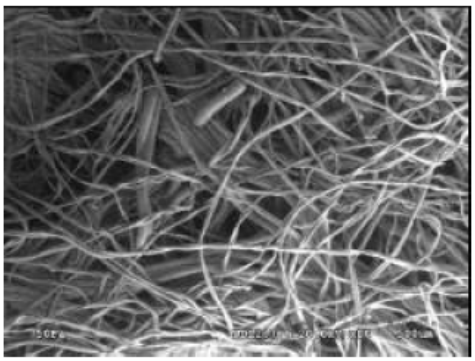

(b) Cotton/Biodegradable Copolyester=50/50

Figure 3. Binder Fiber Distribution of Cotton/Copolyester Webs.

The poor distribution of the biodegradable copolyester fiber is due to the high elasticity of the fiber, which leads to low tensile properties of the final nonwoven fabrics. It is possible to see bundles of biodegradable copolyester fiber in the web indicating poor distribution, which means majority of the bond areas do not have the binder fiber. So a bicomponent fiber, biodegradable copolyester/PP, with biodegradable copolyester *Bio*® GP as the sheath, and polypropylene as the stiffer core was tried as the binder fiber. Instead of the biodegradable copolyester unicomponent the bicomponent has improved processability, which results in better tensile properties of the final fabrics.

Cotton/(Biodegradable Copolyester/PP) Nonwovens

The effect of biodegradable copolyester/PP binder fiber component and bonding temperature on fabric peak load along the machine direction can be seen from the data in Figure 4. The peak loads of cotton/(biodegradable copolyester/PP) nonwovens are much higher than those of cotton/biodegradable copolyester nonwovens shown in Figure 2. Therefore, using the bicomponent fiber as a binder fiber improves the tensile properties of cotton/biodegradable copolyester nonwoven fabrics. This improvement in tensile properties is the result of better binder fiber properties as well as the improved processing characteristics of the modified binder fiber. Higher tenacity of the binder fiber may also contribute to the high strength of the webs.

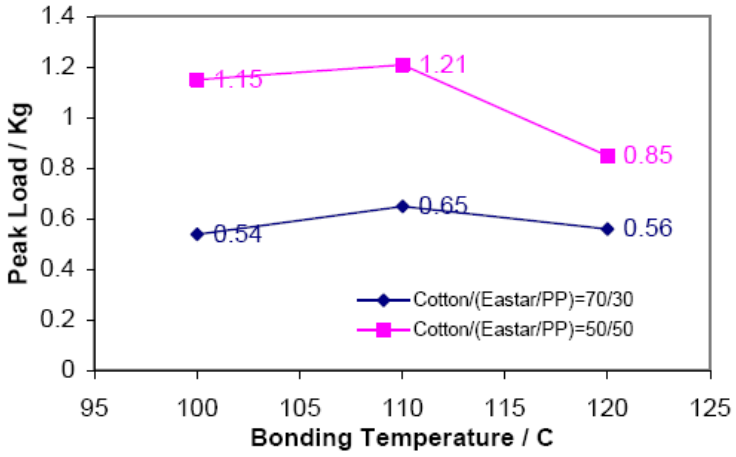

Figure 4. Peak Load of Cotton/(Biodegradable Copolyester/PP) Nonwovens.

With the increase of biodegradable copolyester/PP component, peak load increases at all the three thermal bonding temperatures. This is the result of the increase of biodegradable copolyester/PP fiber, which causes an increase in the really effective bond points and bond area.

For the effect of bonding temperature, it can be seen that with the increase of bonding temperature peak load first increases at lower temperature range (≤110°C). The increase in strength of the fabrics is the result of the formation of better-developed bond structure at lower bonding temperature. This can be verified by observing the SEM pictures of the surface (Figure

5) and the cross-section (Figure 6) of the bonding points. The regular shape of bonding point and smooth surface of the fabrics bonded at high bonding temperature show the well-developed bond structure. It can be found (from Figure 6) that cotton fibers were embedded in the melt of the sheath of the binder fiber and the cores of the binder fibers were deformed by the thermal bonding process.

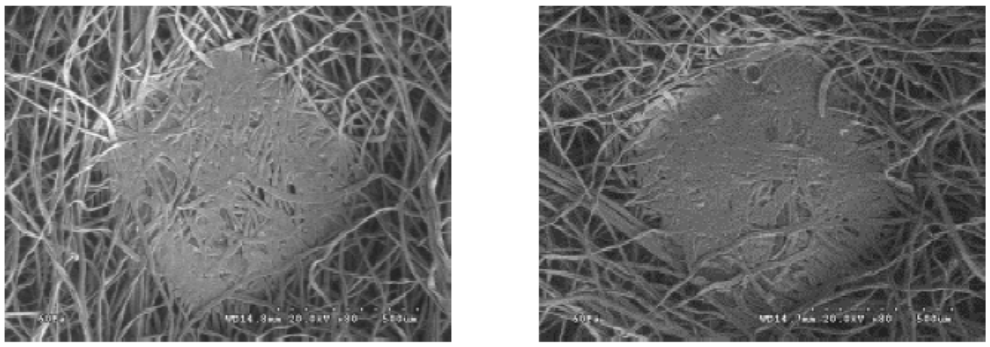

(a) Bonding temperature 100°C (b) Bonding temperature 110°C

Figure 5. SEM Pictures of Bond Points for Cotton/Biodegradable Copolyester/PP (70/30) Fabrics.

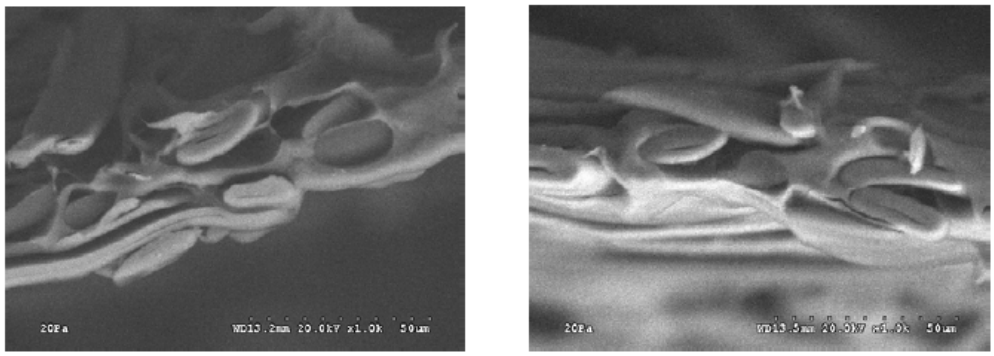

(a) Bonding temperature 100°C (b) Bonding temperature 110°C

Figure 6. Cross-Sections of Bond Points for Cotton/(Biodegradable Copolyester/PP) (50/50) Fabrics.

The peak load decreases with further increase in bonding temperature. This is due to the different failure mechanisms of the nonwoven fabrics bonded at higher temperatures. For fabrics produced at low bonding temperatures, the bond failure mechanism was due to loss of interfacial adhesion at the bond site leading to bond disintegration; for webs produced at higher bonding temperature failure was attributed to the loss of fiber integrity and formation of film-like spots at high temperatures, as well as the reduction in load transfer from fibers to film [5, 6].

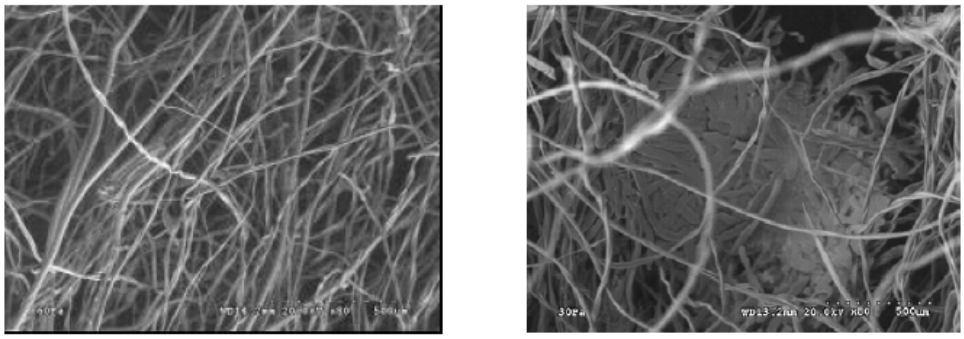

(a) Bonding temperature 100°C (b) Bonding temperature 120°C

Figure 7. SEM Photographs of Failure Structure after Tensile Testing for Cotton/(Biodegradable Copolyester/PP)=50/50 Nonwovens.

This difference in failure mechanism can be confirmed by the SEM pictures of the failure structure of the fabrics produced at different bonding temperature (Figure 7). These observations are consistent with those of Gibson and McGill [7], who have studied the failure mechanism of thermal point-bonded polyester nonwovens as a function of the bonding temperature.

Cotton/Cellulose Acetate Nonwovens

Results from studies with CA as binder fibers were reported earlier [8-10]. The effect of an internal plasticizer compared to no plasticizer in CA is shown in figures 8a and 8b. It is obvious that even at a bonding temperature of 190 °C, ordinary CA (OCA) does not show much strength in the webs. Use of plasticized CA (PCA) results in significant strength development in the cotton/CA webs at a calendering temperature of 190 °C, clearly indicating the effect of added plasticizer in reducing the softening temperature of the binder fiber. Between the two blends, 50/50 cotton/CA webs were slightly stronger than the webs of 75/25 blends.

Comparison of Cotton/Biodegradable Copolyester and Cotton/CA Nonwovens

The peak load comparison between cotton/biodegradable copolyester and cotton/cellulose acetate nonwovens for a blend ratio of 50/50 is illustrated in Figure 9. The data clearly shows that the strength of cotton/(biodegradable copolyester/PP) is higher or comparable to that of cotton/PCA nonwovens.

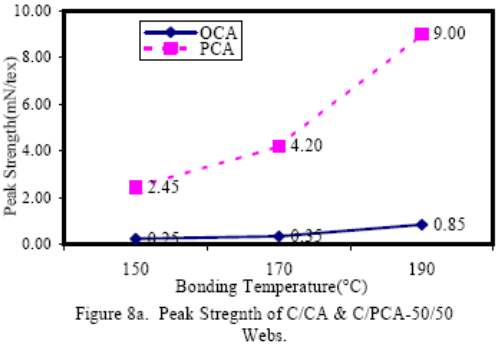

Figure 8a. Peak Stregnth of C/CA & C/PCA-50/50 Webs.

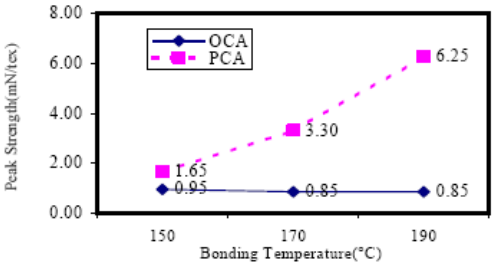

Figure 8b. Peak Strength of C/CA & C/PCA -75/25 Webs.

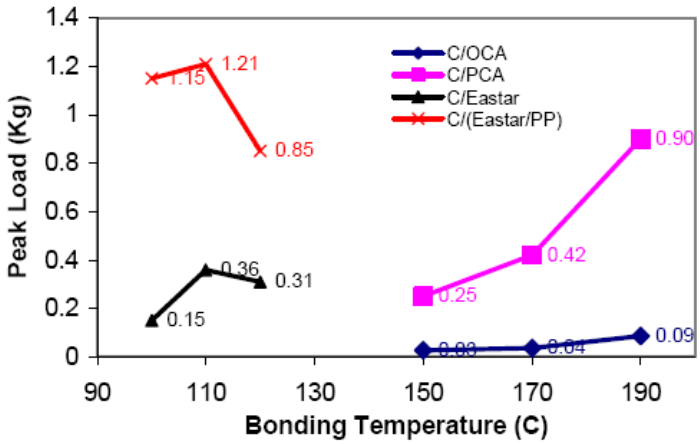

Figure 9. Peak Load of Cotton/(Biodegradable Copolyester/PP) vs. Cotton/Cellulose Acetate Nonwovens.

Based on the results, high strength cotton/(biodegradable copolyester/PP) nonwoven fabrics can be produced using cotton/(biodegradable copolyester/PP) at a blend ratio of 50/50. Also, it is possible to do thermal calendering at relatively low temperatures (<120°C).

SUMMARY

Good quality cotton-based nonwoven fabrics can be made using biodegradable copolyester/PP bicomponent binder fiber at lower bonding temperature (around 110°C). Peak load of cotton/(biodegradable copolyester/PP) nonwoven fabrics are much higher than that of

cotton/biodegradable copolyester nonwoven fabrics. Biodegradable copolyester seems to bond well with cotton producing strong bonds, when there is enough of this polymer in the point bond areas. Of the two cellulose acetate fibers investigated, obviously the plasticized CA is better as stronger webs can be produced at relatively lower bonding temperatures.

ACKNOWLEDGMENTS

This work was supported by funding from the Tennessee Agricultural Experiment Station and Cotton Inc. Raleigh, NC. Authors would like to acknowledge Celanese Acetate, Charlotte, NC and Eastman Chemical Company, Kingsport, TN for providing the binder fibers for this research.

REFERENCES

1. Noda, *et al*., "Spray Processes Using A Gaseous Flow For Preparing Biodegradable Fibrils, Nonwoven Fabrics Comprising Biodegradable Fibrils, And Articles Comprising Such Nonwoven Fabrics", USP 5780368, 1998.
2. Larson, G., "Biodegradable Staple Fiber Nonwovens Calendered with the Assistance of an Aqueous Solvent: Their Fabrication, Properties, and Structural Characteristics", MS Thesis, the University of Tennessee, Knoxville, TN, 1997.
3. Gao, X., Duckett, K. E., Bhat, G., Rong, H., "Effects of Water on Processing and Properties of Thermally Bonded Cotton/Cellulose Acetate Nonwovens," *INJ*, 10(2), 21-25, 2001.
4. *http://www.eastman.com/Brands/Eastar_Bio/Eastar_Bio_products.asp*
5. Bhat, G. S. and Nanjundappa, R. Structure and Properties of Spunbond Nonwovens from Propylene Polymers. *Proceedings of the PP World Congress*, Huddersfield, UK, July 2000.
6. Hansen, S. M., "Nonwoven Engineering Principles," *Nonwovens---Theory, Process, Performance & Testing*. Edited by A. F. Turbak, TAPPI Press, GA, 1993, Chapter 5.
7. Gibson, P.E., McGill, R.L., *TAPPI Nonwovens Conference Proceedings*, TAPPI Press, Atlanta, p. 129, 1987.
8. Bhat, G. S., and Rong, H., "Preparation and Properties of Cotton-Biodegradable copolyester Biodegradable Compostable Nonwovens," *Proceedings of the Sixth Beltwide Nonwovens Conference*, 2003.
9. Bhat, G. S., and Rong, H. and Mclean, E. M., "Effect of Binder Fibers on the Processing and Properties of Cotton-Based Nonwovens," *Proceedings of the Beltwide Conference*, 2002.
10. Duckett, K. E., Bhat, G. S., Giao, X. and Rong, H., "Characterization of Cotton/Cellulose Acetate Nonwovens of Untreated and Aqueous Pretreated Webs prior to Thermal Bonding," *Proceedings of the INTC*, 2000.

Statistical Analysis of the Effect of Processing Conditions on the Strength of Thermally Point-bonded Cotton-based Nonwovens

Haoming Rong, Ramon V. Leon, and Gajanan S. Bhat
The University of Tennessee, Knoxville, TN 37996

Abstract

In this paper, we investigated the effect of thermal calendering temperature, binder fiber type, and binder fiber component (blend ratio) on the tensile strength of resulting thermally point-bonded nonwovens. The experimental results were statistically analyzed using the General Linear Models Procedure in JMP 5.0 to determine the significance of the effects of the variables on the fabric strength. Based on the interactions of binder fiber composition and bonding temperature, empirical models have been developed to predict breaking load of the webs.

Keywords: Nonwoven, statistical analysis, thermal calendering, binder fiber, strength.

Introduction

Nowadays, nonwoven fabrics have been widely used in home furnishings, automotive industry, civil engineering, geotextiles, industrial filters and medical sanitary materials etc [3]. More than 50% of these nonwoven products are disposable products. However, most of these products are made of synthetic fibers, such as polypropylene, polyethylene, polyester and polyamide, which are not biodegradable and end up as solid waste. With [1]the growing environmental awareness throughout the world, environmentally compatible nonwoven products have been receiving increasing attention in recent years.

Cotton-based biodegradable/compostable nonwovens become a major choice, due to the unique properties of cotton fibers, such as biodegradability, softness, absorbency and breathability. There is increasing interest in biodegradable/compostable cotton-based nonwovens with the expansion of nonwovens into novel applications. Cotton/Eastar *Bio*® (/PP) thermally point-bonded biodegradable nonwovens have been produced and evaluated at the University of Tennessee, Knoxville in the recent years [1-2, 5-7]. The resulting nonwoven fabrics have shown great promise. Several variables such as binder fiber type, composition, processing conditions, distribution of fibers in the web and bonding conditions dictate the structure and properties of the resulting webs [4, 8]. Effect of some of the important variables is examined with a statistical approach to come up with predictive models.

Experimental

Materials and Processing

[1] Reprint permitted by TRJ.

The cotton fiber used in this research was supplied by Cotton Incorporated, Cary, NC. The scoured and bleached commodity cotton fiber had a moisture content of 5.2%, a micronaire value of 5.4 and an upper-half-mean fiber length of 24.4 mm (0.96inch). The Eastar *Bio*® GP copolyester (Eastar *Bio*®) unicomponent and bicomponent (Eastar *Bio*®/PP) staple fibers were produced by Eastman Chemical Company, Kingsport, TN. The Eastar *Bio*® GP copolyester has a melting temperature around 110°C and becomes soft around 80°C [5]. The bicomponent fiber has a sheath/core structure, with Eastar *Bio*® GP copolyester as the sheath on a stiffer core of polypropylene. The load-elongation curves for the two binder fibers are shown in Figure 1.

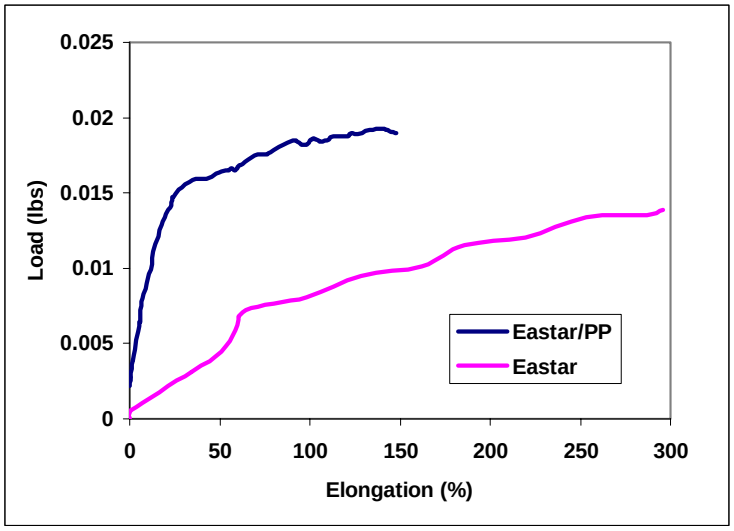

Figure 1. Load-elongation curves for the binder fibers.

Fibers were first opened by hand and then weighed according to the desired blend ratio and fabric weight. The fiber blends were then carded to form a web using a modified Hollingsworth card. The resulting carded fabric weights were around 40 grams/m^2. The carded webs were then thermally point-bonded using a Ramisch Kleinewefers 60cm (23.6 inches) wide five-roll calender with a bonded area of 16.6%. Three blend ratios (85/15, 70/30 and 50/50 of Cotton/Binder fiber), and four calendering temperatures (90°C, 100°C, 110°C, and 120°C) were used for the processing. All the webs were calendered under the same nip pressure, 0.33MPa, at a constant speed of 10 m/min.

Experimental Design

The experimental design used in this research is shown in Figure 2. Three treatment factors (variables) considered in this research were:

Thermal calendering temperature (TEMP, four levels, 90°C, 100°C, 110°C, and 120°C)
Forms of binder fiber (TYPE, two levels, Eastar *Bio*® fiber and Eastar *Bio*®/PP fiber)

Blend ratio (COMP, three levels, Cotton/Binder fiber at 85/15, 70/30, and 50/50 respectively), i.e., binder fiber component (three levels, at 15%, 30%, and 50%)

Since Eastar *Bio*® GP copolyester was the only component which became soft and melt during the bonding process, the same thermal calendering temperature range was settled for both the nonwoven series, and the effects of bonding temperature for both of the nonwoven series are expected to be the same.

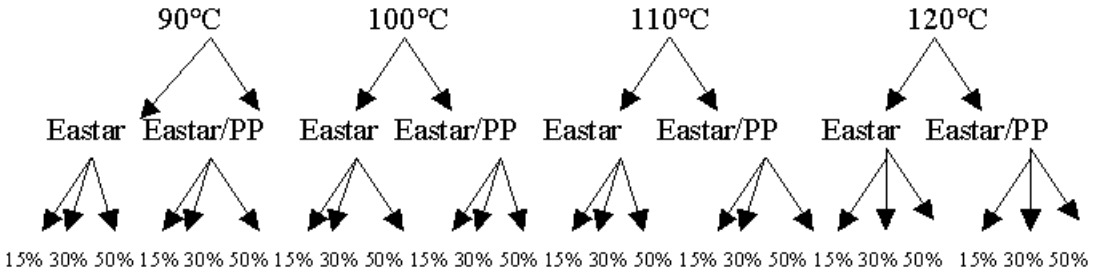

Figure 2. Experimental Design.

Characterization

Basis weight of nonwoven fabrics was determined according to *INDA Standard Test 130.1-92 Standard Test Method for the Mass Per Unit Area of Nonwoven Fabrics*. Fabrics were first conditioned for 24 hours and then test at 20°C and 65% relative humidity. 3 pieces of the sample were cut using a cutting die of an area of 0.01 m^2. Then the weight of the sample pieces was weighed at a balance with an accuracy of 0.0001 gram. The mass per unit area of each test piece was calculated finally based on the measurement.

Tensile strength of the resulting nonwoven fabrics were tested using a united tensile tester according to *ASTM D 5035-95 Standard Test Method for Breaking Force and Elongation of Textile Fabrics (Strip Method).* All the tensile tests were carried out under the standard atmosphere for testing textiles, with temperature of 21 ± 1 °C and relative humidity of 65 ± 2 %. Sample was cut for 1'' wide and 10 '' long. A gauge length of 5'' and an extension rate of 12''/min were used for the test. Five strips were tested for each specimen. Here peak load (LOAD) (kg) of the fabrics was reported to represent the tensile strength of the fabrics.

Statistical Analysis

The experimental results were statistically analyzed using the General Linear Models Procedure in JMP 5.0 to determine the significance of the effects of the parameters (variables) on the fabric strength (responses).

Results

The mean values, standard deviation (σ), and coefficient of variation (C.V.) of peak loads of the resulting nonwoven fabrics are listed in Table 1.

Table 1. Peak loads (kg) of Cotton/Eastar *Bio*® (/PP) nonwovens.

Binder Component (%)	Bonding Temperature (°C)	Cotton/Eastar *Bio*®			Cotton/(Eastar *Bio*®/PP)		
		Mean	σ	C.V.	Mean	σ	C.V.
15	90	0.10	0.03	0.27	0.24	0.04	0.16
	100	0.14	0.03	0.24	0.30	0.05	0.15
	110	0.17	0.02	0.12	0.36	0.05	0.13
	120	0.17	0.03	0.19	0.29	0.06	0.20
30	90	0.12	0.03	0.26	0.42	0.04	0.10
	100	0.15	0.02	0.15	0.54	0.20	0.38
	110	0.30	0.12	0.41	0.65	0.15	0.23
	120	0.30	0.06	0.19	0.56	0.36	0.64
50	90	0.13	0.04	0.34	0.54	0.14	0.26
	100	0.15	0.03	0.21	1.15	0.36	0.32
	110	0.36	0.05	0.15	1.21	0.27	0.22
	120	0.31	0.05	0.16	0.85	0.26	0.31

Analysis

This is not a full factorial design but a split plot design due to the restrictions of experimental conditions. The parameter, bonding temperature, was set only four times due to the experimental restrictions, thus the data are not true replications.

Full model

A model was first fitted where temperature was fitted to the third degree since it had four levels and composition to the second degree since it had two levels and binder type was considered as the only nominal variable. All interactions were included. The R-square of the fit is 0.813, which represents the proportion of variability in peak load accounted by the model [9]. Based on the fit the model was simplified to include only the following effects: TYPE, COMP, TYPE*COMP, TEMP, TEMP*TEMP, TEMP*COMP, TEMP*TEMP*COMP, TEMP*TYPE, TEMP*TEMP*TYPE. We have followed the practice of including lower level terms that are not significant if higher level terms are significant. For example, TEMP*COMP was included in the model because TEMP*TEMP*COMP was significant. Similarly, TEMP*TYPE was included because TEMP*TEMP*TYPE was significant. It should be remarked that the terms not included in the model were not significant even though the experimental variation was less in this split plot design than would have been in the case of true replications. This fact gives confidence in the non-significance of the dropped terms.

Simplified model

Based on above analysis, the simplified model was fitted by TYPE, COMP, TYPE*COMP, TEMP, TEMP*TEMP, TEMP*COMP, TEMP*TEMP*COMP, TEMP*TYPE, TEMP*TEMP*TYPE. The model has an R^2 of 0.8068 versus 0.8127 for the full model so we have not lost much prediction power by simplifying the model as we have done.

The new fitted model is:

$$\begin{aligned} Load = & -0.5792 - 0.2579 \times z + 1.4531 \times COMP - 0.7947 \times z \times (COMP - 0.3167) \\ & + 0.0056 \times TEMP + 0.0186 \times (COMP - 0.3167)(TEMP - 105) \\ & - 0.0006 \times (TEMP - 105)(TEMP - 105) \\ & + 0.0005 \times z \times (TEMP - 105)(TEMP - 105) - 0.000063(TEMP - 105) \times z \\ & - 0.0032 \times (TEMP - 105)(TEMP - 105)(COMP - 0.3167) \end{aligned} \quad (1)$$

where, z = 1 for Eastar *Bio*®; z = -1 for Eastar *Bio*®/PP

Figure 3 shows the predicted profiles for Eastar *Bio*® and Eastar *Bio*®/PP binders respectively according to above model. It can be found that the model predicts that the highest strength for Cotton/Eastar *Bio*® nonwoven is achieved when we use binder component of 0.5 (50%) and a bonding temperature around 111°C; while the highest strength for Cotton/(Eastar *Bio*®/PP) nonwoven is oserved when we use binder component of 0.5 (50%) and a bonding temperature around 108°C. The optimal peak load of Cotton/(Eastar *Bio*®/PP) nonwoven is much higher than that of Cotton/Eastar *Bio*® nonwoven. Thus, Eastar *Bio*®/PP binder fiber give fabrics with increase break load at the temperatures and compositions tested.

Predicted Peak Loads and their Prediction Intervals

For practical applications, prediction interval (PI) was preferred. An interval estimate for an individual observation is called a PI, which is different from confidential interval of the mean of the population [9]. The predicted peak loads and their 95% prediction intervals are shown in Table 2 based on the simplified model (1). Here the prediction interval is where the strength of a future observation will be in the 95% confidence interval. The predicted optimal peak loads and its prediction intervals were also listed in Table 2. It can be seen that the optimal peak load for Cotton/Eastar *Bio*® nonwoven is only 0.3635 kg, relatively lower compared with that for Cotton/(Eastar *Bio*®/PP) nonwoven, which is 1.154 kg. Thus, Eastar *Bio*®/PP fibers give fabrics with superior strength under the conditions tested.

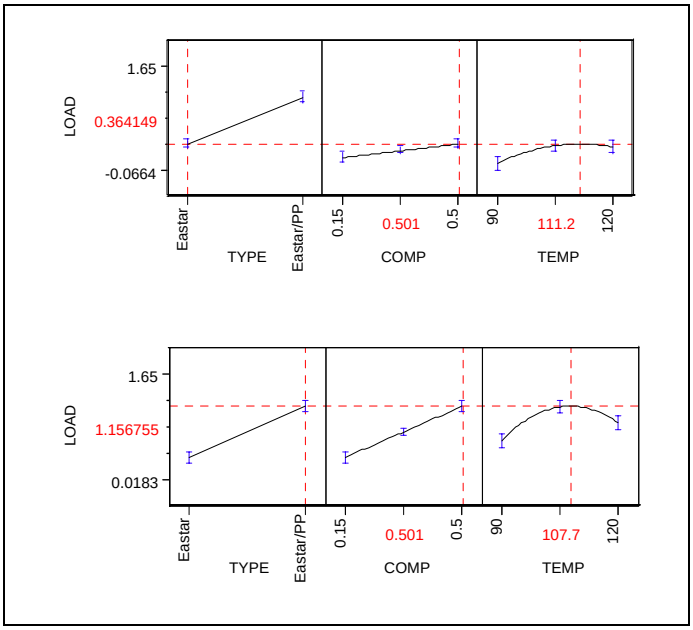

Figure 3. Prediction Profiles.

Summary

All the three variables, binder fiber type, binder fiber component, bonding temperature, and their interactions affect the resulting nonwoven fabric strength significantly. When both temperature and binder component are treated as continuous variables and the effect of temperature and its interactions with other two variables are considered, a fitted model to predict peak loads of the nonwoven webs is developed. The optimal process conditions to obtain high strength nonwoven fabrics are to select Eastar *Bio*®/PP as the binder fiber type, to choose binder fiber component at 50%, and to use 107.7°C as the best bonding temperature. The predicted peak load of the nonwoven fabrics processed under the optimal condition is 1.154 kg. This simplified approach can be very useful in many of the nonwoven processes.

References

[1] Bhat, G. S., Rong, H. M., and Mclean, M., "Biodegradable/Compostable Nonwovens from Cotton-based Compositions," *INTC 2003 Proceedings, September 15-18, 2003.*
[2] Bhat, G. S., and Rong, H. M., "Effect of Binder Fiber on the Processing and Properties of Thermal Bonded Cotton-based Nonwovens," *Proc. Nonwovens Conference Beltwide 2002, Atlanta, GA, January 11-12, 2002*.
[3] Hansen, S. M. Nonwoven Engineering Principles, Nonwovens---Theory, Process, Performance & Testing, Edited by A. F. Turbak, TAPPI Press, GA, 1993, Chapter 1.

[4] Hoyle, A. G., "Thermal Bonding of Nonwoven Fabrics," July 1990, 85-88, Tappi Journal.
[5] Rong, H. M., and Bhat, G. S., "Preparation and Properties of Cotton-Eastar Nonwovens," Int. Nonwovens J., 12(2), 53-57, 2003.
[6] Rong, H. M., and Bhat, G., "Preparation and properties of Cotton-Eastar Biodegradable/compostable nonwovens," *Proc. Nonwovens Conference Beltwide 2003, Nashville, TN, January 6-10, 2003*.
[7] Rong, H. M., Bhat, G. S., Duckett, K. E., and Mclean, M., "Biodegradable Nonwovens From Cotton-based Compositions," *Proc. Nonwovens Conference Beltwide 2001, Anheim, CA, January 2001.*
[8] Shimalla, C. J., and Whitwell, J. C., "Thermomechanical Behavior of Nonwovens, Part I: Responses to Changes in Processing and Post-Bonding," Textile Research Journal, 46, 513-518 (1976).
[9] Tamhane, A. C., and Dunlop D. D., "Statistics and Data Analysis: From Elementary to Intermediate," Prentice-Hall Inc., New Jersey, 2000.

Table 2. Predicted peak loads and their prediction intervals (kg).

Binder Comp. (%)	Bonding Temp. (°C)	Cotton/Eastar *Bio*®			Cotton/(Eastar *Bio*®/PP)		
		Predicted Load	LPL	UPL	Predicted Load	LPL	UPL
15	90	0.162252	-0.15429	0.478799	0.190442	-0.1261	0.506989
	100	0.102685	-0.20747	0.412837	0.328475	0.018322	0.638627
	110	0.127324	-0.18283	0.437477	0.354381	0.044228	0.664534
	120	0.236171	-0.08038	0.552718	0.268161	-0.04839	0.584708
30	90	0.110575	-0.1983	0.419449	0.377184	0.068311	0.686058
	100	0.175418	-0.12953	0.48037	0.639627	0.334676	0.944579
	110	0.227982	-0.07697	0.532934	0.693458	0.388507	0.99841
	120	0.268267	-0.04061	0.577141	0.538676	0.229802	0.84755
50	90	0.041673	-0.27648	0.359823	0.626173	0.308023	0.944324
	100	0.272397	-0.03885	0.583642	1.054498	0.743253	1.365743
	110	0.362193	0.050948	0.673438	1.145561	0.834316	1.456806
	120	0.311062	-0.00709	0.629212	0.899363	0.581212	1.217513
*50	111.2	0.363498	0.022088	0.647734			
*50	107.7				1.154481	0.829364	1.45501

* predicted values for optimal processing conditions.

Effects of Water On Processing and Properties of Thermally Bonded Cotton/Cellulose Acetate Nonwovens

By Xiao Gao, K.E. Duckett, G. Bhat, Haoming Rong, University of Tenessee, Knoxville, TN

Abstract

Environmentally friendly nonwoven fabrics can be formed through thermal bonding of cotton and cellulose acetate fiber blends at reduced bonding temperature with the aid of a plasticizer. Water has been introduced as an external plasticizer to lower the softening temperature of cellulose acetate fibers and to enhance the tensile strength of cotton/cellulose acetate web. It has been found that water can significantly increase the tensile strength of cotton/cellulose acetate thermally-bonded webs at reasonable bonding temperatures. In addition, water can enhance web bonding to essentially the same degree as an acetone treatment does. The mechanisms of water effect are considered and optimal processing conditions are proposed.

Introduction

More and more nonwovens are used in everyday life, but the environmental impact of disposable products remains a major concern [1, 2]. Manufacturers are seeking ways to produce biodegradable textile products by using biodegradable fiber and cotton becomes an obvious choice for the nonwoven industry because of its biodegradability, softness, absorbency and vapor transport properties [13]. However, cotton is a non-thermoplastic fiber and requires the addition of a thermoplastic binder fiber for the fusion of the fibers at relatively low temperature. Most cotton-based nonwovens products are processed with binder fibers using thermal calendering, which is a clean and an economical process. Synthetic fibers such as low melting polyester, polyester copolymer, polypropylene and polyethylene can be used as binder fibers [3-7]. Cellulose acetate fiber also has been used as the biodegradable binder fiber, since it is a thermoplastic, hydrophilic and a biodegradable fiber. A solvent treatment has been introduced in order to modify the softening temperature of cellulose acetate fiber and to lower the calendering temperature, while maintaining enhanced tensile properties. Duckett, Bhat and colleagues [8, 9] have examined the effect of acetone vapor pre-treatment and of 20% acetone solution pre-treatment on cotton/cellulose acetate thermally bonded webs. The results showed that these solvent treatments could decrease the softening temperature of cellulose acetate fiber and produce comparatively stronger webs. However, from a practical standpoint, manufacturers do not like a process involving the use of acetone because acetone evaporates easily, and is flammable and toxic. These detrimental factors create major problems in manufacturing and pollute the working environment. Also, consumers may prefer not to buy acetone-treated products, which they think may contain toxic substances. In our research, the desire was to decrease the softening temperature of cellulose acetate without the aid of acetone treatment by applying water treatment – a treatment noted previously at Celanaese Acetate [10] – prior to thermal bonding. Additionally, an industrially modified (plasticized) cellulose acetate fiber was studied as an alternative choice as binder fiber.

Experimental Procedures

The cotton fiber used in this research is a scoured and bleached cotton fiber provided by Cotton Incorporated. Properties include a 5.2% moisture regain value, 5.4 micronaire value and an upper-half-mean fiber length at 2.44 cm. Celanese Corporation provided both ordinary cellulose acetate (OCA) and plasticized cellulose acetate (PCA). An ultra-light fabric with basis weight around 35 g/m² (1 oz/yd²) was chosen for this research.

The experiment was a four-factor design with two replications. The factors included were:

CA type: Ordinary CA (OCA) and Plasticized CA (PCA)

Temperature: 150°C, 170°C, 190°C

Blend Ratio: 75/25 and 50/50 (by weight) Cotton/Cellulose Acetate

1

[1] Reprint permitted by INJ.

Pre-treatment: Without Water Treatment (nw)
Water Dip-Nip Treatment (dn)
20% Aqueous-Acetone Dip-Nip Treatment

A Saco-Lowell carding machine, with a collector drum circumference of 142.2 cm (56 in.) and a drum width of 22.2 cm (8.75 in.) was used to form the webs. The carded webs were cut away from the drum and placed between two sheets of paper to await pretreatment and thermal calendering. An H.W. Butterworth & Sons padding machine was used for the dip-nip pretreatment. The carded webs were placed between two fine mesh screens and passed through a tray containing water or acetone solution prior to going through padding rolls to squeeze out excess liquid. Following this procedure, the webs were ready to be thermally calendered using a Ramisch Kleinewefers 60 cm (23.6 in.) wide five-roll calender. Only the upper two rolls were used. The top calender roll had an engraved diamond pattern resulting in 16.6 % bonding area and the bottom roll was smooth. Both were made of stainless steel. The rolls were heated by circulating oil and the nip roll pressure was set at 25 KN. Roll feed speed was fixed at 10 m/min.

All pretreated webs were placed in a standard atmosphere for 24 hours before testing. Five 1 X 10 inch test specimens were cut from the web along the machine direction and the tensile properties were obtained using ASTM D 1117– 80 Standard Test Method for Tensile Testing of Nonwoven Materials. A Hitachi S-800 SEM provided information on bond structure and fiber morphology. The SEM was set at 1 Kev, 7 mm working distance, and magnification of 80X and 250X, respectively.

Results and Discussion

In previous studies [11-13], a water spray treatment had been used and there resulted a gradual increase in the peak strength with each increasing bonding temperature compared with those having no water spray treatment. This suggested the possibility that water will act as a plasticizer to enhance fabric tensile properties at reduced bonding temperature.

Treatment Effect

The effect of three different treatments on the tensile strength of cotton/ordinary cellulose acetate (C/OCA) is shown in *Figure 1* for a 50/50 blend ratio.

From statistical analyses and visual observation, it is clear that a water dip-nip treatment can significantly increase the bonding strength of cotton/cellulose acetate thermally bonded webs. Possible mechanisms that are responsible for this strength enhancement are:

1. Water molecules penetrate the whole web with the assistance of the padding machine and are attracted to the cellulose acetate molecules by hydrogen bonding. Thus, the intermolecular forces of cellulose acetate are reduced, and the mobility of the polymer chains is improved. The polymer becomes elastic and more flexible, with the result of a lowered softening temperature. Hence, the softening temperature can be lowered by the external plasticizer-water dip-nip treatment, providing increased cellulose acetate molecular mobility and reducing the necessary thermal energy required to bond the fibers at fiber contact points. This makes it possible to bond at a lower temperature, with the aid of a water dip-nip pre-treatment.

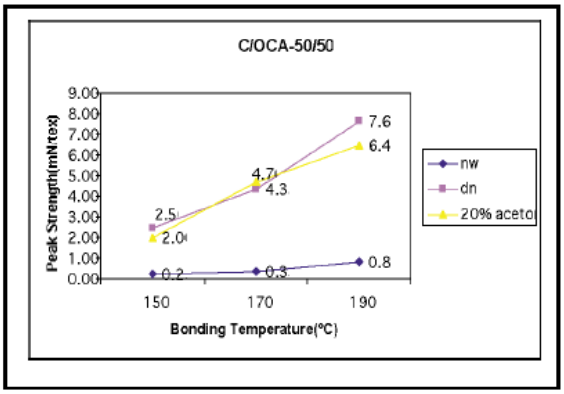

Figure 1
TREATMENT EFFECT ON THE
PEAK STRENGTH OF C/OCA WEBS

2. Due to the hydrophilic nature of the partially crystalline structure of cellulose acetate, it can take up substantial water. Above the softening temperature, the fiber swells as a result of molecular chain relaxation and becomes sufficiently tacky to provide some bonding with other binder fibers and with the base fiber. The swelling, which provides greater free volume for the polymer, will increase the surface area and enhance contact with the other fibers. This might be expected to increase bonding strength by providing more bonding area at the bonding point.

3. When the web is passed through the nip of the pattern and smooth rolls of the thermal calender, heat and pressure are applied to the web. The web at that time is composed of cotton fiber, cellulose acetate fiber and water. Water has very good thermal conductivity – about 10 times that of either cotton or cellullose acetate – and this enables additional heat transfer in the short interval of time when web and rolls are in contact. Thus, enhanced heating produces more polymer flow and better bonding.

The external plasticizer-water bonds physically to the polymer rather than chemically (covalently), which lowers the softening temperature of cellulose acetate. In combination, this enables more heat and polymer flow at the cross-over points of fibers in the bonding region, providing enhanced tensile properties to the web under lower bonding temperature.

From the graph, it can be clearly seen that there is no significant difference between the two different kinds of external plasticizer – water or 20% aqueous solution of acetone when applied to the web by dip-nip pretreatment. Both plasticizations, however, do increase the bonding strength of cotton/cellulose acetate thermally bonded webs. These results suggest that water can replace a 20% acetone concentration and can be used as the external plasticizer in the pre-treatment of cotton/cellulose acetate web, without a reduction in web strength.

Cellulose Acetate Type Effect

The effect of an internal plasticizer on the peak strength of

Cotton/PCA blend was examined, also. The results are shown in *Figure 2*, separately by blend ratio and without any external treatment.

It is clearly observed that the web containing plasticized cellulose acetate (PCA) binder fibers has a significantly higher peak strength than those comprising ordinary cellulose acetate (OCA) binder fibers. The tensile strength rises uniformly to 9.00mN/tex for C/PCA-50/50 webs. This is to be compared to 0.85mN/tex for C/OCA-50/50 webs at the upper temperature of 190°C. This clearly demonstrates that the internal plasticizer enhances the bonding and strength of a thermally bonded cotton/cellulose acetate web.

All webs using PCA as binder fiber have significantly higher peak strengths than those using OCA as binder fiber, except for the 75/25 C/CA web bonded at 150°C. That may be due to the low number of binder fibers (inhomogeneous fiber distribution) and the lower bonding temperature, whereby the web could not get sufficient heat flow and polymer flow to cause suitable bonding. The effect may also be a statistical or processing fluctuation, since the differences are so small.

Combination of PCA and Water Treatment Effect

When the water treatment is applied to Cotton/Plasticized Cellulose Acetate (PCA) webs, the results are as shown in *Figure 3*.

It is seen from the two figures that the cotton/plasticized cellulose acetate webs have higher peak strength when treated with an external plasticizer-water than those cotton/plasticized cellulose acetate webs without water dip-nip treatment. The possible exception may be for C/PCA-50/50-190°C webs, where there is little difference between the two treatments at the highest bonding temperature.

The combination of internal and external plasticizer has a significant effect in lowering the bonding temperature for improved peak strength of cotton/cellulose acetate webs compared to cotton/plasticized cellulose acetate webs, alone. However, when the bonding temperature reaches 190°C, the external plasticizer offers no significant benefit to the web strength compared to the internal plasticizer effect alone. The reasoning is that, at lower temperature, the internal plasticizer helps decrease the softening temperature of cellulose acetate by increasing the polymer chain mobility. The interaction between neighboring polymer chains is still very high at low temperature and more polymer chain flexibility and polymer flow are required for effective bonding. When the external plasticizer – water – is introduced into the web, it can decrease the interaction between polymer chains, giving more mobility of the polymer chain, thereby increasing the bonding surface area and conducting more heat to induce the polymer flow to achieve better bond strength.

When the bonding temperature reaches 190°C, the heat transfer from the calender roll is sufficient for the polymer flow around the other binder fiber or cotton fiber. If water is applied at this time, the thermal dynamics of water may change considerably. More heat may be taken away by evaporation than the heat being conducted by water through the web. In this situation, the water may not be as helpful to web bonding as at

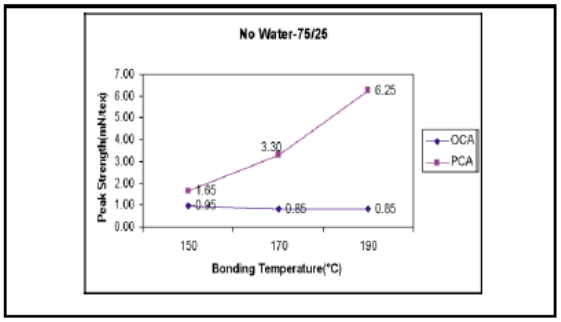

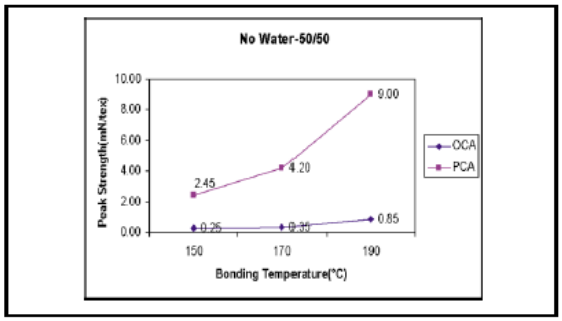

Figure 2
CELLULOSE ACETATE FIBER EFFECT ON THE PEAK STRENGTH OF C/CA WEBS

Figure 3
THE EFFECT OF COMBINATION OF PCA WITH WATER ON THE PEAK STRENGTH OF WEBS

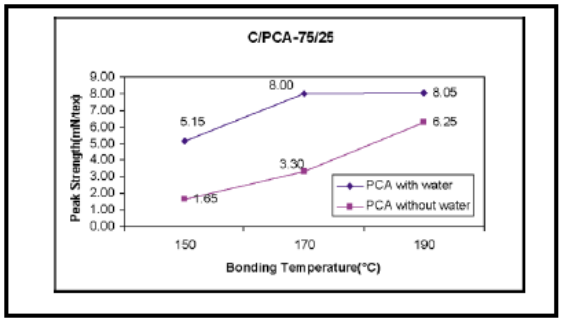

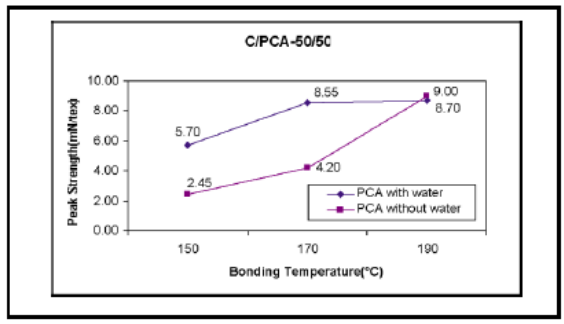

lower temperature. The web peak strength may decrease as a result.

Temperature Effect

The bonding temperature is one of the most important factors that directly affect bonding behavior. For C/OCA webs without an external plasticizing treatment, the temperature has no significant effect on web peak strength. Because the temperature in the experimental range has not reached the softening temperature (around 200°C) of ordinary cellulose acetate, there is limited motion among segments in the polymer chain. The mobility of polymer chains is simply not enough to move out of the intermolecularly constrained structure to bond with surrounding fibers.

When the water dip-nip treatment is applied to the C/OCA web, there is no significant difference in the tensile strength in the range of 150°C and 170°C. The peak strength increases substantially only after the bonding temperature approaches 190°C. Water brings down the softening temperature of the cellulose acetate. But at the higher temperature, the water increases the heat flow into the bonding points and enhances bonding.

The same trend is observed when there is only an internal plasticizer. The higher the bonding temperature, the stronger is the web. When the C/PCA webs have been thermally bonded with the aid of water pre-treatment, the softening temperature of cellulose acetate can be further reduced by decreasing the intermolecular forces in the polymer and increasing the mobility of the polymer chain. Good bonding strength can be achieved even at 170°C.

Blend Ratio Effect

The flow of heat into the fiber blend matrix is affected by fiber distribution and blend ratio. However, based on statistical analysis, there is no significant blend ratio effect on the C/OCA web peak strength when other factors are kept the same.

For C/PCA webs bonded at 150°C and 170°C, there is a significant blend ratio effect on the peak strength of the web that is treated by the 20% aqueous solution of acetone. The reason is apparently that the acetone treatment plays a much more important role on increasing polymer chain mobility in cellulose acetate at lower temperature, when compared to the temperature effect. This goes along with the larger portion of binder fibers that are available; thus, the polymer chain movement and bonding effects are enhanced. At 190°C, significant differences in peak strength are observed for different blend ratios of C/PCA webs when there is no water treatment. The bonding is enhanced as the binder fiber content is increased, when the temperature is appropriate.

Bond Structure

Bonding points taken from C/PCA-50/50 webs were examined and the effect of water treatment on bonding morphology was characterized. From the SEM photos taken on C/PCA-50/50 web bond areas *(Figure 4)*, it is clearly seen that at the same bonding temperature the integrity of bonding points was enhanced with water dip-nip treatment. The edges of the bonding points became much sharper and the fibers became much flatter, thereby increasing the surface contact area and contributing to better bonding. Solvent treatment improves the web bonding structure at lower temperature, also.

In *Figure 4*, A3 and A4 show bonding points taken from C/PCA-50/50 webs bonded at 190°C. These two bonding points show less difference between treatment than those bonded at 150°C. Both bonds are quite good and clearly visible. The reason for the similarity is that the temperature is already high enough for the CA fiber to stick to the surrounding fibers, irrespective of treatment or no treatment.

The same conclusions can be drawn from examining the fiber morphology inside the bonding areas at higher magnification *(Figure 5)*.

The fibers inside the bonding points without treatment look rounder and less altered. However, the fibers inside the bonding points, which have been water pretreated, look much flatter and the edge of the fiber is not very clear. They have been well integrated with surrounding fibers. The fibers became flatter and softer with the water treatment. In the photo taken from acetone treated bonding points, it is difficult to distinguish the fiber inside the bonding point because the acetone treatment has caused part of the cellulose acetate fiber to dissolve, thereby preventing the fiber to retain its integrity. The fibers are well bonded, but the previous comments help explain why acetone treatment did not surpass water treatment as expected. That is, some of the binder fibers were dissolved; therefore, the web strength is decreased.

Figure 4
SEM PHOTOGRAPHS OF BOND POINTS

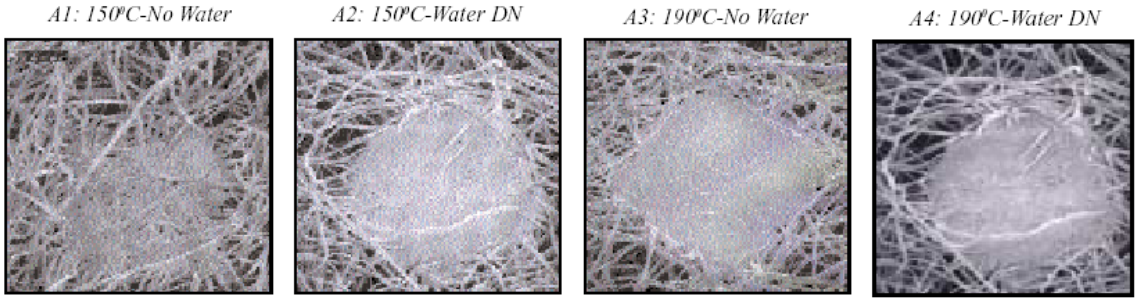

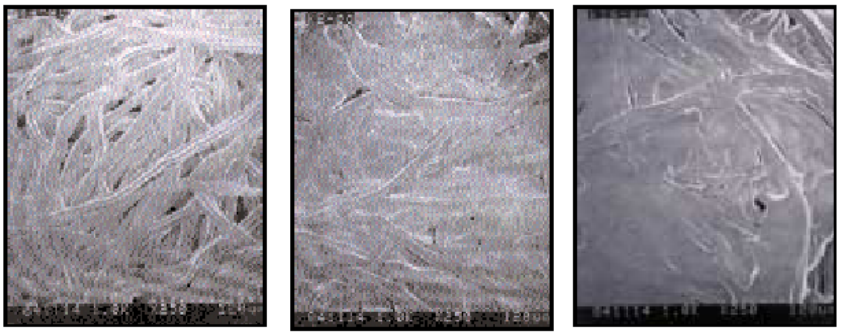

No Water *Water Dip-Nip* *20% Acetone Solution*

Figure 5
FIBER MORPHOLOGY OF C/PCA-50/50-150ºC WEBS
BONDED UNDER DIFFERENT TREATMENTS

When SEM photos at different temperatures are compared *(Figure 4)*, it is observed that the bonding points become much better defined with temperature increase, and the bonding points look more uniform along the edge. It is easier to account for the differences caused by the temperature, especially when one compares the photos showing bonds at 150ºC with those at 190ºC.

Conclusions

1. Water as an external plasticizer, when applied to the web by a dip-nip pretreatment, can significantly increase the tensile strength of cotton/cellulose acetate thermally bonded webs at reduced calender-roll temperatures.

2. Water can enhance the cotton/cellulose acetate web bonding to essentially the same degree as an aqueous acetone treatment and provide a good, safe and more economical choice for industrial manufacturing of nonwovens.

3. The higher the calender roll temperature, the greater the tensile strength of cotton/cellulose acetate thermally bonded webs.

4. Plasticized cellulose acetate as binder fiber provides significantly higher tensile strength to the cotton/cellulose acetate thermally bonded webs than those incorporating ordinary cellulose acetate as binder fiber.

5. The use of internal and/or external plasticizer can provide choices of binder fiber and plasticizing treatment for better bonding with acceptable physical properties. Two choices are:

- Cotton/Plasticized Cellulose Acetate-50/50-170ºC – with water treatment
- Cotton/Plasticized Cellulose Acetate-50/50-190ºC – without water treatment

References

1. John W. Bornhoeft, "The Development of Nonwoven Fabrics and Products that are Friendly to the Environment," TAPPI Proceedings, 1990 Nonwovens Conference, p1

2. A. F. Turbak, "Nonwovens: Theory, Process, Performance, and Testing," TAPPI, Atlanta, GA, 1993

3. K.E. Duckett; Larry Wadsworth, "Tensile Properties of Cotton/Polyester Staple Fiber Nonwovens," TAPPI Proceedings, 1987 Nonwoven Conference, 1987, p121-127

4. K.E. Duckett and L.C. Wadworth, "Physical Characterization of Thermally Point-Bonded Cotton/Polyester Nonwovens," Proceedings of the 1988 TAPPI Nonwovens Conference, 1988, p99-107

5. Jerry P. Moreau, "Cotton Fiber for Nonwovens," June 1990 *TAPPI Journal*, 1990, p179-184

6. K.E. Duckett and L.C. Wadworth, and V. Sharma, "Comparison of Layered and Homogeneously Blended Cotton and Thermally Bonding Bicomponent Fiber Webs," *TAPPI Journal*, 1995, p169-174

7. Hsu-Yeh Huang and Xiao Gao, "Spunbond Technology," http://trcs.he.utk.edu/textile/nonwovens/spunbond.html, 1999

8. Greta Marie Heismeyer, "Biodegradable Staple Fiber Nonwovens Calendered with the Assistance of An Aqueous Solvent: Their Fabrication, Properties, and Structural Characteristics," Thesis, University of Tennessee, December, 1997

9. K.E. Duckett, G. Bhat, H. Suh, "Compostable Nonwovens From Cotton/Cellulose Acetate Blends," TAPPI Proceedings, 1995 Nonwovens Conference, p89-96

10. E. J. Powers, Celanese Acetate, private communication.

11. Gajannan Bhat, Kermit Duckett, and Xiao Gao, "Processing and Properties of Cotton-Based Nonwovens," Proceedings of the Ninth Annual TANDEC Conference, Univ. of Tenn.-Knoxville (Nov. 11, 1999)

12. K.E. Duckett, G.S. Bhat, X. Gao, H. Rong, and E.C. McLean, "Characterization of Cotton/Cellulose Acetate Nonwovens of Untreated and Aqueous Pretreated Webs Prior to Thermal Bonding," Proceeding of INDA/TAPPI, 2000

13. K.E. Duckett, G.S. Bhat, X. Gao, H. Rong, "Advances in the Thermal Bonding of Cotton/Cellulose Acetate Nonwovens of Untreated and Aqueous Pre-treated Webs," Proceeding of 2nd International Conference on Metrology in Textile Engineering, Lodz, Poland, Nov. 23-24, 2000

14. Glenn P. Morton, R.L. McGill, "Thermally Bondable Polyester Fiber Effect of Calendering Temperature," TAPPI Proceedings, 1987 Nonwovens Conference, p129-135 — ***INJ***

Return to Table of Contents

VITA

Haoming Rong was born in Heilongjiang, China in 1970. She will receive her Doctor of Philosophy degree in Materials Science from the University of Tennessee, Knoxville in May 2004. She worked as a graduate research assistant at Textile and Nonwovens Development Center (TANDEC) at the university during her doctoral study. Whereas she was making good progress in her research, she spent the summer 2002 doing internship at Procter & Gamble Company, which has added to her expertise in the area of fiber and nonwoven materials. Before joining the University of Tennessee, she earned a Master of Science degree in Polymer Materials Science and Engineering at the Institute of Carbon Fiber and Composites of Beijing University of Chemical Technology, Beijing, China in June 1997 and worked as a research associate at the institute for two years after the degree. She received a Bachelor of Science degree in Polymer Science and Engineering at Beijing University of Chemical Technology, Beijing, China in July 1991. After that she joined the rubber industry and served as a Design and Quality Control Engineer for three years.